

CARBON STARS: ABSOLUTE MAGNITUDES AND
CARBON AND NITROGEN ISOTOPE RATIOS

by

BERNT INGEMAR OLSON

B.Sc., Simon Fraser University, 1969

M.Sc., University of British Columbia, 1971

A THESIS SUBMITTED IN PARTIAL FULFILLMENT OF
THE REQUIREMENTS FOR THE DEGREE OF
DOCTOR OF PHILOSOPHY

THE FACULTY OF GRADUATE STUDIES
in the Department
of
GEOPHYSICS AND ASTRONOMY

We accept this thesis as conforming to the
required standard

THE UNIVERSITY OF BRITISH COLUMBIA

August 1977



Bernt Ingemar Olson, 1977

In presenting this thesis in partial fulfilment of the requirements for an advanced degree at the University of British Columbia, I agree that the Library shall make it freely available for reference and study. I further agree that permission for extensive copying of this thesis for scholarly purposes may be granted by the Head of my Department or by his representatives. It is understood that copying or publication of this thesis for financial gain shall not be allowed without my written permission.

Department of Geophysics and Astronomy

The University of British Columbia
2075 Wesbrook Place
Vancouver, Canada
V6T 1W5

Date August 19, 1977

ABSTRACT

Carbon stars are relatively uncommon, luminous, cool stars whose spectra exhibit exceptionally strong bands of carbon-containing molecules. This is direct evidence of extensive nucleosynthesis, as will occur in the late stages of stellar evolution. The two aspects investigated here are their luminosities and atmospheric carbon and nitrogen isotope ratios.

The luminosities are derived through the study of those carbon stars which are members of double star systems. Since the companion star is apparently normal and thus of known luminosity, the carbon star luminosity is directly attainable. Photometry and spectroscopy of suspected binaries yield absolute visual magnitudes for a dozen stars as bright as -4.7 , and bolometric magnitudes primarily in the range -4 to -8 . This means they are slightly more luminous than normal giants.

The isotopic ratios have been deduced by a comparison of synthetic spectra with the observed near infrared stellar spectra. The synthetic spectra were calculated by direct integration of the flux emerging from an appropriate model atmosphere, and contain lines primarily of the Red band system of the CN molecule. A new analysis technique, used in time series analysis, which is based on the mutual coherence of the spectra being compared and makes full use of the entire spectrum, has been employed. By varying the parameters describing the synthetic spectrum, including the isotopic ratio, the coherence

can be maximized and the isotopic ratio of the stellar spectrum deduced. Results for five carbon stars yield $^{12}\text{C}/^{13}\text{C}$ ratios in the range 2.5 to 30. A search was also made for the isotopes ^{14}C and ^{15}N ; ^{14}C was not found, while a tentatively positive result is reported for ^{15}N .

TABLE OF CONTENTS

| | |
|--|-----|
| Introduction | 1 |
| Part I. Absolute Magnitudes | 9 |
| Carbon Stars in Clusters | 11 |
| Statistical Studies | 14 |
| Carbon Stars in Binary Systems | 17 |
| The Observational Data | 19 |
| Discussion of Individual Systems | 46 |
| Discussion | 54 |
| Part II. Carbon Isotope Abundance Ratios | 61 |
| The Observational Material | 66 |
| Synthetic Spectra - Theory | 69 |
| Synthetic Spectra - Practice | 73 |
| Molecular Parameters | 73 |
| Molecular Equilibrium Calculation | 82 |
| Spectrum Parameters | 86 |
| Computational Procedure | 88 |
| Analysis Technique | 90 |
| Computational Details | 92 |
| Comments | 95 |
| Tests | 97 |
| Results | 105 |
| The $^{12}\text{C}/^{13}\text{C}$ Ratios | 105 |
| Turbulence | 109 |
| A Note on the Carbon Abundance | 111 |
| The Search for ^{14}C and ^{15}N | 115 |

| | |
|--|-----|
| A Recap of the Coherency Technique | 129 |
| Summary | 131 |
| References | 133 |
| Appendix I. Radial Velocities of Carbon Stars | 138 |
| Appendix II. Use of Microdensitometer and Computer | |
| Programs to Measure Radial Velocities | 147 |
| Appendix III. The Ratio of Total to Selective Absorption . | 161 |
| Appendix IV. Coherency Tables | 169 |
| Appendix V. Parameters of Specific Model Atmospheres | 179 |

LIST OF TABLES

| | | |
|------|---|-----|
| 1. | Summary of Data on Carbon Stars in Clusters | 12 |
| 2. | Summary of Statistical Absolute Magnitudes | 15 |
| 3A. | Observed Photometric Extinction Coefficients | 21 |
| 3B. | Photometric Errors for Standard Stars | 21 |
| 4. | Suspected Binary Systems with Observations | 24 |
| 5. | Data on Observed Systems. Part 1 | 32 |
| 6. | Data on Observed Systems. Part 2 | 35 |
| 7. | Data on Observed Systems. Part 3 | 38 |
| 8. | Data on Observed Systems. Part 4 | 41 |
| 9. | VRI Photometry | 44 |
| 10. | Some Uninvestigated Double Stars | 45 |
| 11. | Model Atmosphere Parameters | 64 |
| 12. | High Dispersion Carbon Star Spectra | 67 |
| 13. | Molecular Data for the Red System of CN | 76 |
| 14. | Molecular Data for the Phillips System of C ₂ | 77 |
| 15A. | Known Energy Levels of the CN Molecule | 78 |
| 15B. | Known Energy Levels of the C ₂ Molecule | 78 |
| 16. | Coherency Peaks for a Test Case | 98 |
| 17. | Summary of Derived Spectral Parameters | 106 |
| 18. | Coherency for γ CVn vs ¹² C ¹⁵ N and ¹³ C ¹⁵ N | 122 |
| 19. | Stars with "A"-quality Velocities Used to Establish Standard Wavelengths in the Infrared | 141 |
| 20. | Standard Wavelengths and Accuracies of Features Defining the Radial Velocity System | 142 |

| | |
|--|-----|
| 21. Acceptance Criteria for Wavelength Standards | 143 |
| 22. Coefficients of Polynomials To Determine R from E(B-V) and (B-V) ₀ | 168 |

LIST OF FIGURES

| | | |
|-----|---|-----|
| 1. | Prominent Features of Carbon Star Spectra | 4 |
| 2. | M _v (Carbon Star) <u>vs</u> M _v (Companion) | 57 |
| 3. | M(bol) (Carbon Star) <u>vs</u> M(bol) (Companion) | 58 |
| 4. | Bolometric Correction <u>vs</u> V-R | 59 |
| 5. | M(bol) <u>vs</u> (V-R) ₀ | 60 |
| 6. | Rotational Energy Level Structure for the Red System of CN | 79 |
| 7. | Rotational Energy Level Structure for the Phillips System of C ₂ | 81 |
| 8. | Pretreatment of Spectra | 94 |
| 9. | Calculated and Observed Spectra of 19 Psc | 102 |
| 10. | C ₂ Features in the Spectrum of 19 Psc | 113 |
| 11. | Coherency Curves for the ¹⁴ C Test Cases | 118 |
| 12. | Coherency Curves for Stars <u>vs</u> ¹⁴ C Abundance | 120 |
| 13. | Coherency Curves for Stars <u>vs</u> ¹⁵ N Abundance | 121 |
| 14. | " ¹⁵ N Features" and the Spectrum of Y CVn | 126 |
| 15. | Identification of Wavelength Features for Near Infrared Radial Velocity System | 144 |
| 16. | R <u>vs</u> E(B-V) for various types of stars | 166 |
| 17. | R [_∂ E(B-V)=0] <u>vs</u> (B-V) ₀ | 167 |

ACKNOWLEDGEMENTS

I would like to express my appreciation to my supervisor, Dr. Harvey Richer, for his continued aid, encouragement and enthusiasm throughout this project. Special thanks go to Dr. Hans Fast for providing the computer programs for spectrogram reduction, and to Dr. Jason Auman for many invaluable discussions and suggestions dealing with the model atmospheres and molecular calculations. I am also indebted to Dr. Hollis Johnson, without whose model atmospheres this thesis would not have been possible in the present form, and especially to Dr. Tad Ulrych, for introducing me to the coherence spectrum technique. The friendly assistance of the staff at Kitt Peak made my visit there very enjoyable, while numerous friends have considerably enhanced the enjoyment of doing this thesis. Finally the U.B.C. Computing Centre was invaluable in the production of the physical copy, while all typing, diagrams and layout were done by myself.

INTRODUCTION

A two dimensional system of stellar classification based on a star's luminosity and temperature does not fully characterize the nature of that star. This is most readily apparent among the late-type giants where abundance differences result in many different classes of stars showing widely dissimilar spectra.

This thesis is about some aspects of one of these classes of stars: the carbon stars. The generic name "carbon star" refers to many different kinds of stars, all of which have one thing in common: their spectra show the presence of carbon-containing molecules in greater strength than in normal stars of similar temperature and luminosity. The classes of carbon stars are:

1. R stars - these stars correspond to the normal K stars, showing spectra with a comparable set of atomic lines plus bands of C_2 and enhanced CN and CH.
2. N stars - generally cooler than the R stars; exhibit extremely heavy blanketing by the bands of C_2 and CN. Most N stars are long period variables.

Every carbon star is either of type R or N. This, the original classification system, depends on the relative visibility of the blue spectral region, with N stars being more heavily blanketed there.

3. J stars - R or N stars with exceptionally strong $^{13}C^{14}N$ bands (especially at 6168 A) and usually also with strong neutral lithium.

4. CH stars - show an abnormally strong G band and other bands of CH, and generally weak metals. These are all high velocity stars and hence belong to population II.
5. Ba II stars - exhibit strong lines of Ba, Sr and other heavy metals, plus enhanced CH.
6. Hd stars - the hydrogen deficient stars, show strong C₂ but weak CH bands. Most Hd stars are also variables of the R CrB type.

The CH, Ba II and Hd stars are subgroups of the R stars.

7. CS (or SC) stars - show conspicuous CN bands, enhanced atomic lines (Ba II, etc.) but very weak bands of ZrO or C₂, making it difficult to decide at low dispersion whether they are C or S stars.

Other chemically peculiar cool stars are the just mentioned S stars which show oxide bands (especially ZrO, plus LaO, YO) and MS stars which are intermediate between S stars and the normal cool M stars, which are characterized by bands of TiO.

The primary factor producing this variety is the C/O ratio; because of the great stability of the CO molecule virtually all the C or O is tied up in the form of CO, so that stars with an excess of carbon form carbon stars while those with excess oxygen form M or S stars. The CS stars are presumably stars with a C/O ratio of almost exactly unity so that small amounts of both C and O are available to form other molecules. Clearly other factors are also important, to produce such different types as the CH and Hd stars; these include the population type

(metal abundance), mass and age to name but the most obvious.

The thing I want to emphasize is that the carbon stars as a whole are a very diverse group indeed. Although each subgroup is a more cohesive set, there is still no a priori reason to assume that the N stars (for example) are sufficiently closely related that they can be described by the same basic parameters. In fact I shall show that their luminosities (in particular) cover quite a wide range. The physical properties of carbon stars have recently been reviewed by Wallerstein (1973).

As a guide to carbon star spectra, Fig. 1 illustrates many of the more prominent and peculiar features that may be present in the visual and near infrared region of cool carbon stars. C_2 is represented by the Swan and Phillips band systems, degrading towards the blue and red, respectively. CN bands from both the Violet and Red systems are present, also degrading in opposite directions; the Red bands show three separate bandheads resulting from different branches of the band. The isotopic bands (not shown) of $^{12}C^{13}C$ are offset from the main bands by approximately +8 Å per unit vibrational quantum number change (Δv) for the Swan bands while for the red bands of C_2 and CN the offset is on the order of +40 Å. CH is present as the G band and several other bands in the 3900 - 4400 Å region; the Merrill-Sanford bands near 4900 Å are almost certainly due to SiC_2 ; CaCl bands are occasionally seen in some stars. [The two redward bands of CaCl shown belong to the Red system and are degraded to the blue; the 5934 Å band belongs to the Orange

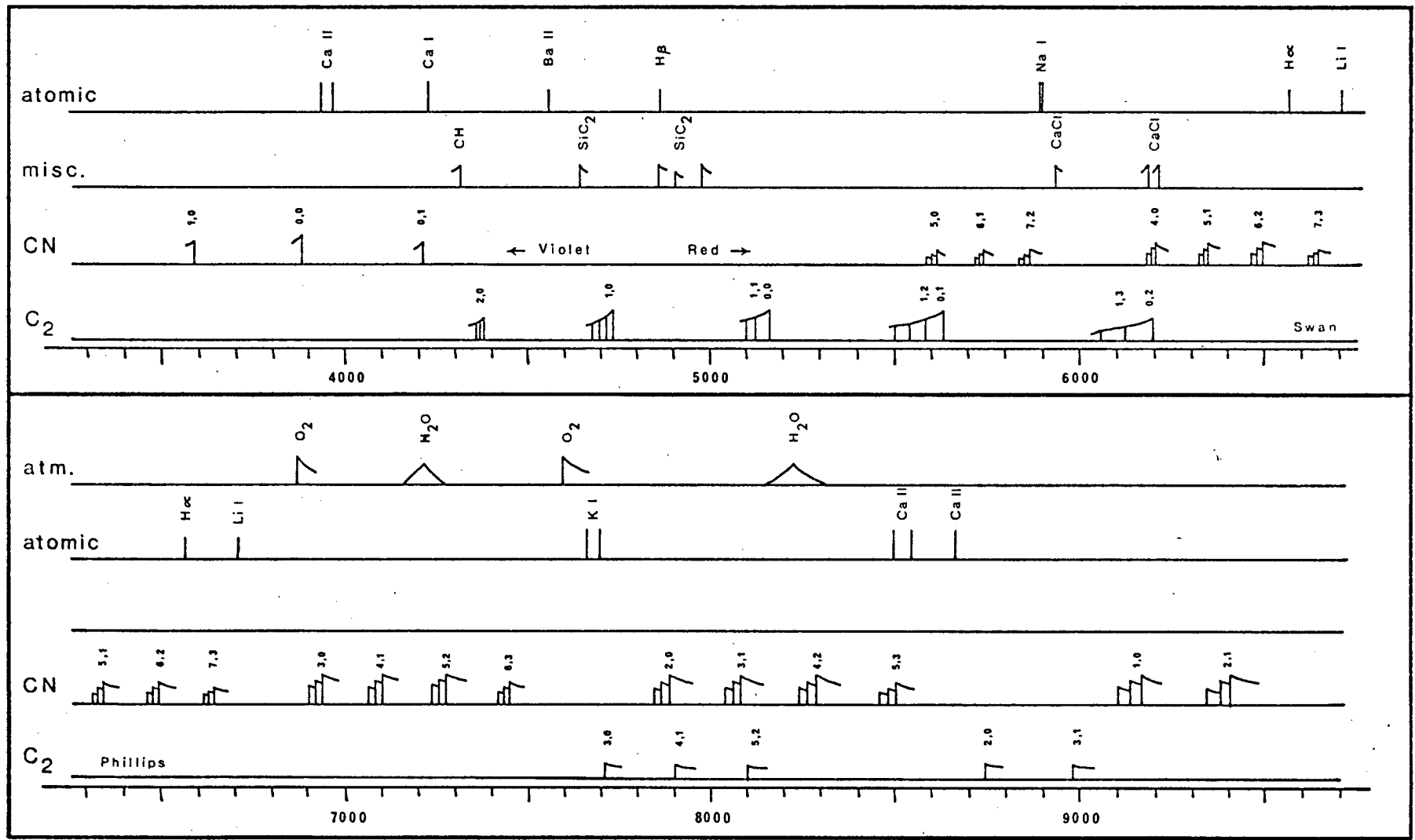


Figure 1. Prominent Features of Carbon Star Spectra

system. According to Pearse and Gaydon (1941) this band is degraded to the red whereas the spectra of Rybski (1973) apparently show the band extending to the blue into the Na D lines.] Polyatomic molecules have also been detected in carbon stars: a C_3 band has been detected at 4050 Å while HCN and C_2H_2 lines have been identified in the 1μ region. Bands of CO do not appear in the visual region, the closest being the $\Delta v=3$ sequence at 1.6μ . The atomic lines indicated are not by any means exhaustive but merely show some of the stronger and/or interesting features.

This thesis is divided into two principal parts. Part I deals with an investigation into the absolute magnitudes of carbon stars. Part II presents a new technique for determining carbon isotope ratios from molecular bands and carries out that analysis for five carbon stars. The remainder of this introduction deals with the origin of the carbon stars.

Although the origin of carbon stars is outside the scope of this thesis it is worthwhile to briefly consider the mechanisms which have been proposed to create carbon stars from the normal oxygen stars. Since carbon stars have $C/O > 1$ it is clear that some nuclear processing must have occurred; this means either hydrogen-burning by the CNO cycle or 3-alpha helium-burning. A means of transporting the processed material to the surface, where we can see it, must also be provided. As it now appears likely that the observed surface abundances of carbon and nitro-

gen are only with difficulty compatible with CNO processing (e.g. Kilston 1975, summary by Irgens-Jensen 1976), a process involving helium-burning reactions, at least in part, must be considered, producing lower N/C ratios.

The evolutionary stage that seems best able to provide for both the processing and transportation requirements occurs during the helium shell-flash phase. During this evolutionary phase the structure of the star is as follows: there is an inert core consisting of the products of helium-burning, C and O, above this is a thick helium-burning shell, followed by an inert helium region, a thin hydrogen-burning shell and a deep convective envelope extending to the surface. As the star evolves the helium-burning shell gradually narrows until a thermal instability develops: the energy released by the helium-burning reactions is not able to escape due to a combination of the high heat capacity of the shell and the pressure in the shell not increasing proportionally to the density change (cf: Sackmann 1977). Since the helium-burning reactions are very temperature sensitive a helium flash occurs. A convective zone then develops, extending almost up to the hydrogen-burning shell. After a while the flash is quenched (Sackmann 1977) and the convective zone decreases and disappears; quiescent helium-burning then continues until the next flash starts. We thus have an evolutionary stage where carbon is produced (violently) and transported upwards; since the convective zone was, however, contained in the interior it is not yet clear how the carbon reaches the surface.

Three basic approaches have been proposed to overcome this difficulty. 1. The deep envelope (DE) model (Sackmann, Smith and Despain 1974) makes the ad hoc assumption that the interior convective zone actually does physically merge with the convective envelope. Though there is nothing impossible about this scheme (e.g. by convective overshooting) the fact remains that no model star yet calculated has exhibited such a continuous convective region. 2. The plume model (Scalo and Ulrich 1973) supposes that, at the maximum extent of the interior convective zone, protons can tunnel through the thin inert helium zone into the convective shell. They would there react with the carbon, setting up convective plumes linking the convective shell with the envelope, thus acting as conduits for the processed material into the envelope. The disadvantages of this scheme are that the plume properties can not be calculated from first principles, and that just the right number of protons need to enter the convective shell to produce the observed distribution of s-process elements. 3. Iben's (1975) scheme, which is a direct result of the evolutionary sequence of stellar model calculations, sees the convective envelope dip down into the helium-burning residue. During the flash the regions within and above the helium-burning shell are pushed outward, and the helium-burning products are distributed throughout the region occupied by the convective shell, which does not quite extend as far as the hydrogen-burning shell. After the flash has stopped the envelope again descends, continuing past its previous

position (in mass) until it encompasses the top part of the residue left behind by the convective shell. This material will then be convected to the surface. Successive flashes will bring more and more processed material into the envelope.

Each of these models will enhance the envelope carbon abundance more than the nitrogen, since nitrogen is not produced during helium-burning. They all also suffer from the difficulty that the just produced carbon will be processed through the CNO reactions as it passes through the hydrogen-burning region and also during the inter-flash periods. An envelope base temperature cool enough to prevent ^{12}C destruction also hinders the production of ^{13}C . Iben's scheme at least has the feature that the luminosity due to hydrogen-burning is considerably reduced during the time that the envelope is actually dipping into the helium-burning residue; the other two schemes necessarily treat the structure as constant during the mixing phase, while Iben's mixing is caused by the structural changes. On the whole, Iben's model is to be preferred at present, primarily because its essential features are directly calculable and involve no additional hypotheses.

Part I.

ABSOLUTE MAGNITUDES

The position of carbon stars in the evolutionary sequence is not well understood. It is not clear, for example, whether most stars become carbon stars or if only some do, whether the carbon star phenomenon is recurrent or occurs only once, or how the core products of nucleosynthesis are transported to the surface. Moreover, as has been mentioned, carbon stars are not a homogeneous group; some are found in globular clusters while others (N stars) are strongly concentrated toward the galactic plane. The problem is compounded by the fact that many of the basic observational data are imprecise, making comparison with theoretical studies difficult. In particular, carbon star temperatures and luminosities are not accurately determined. I shall here address myself to the absolute magnitude problem.

Most previous studies of this question have employed statistical methods to derive mean absolute magnitudes for large groups of stars; this approach does, however, tend to obscure the range of luminosities that actually exists. The only way to reveal this range is to determine the absolute magnitude of as many individual carbon stars as possible. Since this requires a knowledge of the distance to the star this can only be done for carbon stars which are members of clusters or binary systems.

This part of the thesis begins with a brief summary of work dealing with carbon stars in clusters and statistical studies. This is followed by a description of the photometric and

spectroscopic data available pertaining to carbon stars which are members of binary systems and a discussion of the pertinent points of each individual system, plus a general discussion of the derived magnitudes. [Much of the material discussed in this part has already been published (Olson and Richer 1975).]

CARBON STARS IN CLUSTERS

The data on carbon stars in the line of sight to clusters has been summarized by Gordon (1968). Assuming that the carbon stars actually are cluster members she finds absolute visual magnitudes ranging from +0.5 to -3.5. Unfortunately the supporting observational data is rather sketchy and the absolute magnitudes hence somewhat uncertain. Since that time several other cases have been discovered and more data gathered on other suspected cluster members. Table 1 summarizes the current status of carbon stars in clusters.

The carbon star near NGC 2477 is approximately two cluster radii from the cluster center. Its radial velocity of $+5.5 \pm 3$ km/s agrees well, however, with that of an early M-star ($+7 \pm 3$) which is a cluster member on the basis of its proper motion; furthermore the galactic field velocity at the distance of the cluster is +27 km/s, making this star a probable member. The magnitude range shown is caused by nonuniform reddening across the cluster.

Hartwick and Hesser (1973) find that if the carbon star which is 2' from the center of NGC 2660 is a cluster member its $M_v = -2.0$ and it has a mass of about $1.8 M_{\odot}$.

The radial velocity of MSB 75 (-46 ± 3 km/s) makes it a probable member of the very old cluster NGC 7789 (-45 ± 7 km/s) when compared with the field velocity (-25 km/s).

Walker (1972) has found another very red star ((B-V) =

TABLE 1. SUMMARY OF DATA ON CARBON STARS IN CLUSTERS

| Cluster | Star | V | B-V | Clus. | (m-M) | Cluster | | Mv | Ref |
|-------------|--------|--------|-------|--------|-------|---------|--------------------|-------|------|
| | | | | E(B-V) | app | Type | Age | | |
| NGC 2477 | | 10.7 | 2.9 | 0.20 | 11.2 | Open | 10 ⁹ | -0.5 | 1,2 |
| | | | | 0.40 | 11.8 | | | -1.1 | |
| NGC 2660 | | 11.53 | 4.26 | 0.38 | 13.55 | Open | 10 ⁹ | -2.0 | 3 |
| NGC 7789 | MSB 75 | (10.2) | | 0.26 | 12.1 | Open | 10 ⁹⁻¹⁰ | -1.9 | 4,8 |
| SMC-NGC 419 | Anon 1 | 16.3 | | | 19.4 | Glob | 10 ⁹ | -3.1 | 5 |
| SMC-Kron 3 | #24 | 16.48 | 2.37 | | 19.4 | Glob | 10 ⁹⁻¹⁰ | -2.9 | 5 |
| SMC-NGC 121 | V8 | <16.4> | <1.9> | | 19.4 | Glob | 10 ¹⁰ | -3.0 | 5 |
| ω Cen | RG0 55 | 11.56 | 1.55 | | 14.28 | Glob | 10 ¹⁰ | -2.72 | 7,9 |
| | RG0 70 | 11.61 | 1.80 | | | | | -2.67 | 10,6 |
| | anon | 12.16 | 1.50 | | | | | -2.12 | 11 |
| LMC | many | 15.7 | | | 18.7 | | | -3 | 12 |

Refs:

- | | |
|----------------------------------|-----------------------|
| 1. Catchpole and Feast (1973) | 7. Harding (1962) |
| 2. Hartwick <u>et al.</u> (1972) | 8. Haqen (1970) |
| 3. Hartwick and Hesser (1973) | 9. Arp (1965) |
| 4. Gaustad and Conti (1971) | 10. Dickens (1972) |
| 5. Feast and Lloyd Evans (1973) | 11. Bond (1975) |
| 6. Cannon and Stobie (1973) | 12. Westerlund (1964) |

+4.2, $M_v = -1.9$) in NGC 419 in the Small Magellanic Cloud. Although no spectra of this star exist, it seems probable that it is a carbon star. The three SMC stars in Table 1 are all located right at the tip of the red-giant branch (Feast and Lloyd Evans 1973), as are the three known CH stars in ω Cen (Smith and Wing 1973; Bond 1975). All carbon stars so far found in globular clusters have been located at the tip of the giant branch.

The approximately 400 carbon stars found by Westerlund (1964) in the LMC have a mean estimated visual magnitude of 15.7 with a spread of about half a magnitude, indicating an absolute visual magnitude of about -3.

Because of the scarcity of C-stars near clusters and the difficulty in establishing whether a star is a cluster member in our galaxy, the large numbers of carbon stars in the Large Magellanic Cloud hold great promise in regard to absolute magnitude studies. Recently a small sample of these have been studied by Crabtree, Richer and Westerlund (1976); they range in apparent magnitude from 13.9 to their instrumental limit of 16.8, resulting in absolute visual magnitudes as bright as -4.6 (using $m-M = 18.5$).

STATISTICAL STUDIES

Since most carbon stars are field stars, their absolute magnitudes can only be calculated on a statistical basis using the observed radial velocities and/or proper motions in conjunction with the apparent magnitudes.

Sanford (1944) found $\langle M_V \rangle = -0.4 \pm 0.4$ for 62 R-stars and -2.3 ± 0.2 for 171 N-stars. The R-stars were further subdivided by Vandervort (1958) who derived $\langle M_V \rangle = +0.44 \pm 0.29$ from 43 R0 and R2 stars, and -1.10 ± 0.49 from 42 R5 and R8 stars. Richer (1971) calculated $\langle M_V \rangle = -2.7 \pm 0.7$ for 33 stars classified C3 to C7 on his infrared classification system; these stars were mostly of type N.

Baumert (1972) has calculated near infrared 1.04 micron narrowband absolute magnitudes $\langle M(104) \rangle$ of -1.7 ± 0.5 and -4.3 ± 0.6 for R and N-stars, respectively. To convert these numbers to visual magnitudes the colour index $(V-I(104))$ was formed for a sample of stars in common with the lists of Richer (1971) and of Mendoza and Johnson (1965). This resulted in $\langle V-I(104) \rangle = +2.4 \pm 0.9$ (st. devn) for the R-stars and $+3.9 \pm 0.7$ for the N-stars. The average $(B-V)$ indices for the samples were $+1.67$ and $+3.13$, as compared to the more complete sample values of $+1.67$ for Vandervort's R-stars and $+3.10$ for Richer's N-stars, indicating that the samples used are representative of the general population. The resulting M_V 's are $+0.7$ and -0.4 , significantly fainter than the previous results.

| Author | Type | Mv | N | Type | Mv | N |
|----------------------|----------|---------------------------------------|-----|----------|---------------------------------------|-----|
| Sanford (1944) | R | -0.4 ± 0.4 | 62 | N | -2.3 ± 0.2 | 171 |
| Vandervort (1958) | R0 R2 | +0.44 ± 0.29 | 43 | | | |
| -- " -- | R5 R8 | -1.10 ± 0.49 | 42 | | | |
| Richer (1971) | | | | C3 C7 | -2.7 ± 0.7 | 33 |
| Baumert (1974) | R | M(104) = -1.7 ± 0.5 Mv = +0.7 # | 115 | N | M(104) = -4.3 ± 0.6 Mv = -0.4 # | 202 |

See text.

TABLE 2. SUMMARY OF STATISTICAL ABSOLUTE MAGNITUDES OF CARBON STARS

Peery (1975), assuming that most of the dispersion in colour of Baumert's photometric data is due to interstellar reddening, has deduced bolometric magnitudes for a sample of N irregular variables in the range -4 to -6 , again considerably brighter than Baumert's value for a similar group. Baumert (1975) subsequently revised his value for this group of stars by -1.5 magnitudes by deleting a single star from his sample. Thus it seems plausible that similar errors may be responsible for a large part of the above mentioned discrepancy.

CARBON STARS IN BINARY SYSTEMS

The other major approach to determining absolute magnitudes of individual carbon stars makes use of binary systems with one member a carbon star. This method is essentially identical to that used for carbon stars in clusters; namely, determine the distance modulus to the system (cluster) and use the apparent magnitude to calculate the absolute magnitude. To do this one must: a) establish the reality of the physical proximity of the C-star and its suspected companion (or the cluster), and b) calculate the distance modulus of the companion (cluster).

The distance modulus of a cluster is far easier to derive accurately than that of a single star, however, since in that case we have access to all the cluster members. Comparison of the observed colour-magnitude diagram with the zero age main sequence yields the distance modulus and reddening as well as the age of the cluster and the mass of the carbon star, though this is more strongly dependent on the evolutionary model sequence used. A cluster distance modulus is obtainable to an accuracy of a few tenths of a magnitude. In contrast to this the modulus of a single star must be computed from a knowledge of its absolute magnitude, which, in turn, must be inferred from some observational parameter that has been calibrated in terms of absolute magnitude. In practice this would normally entail MK spectral classification, H_{β} photometry for B-stars, or H_{β} plus uvby photometry for A and F-stars. Whereas the absolute magnitude calibrations for single stars of early type may be

comparable in accuracy to the cluster moduli, later types can often not be placed to better than a magnitude. In this investigation the first two methods have been employed.

The most conclusive ways of proving the reality of a suspected binary system would be to observe either an orbit or one star eclipsing the other. No such cases are known among carbon stars although a few do show composite spectra, indicating a very close companion. That these are the result of a chance superposition is highly unlikely. As the angular separation of the two stars increases there is an increasing need for corroborating evidence of their physical association. Agreement of their radial velocities, or common proper motion, would strongly support this conclusion, as would the presence of the same set of interstellar absorption lines in both stars, although this would be difficult to apply to carbon stars because of the complexity of their spectra. Finally, the absolute magnitude derived for the carbon star ought to be "reasonably" close to the range indicated by the statistical studies and those carbon stars which are members of clusters (see previous sections).

The Observational Data

The list of candidate carbon stars which may be members of binary systems has been compiled from several sources. The initial list was prepared by Dr. H. B. Richer during his observing run at Cerro Tololo in 1969, when, while taking spectra of the C-stars, he noticed that several stars had fairly close companions. Three systems were added when his photometry indicated that the (U-B) indices of the supposedly single carbon stars were much too blue compared to (B-V). The results for these systems have already been published (Richer 1972). A secondary list was kindly supplied by Dr. H. E. Crull, Jr. (1972) of the U.S. Naval Observatory at Washington, D.C., while a few systems were chosen from the A.A.V.S.O. charts and some were gleaned from the literature. With the aid of the Palomar Sky Survey prints and visual observations of the candidates through the department's 30-cm (12-inch) telescope, this preliminary list was narrowed down to those systems with companions thought bright enough to be feasibly investigated further.

Photometric and spectroscopic observations of some of these systems were obtained at the Kitt Peak National Observatory near Tucson, Arizona, during the periods Sept. 10-12 (photometry) and Sept. 18-24 (spectroscopy) of 1972, by the author. In addition, Dr. Richer has obtained some VRI photometry from Cerro Tololo during the periods Oct. 12-14, 1971 and June 5-7, 1974.

UBV and $H\beta$ photometry was obtained of 17 suspected systems using the Kitt Peak #2 36-inch (91-cm) telescope and the

reductions were done by a computer program written by the author using standard reduction methods; taking into account the red leak of the U filter. The red leak filter is a standard U filter with the U bandpass region blocked, allowing a direct measure of the leak in the red region. Use of this filter is necessary for the C-stars because of their extremely red colours.

The photometer deflections through the ultraviolet, blue, visual and red leak filters are denoted by u , b , y and rl , respectively, and the raw colours are

$$\begin{aligned} C_y &= -2.5 \log (b/y) \\ C_u &= -2.5 \log (u'/b) \end{aligned} \quad (1)$$

where $u' = u - rl$. These are related to the magnitude and colors above the atmosphere via

$$\begin{aligned} y(0) &= y - k_m * \sec z \\ C_y(0) &= C_y - k_y * \sec z \\ C_u(0) &= C_u - k_u * \sec z \end{aligned} \quad (2)$$

where $k_y = k_1 + k_2 * C_y(0)$, and $\sec z$ is the air mass of the observation. The calculated extinction coefficients for each of the three photometric nights are tabulated in Table 3A, along with standard Kitt Peak values (Barnes 1974). Finally UVB colours are calculated from

$$\begin{aligned} V &= c_1 + c_2 * (B-V) + y(0) \\ B-V &= c_3 + c_4 * C_y(0) \\ U-B &= c_5 + c_6 * C_u(0) \end{aligned} \quad (3)$$

| Date (1972) | k1 | k2 | ku | km |
|---------------------|--------|--------|--------|--------|
| Sept. 10/11 | 0.107 | -0.006 | 0.234 | 0.117 |
| Sept. 11/12 | 0.087 | -0.029 | 0.136 | 0.101 |
| Sept. 12/13 | 0.088 | -0.025 | 0.269 | 0.145 |
| Average: | 0.094 | -0.020 | 0.213 | 0.121 |
| St. Devn: | ±0.011 | ±0.012 | ±0.069 | ±0.022 |
| Std. KPNO values | 0.100 | -0.020 | 0.340 | 0.150 |

TABLE 3A. OBSERVED PHOTOMETRIC EXTINCTION COEFFICIENTS

| Colour | V | B-V | U-B |
|----------|-------|-------|-------|
| St. Devn | 0.019 | 0.016 | 0.023 |

TABLE 3B. PHOTOMETRIC ERRORS FOR STANDARD STARS

where the "c" coefficients are calculated from observations of standard stars. The expected uncertainties are given in Table 3B. Since the magnitudes of the very red carbon stars are calculated, in part, from an extrapolation of the relation defined by the (bluer) standards, one would expect the uncertainties of the C-star magnitudes to be somewhat greater than those of bluer stars, and may be systematically in error. No attempt has been made to try to combat this problem. The VRI reductions were carried out in a similar manner.

Blue plates of 127 A/mm dispersion at H_γ were secured of the companions in 10 systems, as well as several MK and velocity standards. Spectral classification was done relative to the known standards using the criteria outlined in the Kitt Peak Spectral Atlas (Abt et al. 1968). The radial velocities were measured on the Grant oscilloscope measuring engine in this university's Physics Department. The internal errors resulting from the measurement of (typically) a dozen lines were about 16 km/s (st. devn), whereas a comparison of measured and standard velocities gave standard deviations of 15.2 and 11.8 km/s for B, A and F-stars and for G and K-stars, respectively, indicating that there were no systematic errors present.

Several additional spectra have also been obtained at the Dominion Astrophysical Observatory, Victoria. These were obtained with the 183-cm (72-inch) telescope at a dispersion of 78 A/mm. The internal accuracy of these plates is about 10 km/s (st. devn) from a half dozen lines. Also available were 200

A/mm blue plates of many of the suspected companions obtained by Dr. Richer at Cerro Tololo in September 1971. Unfortunately these plates turned out to be unusable for radial velocity measurements as there were large random unexplained systematic shifts between the stellar spectra and the comparison arcs, amounting in some cases to equivalent velocities of several hundred km/s.

A list of suspected carbon star binary systems for which observations exist is given in Table 4, along with two suspected systems containing S-stars. Columns 1, 2 and 3 give the name and equatorial and galactic coordinates of the C-star. Column 4 refers to the RN spectral type, the Keenan-Morgan C-type as defined on the Okayama system (Yamashita 1972), and Richer's (1971) infrared C-type. Column 5 gives the companion's name, while column 6 gives the angular separation of the two stars in seconds of arc and the position angle of the vector from the C-star to the companion, measured counterclockwise from the north point (i.e., N-E-S-W). The observational data that are relevant to determining the reality of the systems and the C-stars' absolute magnitudes are given in Tables 5 through 8. The last column of Table 4 gives which of these four tables contains the observations for that system.

The stars have been divided into four groups depending on the probability that the systems are real and the status of the observational data. Those systems which have several items of supporting evidence and no negative ones are considered to be

| Name HD DM | R. A. Dec. (1900) | l b | RN KM Rh | Comp. | Sep. P. A. | Tb No |
|------------------|-------------------------|--------|----------------|-----------|---------------|----------|
| X Cas | 01 49.8 | 131.2 | Ne | | 60 | 8 |
| | +58 46 | -2.6 | C5,4e | | 70 | |
| U Cam | 03 33.2 | 141.2 | N | +62 594 | 208 | 7 |
| 22611 | +62 19 | 6.0 | C5,4 | | 349 | |
| +62 596 | | | | | | |
| | 04 44.9 | 183.8 | N | | | 8 |
| 30710 | +15 37 | -17.9 | C5,3 | | | |
| +15 691 | | | C4 | | | |
| | 05 12.5 | 171.2 | N | | 24 | 6 |
| 34467 | +35 41 | -0.9 | C6,3 | | 44 | |
| +35 1046 | | | C4 | | | |
| UV Aur | 05 15.3 | 174.2 | Ne | ADS 3934B | 3 | 5 |
| 34842 | +32 24 | -2.4 | C8,1Je | | 4 | |
| +32 957 | | | C9 | | | |
| TU Tau | 05 39.1 | 183.8 | N | | 0 | 5 |
| 38218 | +24 23 | -2.4 | C5,4 | | | |
| +24 943 | | | C5 | | | |

TABLE 4. SUSPECTED BINARY SYSTEMS WITH OBSERVATIONS

| Name HD DM | R.A. Dec. (1900) | l b | RN KM Rh | Comp. | Sep. P.A. | Tb No |
|------------------------------|------------------------|--------------|-----------------|--------|--------------|----------|
| SZ Sgr 161208 -18 4634 | 17 39.1 -18 37 | 8.7 5.5 | N C7,3 C5 | | 2 215 | 5 |
| T Dra +58 1772a | 17 54.9 +58 14 | 86.8 29.9 | Ne | UY Dra | 15 225 | 7 |
| HK Lyr 173291 +36 3243 | 18 39.4 +36 51 | 66.1 17.5 | N C7,4 C5 | | | 8 |
| MSB 64 + 5 3950 | 18 42.6 +05 20 | 37.3 3.4 | N C6 | | 28 | 5 |
| S Sct 174325 - 8 4726 | 18 44.9 -08 01 | 25.8 -3.4 | N C6,4 C5 | | - | 8 |
| UV Aql 176200 +14 3729 | 18 54.0 +14 14 | 46.6 5.0 | N C6 | | 20 | 6 |

TABLE 4. (Cont.)

| Name HD DM | R. A. Dec. (1900) | l b | RN KM Rh | Comp. | Sep. P.A. | Tb No |
|------------------------------|-------------------------|--------------|--------------------|--------------------------|-------------------------|----------|
| X Sge 190606 +20 4417 | 20 00.7 +20 22 | 59.7 -5.9 | N C6 | | 6 | 6 |
| SV Cyg 191738 +47 3031 | 20 06.4 +47 33 | 83.2 8.0 | N3 C7,4 | +47 3032 | 145 140 | 5 |
| RS Cyg 192443 +38 3957 | 20 09.8 +38 26 | 75.9 2.4 | Ne C8,2e C5 | +38 3956 +38 3960 | 132 355 56 106 | 7 |
| U Cyg 193680 +47 3077 | 20 16.5 +47 35 | 84.2 6.6 | Ne C8,2 C em | +47 3078 | 64 51 | 7 |
| MSB 41 +32 3954 | 20 45.2 +32 51 | 75.8 -6.7 | N | cp. 1 cp. 2 | 10 18 | 6 |

TABLE 4. (Cont.)

| Name HD DM | R.A. Dec. (1900) | l b | RN KM Rh | Comp. | Sep. P.A. | Tb No |
|------------------------------|------------------------|----------------|---------------------|-------|--------------|----------|
| RV Aqr | 21 00.7 -00 36 | 49.6 -29.6 | Ne C em | | | 8 |
| 209596 | 21 59.5 +45 05 | 94.7 -7.9 | N | | 9 | 6 |
| 209621 +20 5071 | 21 59.7 +20 34 | 78.6 -27.1 | R3 C2,2CH C2 | | | 8 |
| RZ Peg 209890 +32 4335 | 22 01.5 +33 02 | 87.6 -17.8 | Ne C9,1e C em | | 15 | 6 |
| MSB 73 +48 3827 | 22 40.7 +48 57 | 102.8 -8.4 | N | | 6 325 | 6 |
| SU And 225217 +42 4827 | 23 59.4 +43 00 | 114.0 -18.5 | N C6,4 C5 | | 15 | 5 |

TABLE 4. (Cont.)

| Name HD DM | R. A. Dec. (1900) | l b | RN KM Rh | Comp. | Sep. P. A. | Tb No |
|------------------|-------------------------|--------|----------------|----------|---------------|----------|
| R Cyg | 19 34.1 | 82.7 | | +49 3065 | 91 | 6 |
| 185456 | +49 58 | 13.8 | S4,9 | | 14 | |
| +49 3064 | | | | | | |
| S Cyg | 20 03.4 | 91.8 | | | 31 | 6 |
| | +57 42 | 13.7 | S5,2e | | | |
| +57 2134 | | | | | | |

TABLE 4. (Concl.)

real (Table 5), while the systems with strongly discordant data are considered to be not real (Table 7). Systems with few supportive (or mildly conflicting) data are considered in Table 6; these systems frequently lack some vital observation and cannot be decided one way or the other on the basis of the present observational data. Finally there are those systems (Table 8) for which so little data is available that it would be meaningless to claim their reality or otherwise.

The Tables 5 to 8 have, because of space limitations, been divided into three parts each (A, B and C). The photometry of parts A refers to the carbon stars (columns 2 - 4) and their companions (columns 5 - 7) for the years indicated [1969 = Sept./Oct. 1969 (Richer 1971); 1971 = Sept. 1971 from Cerro Tololo (by Dr. Richer, mostly unpublished); 1972 = Sept. 1972, author's data from Kitt Peak]. All the $H\beta$ photometry was done in 1972. The carbon star V magnitudes at maximum (col. B.2) are derived from the present photometry (p) unless otherwise indicated. The colour excesses (col. A.7) and absolute magnitudes (col. B.5) of the companions are based on the calibrations of Johnson (1966) and Blaauw (1963), respectively. Column C.4 gives the radial velocity of the galactic field at the distance of the companion, calculated from the Oort galactic rotation formula and corrected for the standard solar motion. Columns C.5 and C.6 give the dereddened colour index (cf. Appendix III) and the calculated brightest absolute visual magnitude of the carbon star. Finally, column C.7 gives the author's confidence level, on a scale from 0 to 10, in these derived absolute magni-

tudes. This is a combination of the confidence level of a physical connection between the component stars and the reliability of the companion's luminosity class.

The letters also appearing in some of the columns of parts B and C refer to the sources of the data. These are:

- A - A.A.V.S.O. magnitude estimates (Barnes 1974),
- E - Eggen (1972),
- F - Franz and White (1973),
- G - Gordon (1968),
- M - Mendoza and Johnson (1965),
- W - Wilson (1953),

- p - brightest V magnitude from part A of Table 5,
- a,b,c,d,e - Sanford's (1944) probable error of velocity:
a=±1, b=±2-3, c=±4-5, d=±6-8, e=±>10 (km/s).

- VI - Victoria - 78 A/mm spectra.
- KP - Kitt Peak - 128 A/mm spectra.
- CT - Cerro Tololo - 200 A/mm spectra - companions.
- 124 A/mm IR spectra - C-stars.

The carbon star radial velocities mentioned on the previous line have been measured on a system developed here and described in Appendix I. The VRI photometry is presented in Table 9, while a few additional double stars from Crull's (1972) list which have not been investigated at all are given in Table 10. These companions' magnitudes are guesses from the Palomar Sky Survey prints.

| Star | C-star | | | Companion | | |
|----------|-------------|-------------|-------------|-------------|-------------|---------|
| | V | V | V | V | V | H beta |
| | B-V | B-V | B-V | B-V | B-V | E (B-V) |
| | U-B 1969 | U-B 1971 | U-B 1972 | U-B 1971 | U-B 1972 | |
| UV Aur | | 9.59 | 9.39 | | 10.96 | 2.679 |
| % | | 1.42 | 1.67 : | | 0.21 | 0.20 |
| | | -0.26 | -0.13 | | -0.30 | |
| -26 2983 | 8.58 | 8.56 | | (12.8) | | -- |
| % | 3.47 | 3.26 | | | | 0.0 |
| | 1.00 | 1.35 | | | | |
| SZ Sgr | | 8.44 | | (11.8) | | -- |
| % | | 2.31 | | | | 0.21 |
| | | 1.72 | | | | |
| TU Tau | 8.42 | 8.29 | 8.45 | (11.7) | | -- |
| % | 2.95 | 2.72 | 2.73 | | | 0.44 |
| | -- | 1.36 | 1.49 | | | |
| W CMa | 6.77 | 6.55 | 7.48 | 8.76 | 8.82 | 2.642 |
| | 2.53 | 2.38 | 2.50 | 0.00 | -0.01 | 0.24 |
| | 4.68 | 4.24 | 4.32 | -0.69 | -0.69 | |
| SU And | 8.22 | 8.19 | | 12.77 | | -- |
| | 2.58 | 2.45 | | 0.38 | | 0.07 |
| | 4.13 | 4.85 | | 0.01 | | |
| SV Cyg | | | 8.55 | | 9.75 | -- |
| | | | 3.19 | | 1.21 | 0.11 |
| | | | 5.2 : | | 1.24 | |
| MSB 64 | | 9.60 | 9.51 | 11.81 | 11.85 | 2.818 |
| | | 3.79 | 3.46 | 0.73 | 0.72 | 0.58 |
| | | -- | -- | 0.49 | 0.48 | |
| HD 75021 | | 7.08 | | 7.58 | | -- |
| | | 1.94 | | 1.45 | | 0.35 |
| | | 3.17 | | 1.60 | | |
| MSB 31 | 9.0 | | | 10.8 | | |
| # | | | | 0.2 | | |
| V Hya | 6.7 | | | 11.58 | | |
| # | | | | | | |

% C-star photometry includes companion.

See text.

TABLE 5.A DATA ON OBSERVED SYSTEMS - PROBABLY REAL PHOTOMETRY

| Star | V(max) C-star | ΔV C-star | Spectrum Comp | Mv Comp | V max, C* -V (cp) | |
|----------|------------------|----------------------|------------------|------------|----------------------|-------|
| UV Aur | 7.4 F | 3.2 F | B9 V | KP | -0.1 | -3.5 |
| -26 2983 | 8.55 p | | A5 V | CT | +1.8 | -4.25 |
| SZ Sgr | 8.4 p | | A7 V | CT | +2.0 | -3.4 |
| TU Tau | 8.3 p | 0.2 p | A2 III: | CT KP | -0.6 # | -3.4 |
| W CMa | 6.55 p | 0.9 p | B2 V | KP CT | -2.5 | -2.2 |
| SU And | 8.2 p | | F0 V: | VI | +2.4 | -4.6 |
| SV Cyg | 8.4 A | 0.5 A | K1 III | KP | +0.8 | -1.4 |
| MSB 64 | 9.4 p | | A6 IV: | CT VI | +1.5 | -2.4 |
| HD 75021 | 7.1 p | 0.1 M | K1 III | G, E CT | +0.8 | -0.5 |
| MSB 31 | 9.0 | | A6 III-V: | G | +1.9 # | -1.8 |
| V Hya | 6.7 | | K0 III: | G | +0.8 | -4.3 |

See text.

TABLE 5.B DATA ON OBSERVED SYSTEMS - PROBABLY REAL
MAGNITUDES AND SPECTRA

| Star | Radial C-star | Velocity Comp | Gal | (B-V) o C-star | Mv C-star | Wt |
|----------|------------------|------------------|-----|-------------------|--------------|----|
| UV Aur | -10 a | -17 KP | +6 | 3.0 | -3.6 | 10 |
| -26 2983 | +23 e -6 CT | | +38 | 4.1 | -2.4 | 10 |
| SZ Sgr | +19 b | | -10 | 2.4 | -1.4 | 10 |
| TU Tau | -24 c -19 CT | | +15 | 2.8 | -3.9 | 8 |
| W CMa | +21 d | +19 G | +37 | 2.2 | -4.7 # | 7 |
| SU And | -6 b -11 CT | -6 VI | -20 | 2.4 | -2.2 | 9 |
| SV Cyg | -8 c | -15 KP | -14 | 3.1 | -0.5 | 6 |
| MSB 64 | -17 c +4 CT | +1 VI | -10 | 3.0 | -0.8 | 7 |
| HD 75021 | +11 a | # | +18 | 1.6 | +0.3 | 8 |
| MSB 31 | +4 | | | | +0.1 | |
| V Hya | -8 | | | | -3.5 | |

See text.

TABLE 5.C DATA ON OBSERVED SYSTEMS - PROBABLY REAL VELOCITIES AND DERIVED MAGNITUDES

| Star | C-star | | | Companion | | |
|----------|-------------|-------------|-------------|-------------|-------------|--------|
| | V | V | V | V | V | H beta |
| | B-V | B-V | B-V | B-V | B-V | E(B-V) |
| | U-B 1969 | U-B 1971 | U-B 1972 | U-B 1971 | U-B 1972 | |
| RY Mon | 8.10 | 7.91 | | | 12.29 | -- |
| | 4.15 | 4.03 | | | 0.49 | 0.11 |
| | -- | -- | | | 0.01 | |
| RZ Peg | | 9.25 | | 12.31 | | -- |
| | | 3.93 | | 0.57 | | 0.0 |
| | | 2.66 | | 0.13 | | |
| UV Aql | | 8.39 | | 12.05 | | -- |
| | | 3.55 | | 1.53 | | 0.88 |
| | | -- | | 1.50 | | |
| HD 34467 | 9.20 | | 9.20 | | 12.90 | 2.826 |
| | 2.75 | | 2.78 | | 0.53 | -- |
| | -- | | 4.28 | | 0.30 | |
| MSB 41 | | 9.61 | 9.52 | 10.72 | 10.81 | -- |
| | | 4.14 | 4.36 | 0.89 | 0.88 | 0.0 |
| | | -- | -- | 0.44 | 0.44 | |
| cp.2 | | | | 11.94 | 12.00 | -- |
| | | | | 1.08 | 1.10 | 0.0 |
| | | | | 0.80 | 0.86 | |
| X Sge | 8.36 | 8.53 | | 13.18 | | -- |
| | 3.29 | 3.35 | | 0.77 | | 0.41 |
| | -- | -- | | 0.16 | | |
| HD209596 | | | 10.18 | | 12.96 | 2.608 |
| | | | 2.40 | | 0.85 | -- |
| | | | 4.05 | | 0.39 | |
| MSB 73 | | | 10.29 | | 12.74 | 2.615 |
| | | | 2.30 | | 0.74 | 0.29 |
| | | | 3.44: | | 0.08 | |
| R Cyg | | | 6.80 | | 9.88 | 2.899 |
| | | | 1.91 | | 0.09 | 0.0 |
| | | | 2.18 | | 0.11 | |
| S Cyg | | | 11.24: | | 9.17 | -- |
| | | | 2.01 | | 1.00 | 0.0 |
| | | | 1.00 | | 0.80 | |

TABLE 6.A DATA ON OBSERVED SYSTEMS - POSSIBLY REAL PHOTOMETRY

| Star | V(max) C-star | | ΔV C-star | | Spectrum Comp | | Mv Comp | V max,C* -V(cp) |
|----------|------------------|---|----------------------|---|------------------|---------|--------------------|--------------------|
| RY Mon | 7.9 | p | 1.5 | A | F3 IV | CT | +2. | -4.4 |
| RZ Peg | 8.2 | A | 4.0 | A | F9 V | CT | +4.2 | -4.1 |
| UV Aql | 8.4 | p | | | G4 V: | CT | +1.8 # | -3.7 |
| HD 34467 | 9.2 | p | | | | | +2.1 | -3.7 |
| MSB 41 | 9.5 | p | | | G6 III | G | +0.4 | -1.3 |
| cp.2 | | | | | K | VI | | -2.5 |
| X Sge | 8.4 | p | | | F2 V | VI | +2.8 | -4.7 |
| HD209596 | 10.2 | p | | | F8 III-V | G VI | +1.0 OR +4.0 | -2.8 |
| MSB 73 | 10.3 | p | | | F6 III-V | G | +1.0 OR +3.5 | -2.4 |
| R Cyg | 6.8 | A | 7.1 | A | A5 V | KP | +1.8 | -3.1 |
| S Cyg | 9.5 | A | 5.7 | A | K0 III | KP | +0.8 | -0.2 |

See text.

TABLE 6.B DATA ON OBSERVED SYSTEMS - POSSIBLY REAL
MAGNITUDES AND SPECTRA

| Star | Radial C-star | Velocity Comp | Gal | (B-V) o C-star | Mv C-star | Wt |
|----------|------------------|------------------|-----|-------------------|--------------------|----|
| RY Mon | +2 c +4 CT | | +32 | 4.0 | -2.4 | |
| RZ Peg | -27 d -21 CT | | -15 | 3.9 | +0.1 | |
| UV Aql | +21 b | | -17 | 2.9 | -1.9 | 3 |
| HD 34467 | +15 d | | | 2.5: | -1.6 | 4 |
| MSB 41 | -11 e | +9 VI +21 G | -9 | 4.1 | -0.9 | 4 |
| cp.2 | | +1 VI | | | | |
| X Sge | +26 e +32 CT | +3: VI | -10 | 3.1 | -1.8 | 2 |
| HD209596 | -18 c | +1 VI | | | -1.8 or +1.2 | 3 |
| MSB 73 | -13 b | | | | -1.4 or +1.1 | |
| R Cyg | -30 W | -15 KP | +2 | 1.9 | -1.3 | 3 |
| S Cyg | | -23 KP | 0 | 2.0 | +0.6 | |

TABLE 6.C DATA ON OBSERVED SYSTEMS - POSSIBLY REAL VELOCITIES AND DERIVED MAGNITUDES

| Star | C-star | | | Companion | | |
|--------|--------|------|-------|-----------|-------|--------------------|
| | V | V | V | V | V | H. beta E (B-V) |
| | B-V | B-V | B-V | B-V | B-V | |
| | U-B | U-B | U-B | U-B | U-B | |
| 1969 | 1971 | 1972 | 1971 | 1972 | | |
| T Dra | | | 12.48 | | 10.99 | |
| | | | 5.6 : | | 1.16 | |
| | | | -- | | 1.15 | |
| U Cam | | | 7.55 | | 9.63 | 2.816 |
| | | | 4.29 | | 0.21 | 0.30 |
| | | | 4.49 | | -0.05 | |
| U Cyg | | | 10.08 | | 7.87 | -- |
| | | | 5.18 | | 0.80 | 0.0 |
| | | | -- | | 0.51 | |
| RS Cyg | 7.48 | | 8.32 | | 7.09 | 2.561 |
| | 2.86 | | 3.45 | | 0.50 | 0.75 |
| | 3.90 | | 3.61 | | -0.45 | |
| cp.2 | | | | | 9.24 | -- |
| | | | | | 1.93 | 0.31 |
| | | | | | 2.24 | |

TABLE 7.A DATA ON OBSERVED SYSTEMS - NOT REAL
PHOTOMETRY

| Star | V(max) C-star | ΔV C-star | Spectrum Comp | Mv Comp | V max,C* -V(cp) |
|--------|------------------|----------------------|------------------|------------|--------------------|
| T Dra | 9.6 A | 2.5 A | K2 III-IV KP | +1. | -1.2 |
| U Cam | 7.2 A | 0.6 A | B8 V KP | 0. | -2.4 |
| U Cyg | 7.1 A | 3.5 A | G2 III KP | +0.4 | -0.8 |
| RS Cyg | 7.2 A | 0.7 A | B0.5 Ib KP | -6.1 | +0.1 |
| cp.2 | | # | K7 II KP | -2 | -2.0 |

See text.

TABLE 7.B DATA ON OBSERVED SYSTEMS - NOT REAL
MAGNITUDES AND SPECTRA

| Star | Radial C-star | Velocity Comp | Gal | (B-V) o C-star | Mv C-star | Wt |
|--------|------------------|------------------|-----|-------------------|--------------|----|
| T Dra | -23 a | -84: KP | | | -0.2 | 0 |
| U Cam | -3 c | -35 KP | -10 | 4.1 | -2.4 | 0 |
| U Cyg | +13 a | -25 KP | -15 | 5.2 | -0.4 | 0 |
| RS Cyg | -50 a | -14 KP -2 W | -7 | | -6 | 0 |
| cp.2 | | -18 KP | -9 | | -4 | |

TABLE 7.C DATA ON OBSERVED SYSTEMS - NOT REAL
VELOCITIES AND DERIVED MAGNITUDES

| Star | C-star | | | Companion | | | H beta E (B-V) |
|----------|-------------|-------------|-------------|-------------|-------------|-------|-------------------|
| | V | V | V | V | V | | |
| | B-V | B-V | B-V | B-V | B-V | | |
| | U-B 1969 | U-B 1971 | U-B 1972 | U-B 1971 | U-B 1972 | | |
| X Cas | | | 11.01 | | 11.15 | 2.665 | |
| | | | 4.99 | | 0.53 | -- | |
| | | | -- | | 0.02 | | |
| HD 30710 | 9.43 | 9.17 | | 14.04 | | | |
| | 2.75 | 2.58 | | 1.39 | | | |
| | 4.27 | 3.44 | | 0.97 | | | |
| HK Lyr | | 7.97 | | 14.26 | | | |
| | | 3.24 | | 0.84 | | | |
| | | -- | | 0.01 | | | |
| S Sct | 6.70 | | 6.87 | | 12.2: | | |
| | 2.93 | | 2.91 | | 1.9: | | |
| | -- | | 5.48 | | 2.1: | | |
| RV Aqr | | 9.20 | | 14.92 | | | |
| | | 4.56 | | 1.22 | | | |
| | | -- | | 0.20 | | | |
| HD209621 | | 8.82 | | 13.10 | | | |
| | | 1.42 | | 1.43 | | | |
| | | 1.13 | | 1.23 | | | |

TABLE 8.A DATA ON OBSERVED SYSTEMS - INADEQUATE DATA
PHOTOMETRY

| Star | V(max) C-star | ΔV C-star | Spectrum Comp | Mv Comp | V max, C* -V (cp) |
|----------|------------------|----------------------|------------------|------------|----------------------|
| X Cas | 9.6 A | 2.3 A | | | -1.6 |
| HD 30710 | 9.2 p | | | | -4.8 |
| HK Lyr | 8.0 p | | | | -6.3 |
| S Sct | 6.7 p | 0.7 A | | | -5.5 |
| RV Aqr | 9.2 p | | | | -5.7 |
| HD209621 | 8.8 p | | G (?) | VI | -4.3 |

TABLE 8.B DATA ON OBSERVED SYSTEMS - INADEQUATE DATA
MAGNITUDES AND SPECTRA

| Star | Radial C-star | Velocity Comp | Gal | (B-V) o C-star | Mv C-star | Wt |
|----------|------------------|------------------|-----|-------------------|--------------|----|
| X Cas | -55 | a | | | | |
| HD 30710 | +38 | c | | | | |
| HK Lyr | -5 | a | | | | |
| S Sct | 0 | a | | | | |
| RV Aqr | -1 -4 | b CT | | | | |
| HD209621 | -381 | a | | | | |

TABLE 8.C DATA ON OBSERVED SYSTEMS - INADEQUATE DATA
VELOCITIES AND DERIVED MAGNITUDES

| Star | V | V-R | V-I | Year |
|----------|-------|------|------|------|
| UV Aur | 10.01 | 2.43 | 4.26 | 71 |
| -26 2983 | 8.72 | 2.15 | 3.56 | 71 |
| SZ Sgr | 8.74 | 1.99 | 3.45 | 74 |
| W CMa | 6.59 | 1.74 | 3.02 | 71 |
| | 6.65 | 1.78 | 3.20 | 74 |
| MSB 64 | 9.40 | 2.41 | 4.05 | 74 |
| HD 75021 | 7.26 | 1.51 | 2.88 | 71 |
| V Hya | 8.36 | 3.03 | 4.69 | 74 |
| RY Mon | 8.26 | 2.47 | 4.06 | 71 |
| RZ Peg | 8.42 | 1.92 | 3.34 | 74 |
| UV Aql | 9.05 | 2.46 | 3.93 | 74 |
| X Sge | 8.58 | 2.20 | 3.59 | 74 |

TABLE 9. VRI PHOTOMETRY

| Star | RA Dec 1900 | Spec | V | Sep (") | V cp | |
|----------|-------------------|-------|-----|------------|---------|-----------|
| V Cnc | 08 16.0 +17 36 | S2,9e | 7.1 | 10 | >13 | |
| HD 76115 | 08 49.1 +75 50 | R0 | 8.0 | 31 | 14 | |
| RT Cap | 20 11.3 -21 38 | C5,3 | 8.6 | 26 | 15 | ADS 13616 |

TABLE 10. SOME UNINVESTIGATED DOUBLE STARS

Discussion of Individual Systems

UV Aur The spectral type of the 3.4" distant companion is B9 V, in excellent agreement with Gordon's (1968) type of B8.5 V; the photometric data may, however, have been contaminated by the brighter carbon star. Franz and White (1973) have measured $V = 10.92$ and $B-V = 0.12$ for the companion; this agrees well with the present V value but is bluer by 0.09 mag. The Q index [$Q = (U-B) - 0.72(B-V)$] corresponding to the B9 spectral type points to the star being above the main sequence, while the $H\beta$ value indicates an absolute magnitude of -1.5 (Stromgren 1966). As these data could also have been contaminated an absolute magnitude of -0.1 has been adopted; this corresponds to a point barely above the main sequence at B9. Recently Garrison (1977) has expressed the opinion that this star is brighter than luminosity class V, possibly as bright as class III. This agrees quite well with the assigned absolute magnitude. A normal star of this spectral type is expected to have a mass of 3.5 to 4 M_{\odot} (Allen 1973), and Iben (1967) indicates that such a star would be $\sim 1 - 1.5 \times 10^8$ years old. Since the post main sequence evolution of the companion carbon star is much faster than this we can assign it a main sequence mass of $\geq 4 M_{\odot}$; as it may subsequently have suffered mass loss, however, this is only an upper limit to its present mass. Since the velocities agree reasonably well and are significantly different from the expected galactic field velocity there is no reason to suppose that these stars do not form a physical pair. The carbon star absolute magnitude is

variable between -3.6 and -0.4. The period of this variability is approximately 390 days.

-26° 2983

SZ Sgr

These stars with composite spectra have been discussed by Richer (1972), and no further observations have been obtained.

He derives absolute magnitudes of -2.4 and -1.4, respectively, under the assumptions that the U magnitudes are influenced only by the early-type companion and that the reddening can be obtained from the nearby field stars. As there is no reason to doubt the validity of these assumptions, these magnitudes will be adopted.

TU Tau

This system was also discussed by Richer, who derived a carbon star absolute magnitude of -3.9 based on the same assumptions as above and using a spectral type for the companion of A2 III. One additional spectrum has been obtained of this star. Unfortunately it is rather weak and does not permit either verification or disproof of Richer's assigned luminosity class. The only features definitely present between H-gamma and H-delta are 4315 (Fe I), G-band (CH), 4260 (?) and 4226 (Ca I); all attributable to the carbon star. Even if the luminosity sensitive blend 4173-8 is weakly present it would be more difficult to detect on the weak plate because of the higher dispersion used (128 vs 200 A/mm). It is interesting to note, however, that SZ Sgr, wherein the carbon star is relatively brighter in the blue region than TU Tau, also shows (in Richer's Fig. 1) a

line at the same position, indicating that this feature may be from the carbon star spectrum. If this is the case the companion's absolute magnitude must be decreased by 1.8 mag to +1.2, corresponding to a main sequence star. Because of the small separation (zero) there is little room for doubt as to the physical reality of this system, even though corroborating radial velocity data is lacking. Thus the absolute magnitude of TU Tau is either -3.9 or -2.1.

W Cma Despite the large separation of the two stars (158") there are several reasons for supposing their physical proximity. Primary is the observation that W Cma illuminates a reflection nebula which is probably part of the Cma OB1/Cma R1 complex (Herbst, Racine and Richer 1977). The spectral type of the companion is B2 V, given by several spectra and confirmed by the Q-value (-0.69) as well as the luminosity indicated by the $H\beta$ index, and not B5 as given by Gordon (1968). The galactic field radial velocity at the distance of this star is +37 km/s, significantly different from both the B-star itself (+19 km/s) and the C-star (+21 km/s) which agree quite well. Since the solar motion component in this direction contributes +18 km/s to these velocities it is clear that the B-star motion differs greatly from the galactic field. Furthermore the declination components of the proper motions agree very well (+0.023" and +0.019" \pm 0.020" (st. devn)) although the right ascension components are somewhat discordant (-0.036" and +0.017" \pm 0.027") (SAO Catalog 1966). It should be noted, however, that the C-star velocity (though of

poor quality) does not differ greatly from the LSR velocity and hence is not inconsistent with a much fainter absolute magnitude.

SU And The F0 spectral type is based on two medium well to weakly exposed spectra. As these make it rather difficult to determine the luminosity, class V has been assumed because of the width of the Balmer lines. Because of the excellent agreement of the velocities this system seems to be on a solid basis.

SV Cyg The radial velocity data for these stars can't be used to verify the reality of this system as both of the velocities agree well with the galactic field velocity and the system is in a direction ($l=83^\circ$) where the velocity is rather insensitive to distance. Since the derived C-star absolute magnitude is in the right ballpark, however, and there is no contradictory data this system cannot be ruled out as real.

MSB 64 The luminosity classification of the companion is based on the width of the Balmer lines; if the star is on the main sequence the absolute magnitude will be fainter by 0.4 magnitudes. The Victoria radial velocity agrees well with the infrared C-star velocity but not with Sanford's "c"-quality (± 5 km/s according to Sanford) blue velocity. Better radial velocities are obviously needed to settle this question.

HD 75021 Most of the data on these stars have
 MSB 31 been taken from Gordon (1968). New pho-
 tometry of HD 75021 has yielded improved
 colours, and the spectral type is a compromise of Gordon, Eggen
 (1972) and a low dispersion spectrum. Proper motion data for
 this double agrees in declination ($-0.010''$ and $-0.008'' \pm 0.013$
 (st. devn)) but not in right ascension ($-0.028''$ and $+0.002''$
 ± 0.013) (SAO 1966). Gordon says the radial velocities agree to
 within the measurement errors but the galactic velocity gradient
 in this direction is very small and hence this datum does not
 carry much positive weight. The magnitude data for the compa-
 nion to MSB 31 is based on a photographic magnitude by Sanford
 (1940) of 11.0 and Gordon's spectral type. Although she cannot
 distinguish between luminosity classes III and V, the main
 sequence class has been assumed in Table 5. The small
 separation of this pair lends credibility to the reality of this
 system.

V Hya VRI photometry of this double gives
 (V-R, V-I) colours for the companion of
 (0.81, 1.56), consistent with a spectral type of K1 or K2 III,
 or K0 III:, the spectral type given by Gordon (1968). If this
 system is real, V Hya is both the reddest and intrinsically
 brightest star investigated here.

RY Mon This star lacks sufficient data to be either accepted or rejected as a real system. The photometry is consistent with an unreddened F6 V star, considerably later than is indicated by the available spectrum, which has been given the greater weight. Should this system be real the photometric spectral type would set a faint limit to the C-star absolute magnitude of -0.9.

RZ Peg This star also lacks data. Here, however, at least the spectral type is not open to question as both the photometry and the spectrum agree. A radial velocity for the companion would be most interesting here as the suggested C-star absolute magnitude would be among the faintest known for N-stars if the system is real. It is interesting to note that the carbon star shows emission in the infrared Ca II triplet (Richer 1971).

UV Aql This double lacks both a radial velocity and reliable spectral classification. The spectral type is based on a rather weak spectrum; hence the uncertain luminosity class. The photometry is consistent with a K2 giant and supergiant but only marginally acceptable as a main sequence star and then as a late K dwarf. This double is best left until more data is available.

HD 34467 This double is severely lacking in data. The UBV photometry is consistent with spectral types B9 V, A8 V and gF, while the $H\beta$ value is compatible with the B9 V and A8 V types only. If the A8 V type is

assumed (this requires the least reddening and sets the faint limit to the C-star) the carbon star would have an absolute magnitude of -1.6 if the system is real.

MSB 41 The C-star velocity does not agree well with either of the companions but its poor quality makes this of little significance.

X Sge The photometry is indicative of a slightly later spectral type for this companion than is given by the spectrum. The weakness of the Ca I 4226 line and the G-band is strongly supportive of the earlier type however; perhaps the star is metal poor. Sanford's C-star velocity is confirmed by the presently measured infrared velocity, while the companion's velocity seems to be significantly different although this is based on only three wide lines and thus is of low weight. This system does not seem to be real.

HD 209596 The C-star absolute magnitudes for these
MSB 73 doubles are based on Gordon's (1968) spectral types for the companions and the present improved photometry. The velocity for HD 209596's companion is based on but four broad lines on a weak plate; these do agree fairly well however.

S Cyg This star is a member of the triple star ADS 13385. The K-star is the A-component while the S-star is a binary with 0.6" separation (BC). No data is available for the C-component because of its close proximity and the faintness of the system (BC) as a whole.

T Dra The large velocity differences between
 U Cam the carbon stars and the suspected com-
 U Cyg panions rule out these doubles as real
 RS Cyg systems. According to the A.A.V.S.O.
 data the visual magnitude variation of
 RS Cyg has been steadily decreasing from at least the early
 60's. The amplitude has changed from about 1.4 mag to the
 present 0.5 magnitude.

S Sct This star is in a very rich region of
 the Milky Way and has several fairly
 close companions. The photometry reported here refers to the
 brightest of these. Because of the crowded field this star is
 not worth investigating further.

Discussion

The relation between the absolute visual magnitudes of the C stars and their companions is shown in Figure 2. The faint limits shown in this figure are at least partially affected by observational selection. Nonetheless, there seems to be some indication of a trend in the sense that the early A and B type companions are associated with the brightest C stars, and the higher weighted late-type giants are associated with fainter C stars. Use of the bolometric absolute magnitudes (see below), instead of the visual magnitudes, still shows this trend (Figure 3): carbon stars with B type companions tend to be more luminous than those with A and K type companions. Since the early-type stars are expected to be younger (on the average) and their evolved companions therefore more massive (initially at least) this may be taken as a mild indication for a mass - luminosity relation for carbon stars.

If the stars for which only Gordon's (1968) absolute magnitudes are available as well as the R stars are deleted, and if we apply the weights indicated in the last column of Tables 5 and 6 the group properties can be derived. The average absolute visual magnitude of the remaining 13 N stars is -2.3 ± 1.1 (st. devn). Since the average intrinsic (B-V) colour of these stars is +3.0 (cf. the "Statistical Studies" section), and there is nothing obviously peculiar about them other than having companions, they can be taken to be a typical sample of N stars.

Since most of the energy from carbon stars is radiated in

the infrared, their visual absolute magnitudes are not as physically meaningful as their bolometric absolute magnitudes. To properly calculate the bolometric corrections, however, one needs photometric information extending far into the infrared, and such data exist for but a few dozen stars (Mendoza and Johnson 1965). Fortunately, their data show that there exists a good correlation between the calculated bolometric corrections and the V-R colour index for both R and N stars. These relations are shown in Figure 4. Since one would expect the stars in Figure 4 to be reddened by different amounts, it is surprising at first that the correlation is as tight as is indicated. The effect of interstellar reddening is, however, not only to make the observed colours redder, but also to increase the ratio of the nonvisual to visual flux (since most of the flux is in the infrared), thus causing an overestimate of the bolometric corrections based on the reddened colours. Hence reddening will cause a star to move more or less along the lines of Figure 4, rather than across them, retaining the tightness of the relation.

To derive bolometric corrections the observed (V-R) colours, where available (Table 9; Mendoza and Johnson 1965) were corrected for the reddening shown by the companions according to $E(V-R) = 0.75 E(B-V)$. The bolometric corrections were then read off from Figure 4. These are expected, in most cases, to be good to a few tenths of a magnitude. The resulting bolometric absolute magnitudes have been plotted in Figure 5 versus the deduced intrinsic (V-R) colours. For reference the

normal giant and supergiant branches from M0 to M6 are also included (Blaauw 1963; Johnson 1966). It is thus apparent that the late-type carbon stars are not confined to a narrow luminosity range, but in fact populate a wide band (about 4 magnitudes wide) corresponding to the region between the normal giant branch and the supergiants.

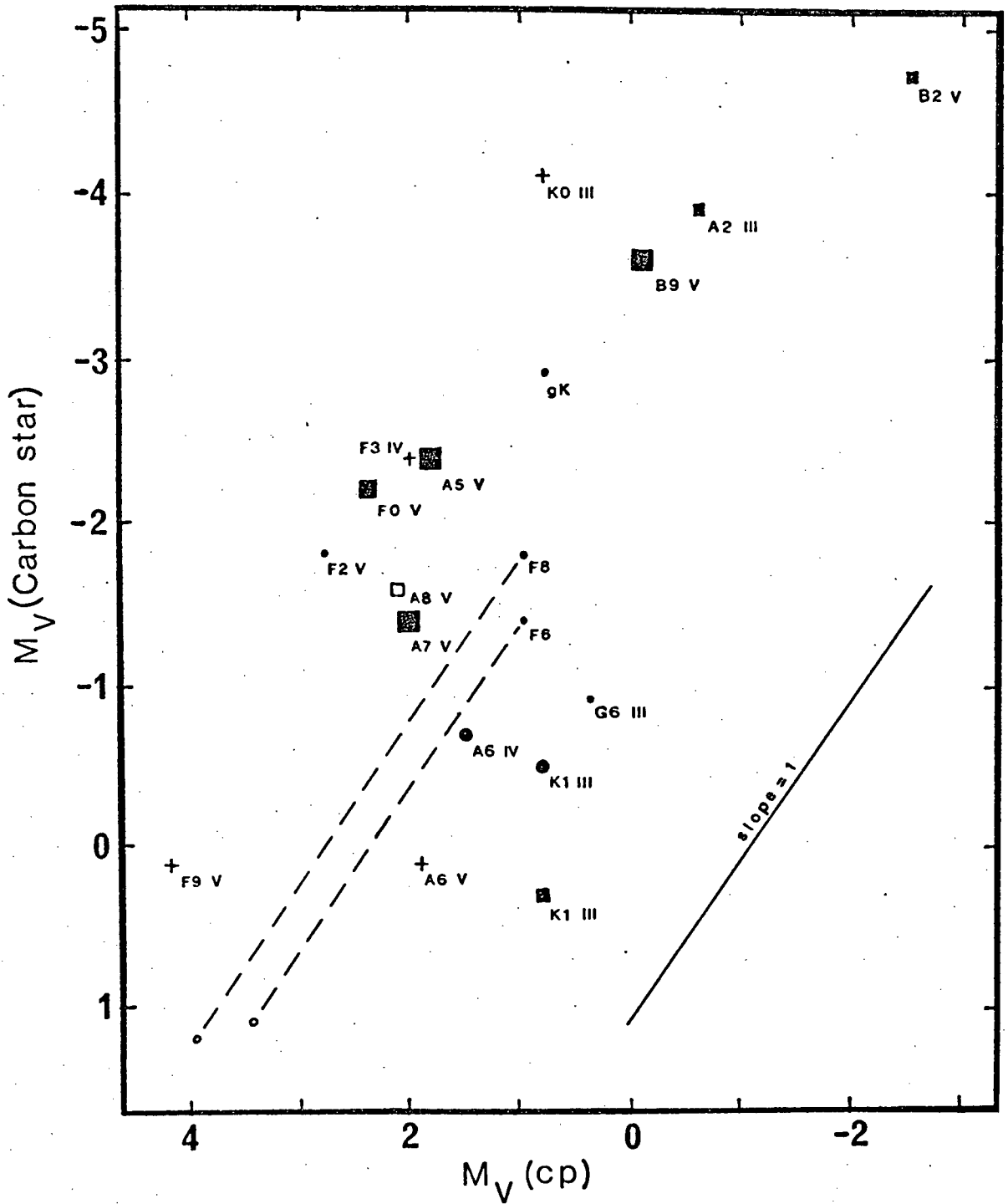


Figure 2. M_V (Carbon Star) vs M_V (Companion)

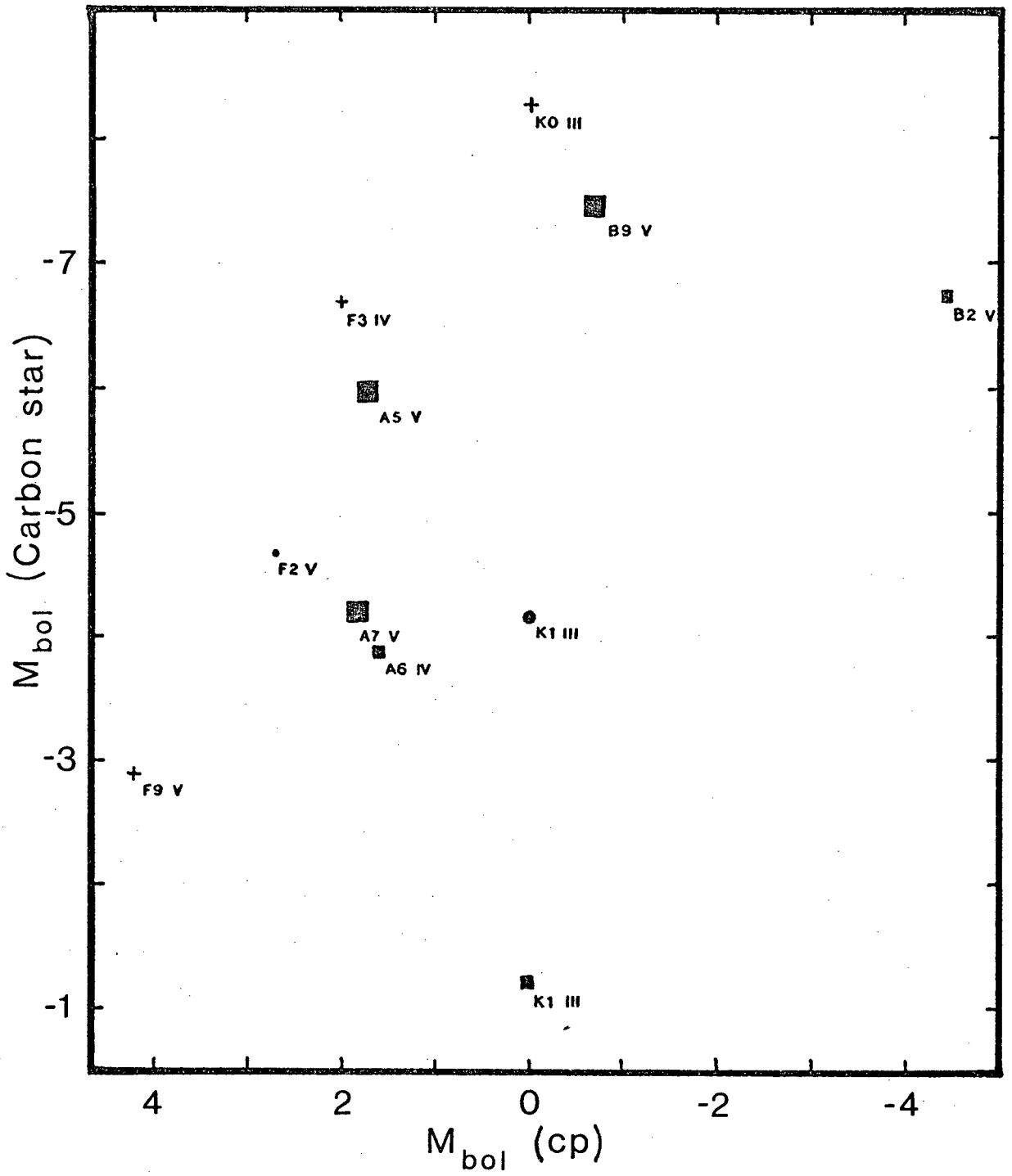


Figure 3. M_{bol} (Carbon star) vs M_{bol} (Companion)

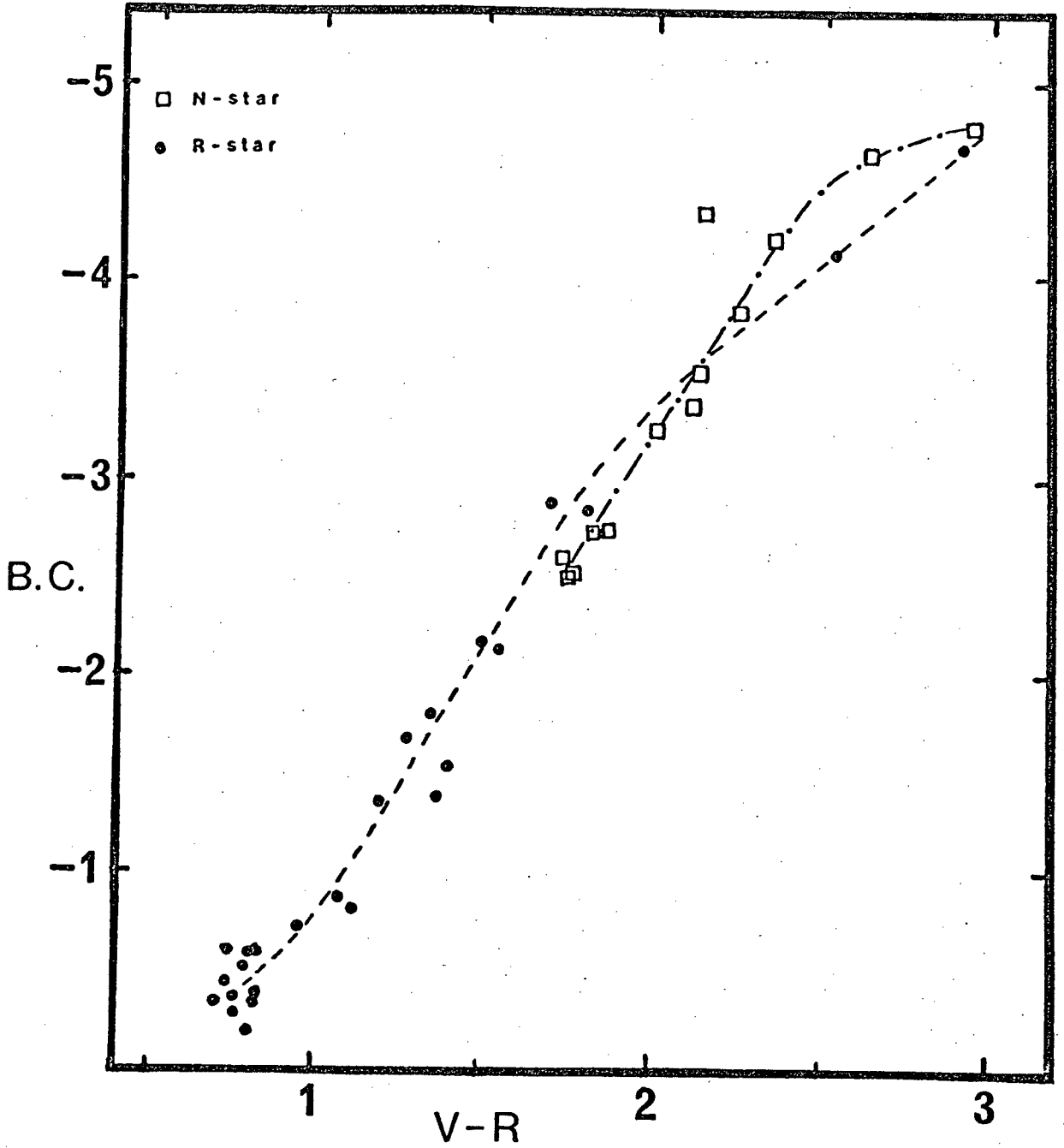


Figure 4. Bolometric Correction vs V-R

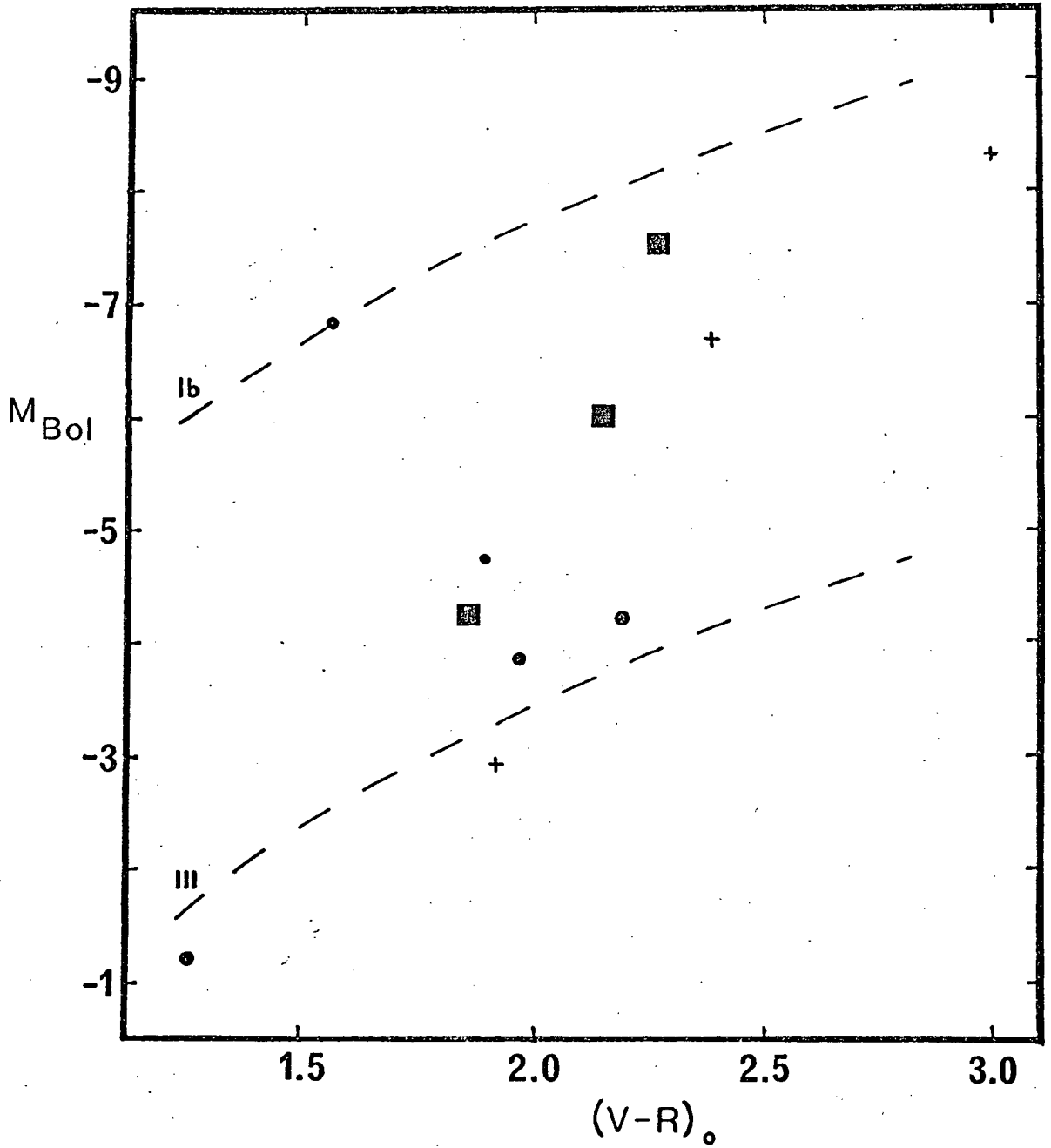


Figure 5. $M(\text{bol})$ vs $(V-R)_0$.

Part II.

CARBON ISOTOPE ABUNDANCE RATIOS

Carbon exists in nature in only two stable isotopic forms (viz. ^{12}C & ^{13}C). The terrestrial $^{12}\text{C}/^{13}\text{C}$ ratio is approximately 90, while reported results for carbon stars range from a low of 2 to highs of greater than 100. For normal late-type stars (mostly K giants) ratios have recently been reported primarily in the 10 to 30 range (Tomkin, Luck and Lambert 1976; Dearborn and Eggleton 1976).

A knowledge of the $^{12}\text{C}/^{13}\text{C}$ ratios in carbon stars is important because of the constraints it places on the models of C stars, which should tell us something about their evolutionary state, nucleosynthesis reactions (to produce the isotopes) and structure (convection zones to transport them to the surface).

In carbon stars we can observe carbon primarily in three forms: the molecules CO, CN and C_2 ; the observational problems involved in determining the abundance ratios differ depending on which molecule and spectral region is to be studied. The CO vibration-rotation bands are all in the infrared (from 5μ to 1.6μ for $\Delta v = 1$ and 3, resp.) and thus are not accessible using conventional methods; the CN and C_2 bands in the blue and visual regions are all very crowded, resulting in great problems with line blending. The Red system of CN in the near infrared avoids both these problems: the spectral region is readily available using both photographic N-type emulsions and the newer solid state detectors, and the rotational band structure is suffi-

ciently open that individual rotational lines are frequently resolved, even at moderate dispersions.

Past values of the $^{12}\text{C}/^{13}\text{C}$ ratio in carbon stars have been derived using three main techniques. Most quoted values have been obtained using some variant of the standard curve-of-growth method. Line blending is often severe, resulting in relatively few usable lines; in the extreme, Wyller (1966) based his results on only 2 lines. Even more serious is the question of locating the continuum, in a strong-CN star like γ CVn the spectrum hardly ever approaches anything that can be called a continuum level. In their analysis of UU Aur Querci and Querci (1970) determined their continuum through an iterative procedure based on the temperature and lines that should be on the flat part of the curve of growth. The iso-intensity method of Fujita (1970) avoids the problem of the continuum by using the central depths of the lines and a pseudo-curve-of-growth analysis. This method is, however, very sensitive to the excitation temperature adopted. The third method (Climenthaga 1960) uses calculated synthetic spectra which are then matched to the observed spectrum. His synthetic spectra were calculated using the empirical Minnaert formula and the matching was done visually.

The present investigation is a greatly improved version of Climenthaga's basic approach. Since it is well known that carbon stars are at least giants and probably somewhat brighter [see Part I of this thesis] their atmospheres must be quite extended,

and one would not expect methods which are based on a uniform slab model of that atmosphere to necessarily produce reliable results. Thus I decided to calculate synthetic spectra by directly integrating the flux through an appropriate model atmosphere. It would also be desirable to have an analysis technique that was independent of the prejudices of the observer. Ideally such a technique should make use of the entire information content of the spectrum, rather than just certain selected pieces, it should also be relatively insensitive to those spectral features that one is not interested in (e.g. telluric lines). For spectra such as these of molecular bands in carbon stars, where the vast majority of spectral features are in fact due to the molecule(s) being studied, I believe that the method based on the coherence spectrum (to be described later) satisfies the above conditions. It also has the further advantage of being insensitive to the assumed continuum level.

The only model atmospheres appropriate to the cool carbon stars investigated here that I have been able to obtain are those of Johnson (1974). These were calculated on a loose grid of parameters to explore the effects of temperature, surface gravity, composition and opacities. The model parameters are outlined in Table 11; most of the models are arranged in sequences with one or two of the parameters variable. The number of possibly useful models is 17. The models were calculated under the usual assumptions of a plane parallel atmosphere, LTE and using straight mean opacities. In spite of

| Parameter | Range | principally |
|-------------|----------------------|-------------|
| C/O | [1, 50] | 2, 5 |
| T(eff) (°K) | [2000, 3500] | 3500 |
| C/H | [0.1, 100] (C/H) ● | |
| log g | [0, +4] | 0 (giants) |
| N/H | [1, 120] (N/H) ● | |

TABLE 11. MODEL ATMOSPHERE PARAMETERS

these limitations they are still better than the uniform slab model.

This part of the thesis opens with a brief description of the observational material used here. This is followed by a description of how to calculate synthetic stellar spectra, both a theoretical summary and the practical details appropriate to molecular band spectra. The analysis technique is then presented, along with some comments on its advantages and a few tests illustrating its applicability. Next the results of the carbon isotope ratio analysis are shown, including remarks on the microturbulence and carbon content of the carbon stars, as well as a search for the ^{14}C and ^{15}N isotopes. A resume of the pros and cons of the analysis technique concludes this part.

The Observational Material

The basic observational material for this part of the study consists of near infrared photographic spectra of five carbon stars (Table 12). The spectra were obtained by Dr. H. B. Richer at the 122-cm (48 inch) telescope of the Dominion Astrophysical Observatory in Victoria during the period Nov. 21, 1970 to Dec. 18, 1970. The plates are at a dispersion of 13 Å/mm on IN hypersensitized emulsions covering the wavelength region 7500 - 8800 Å.

The region of the spectra from 7800 Å to 8300 Å was digitized with the department's automated Joyce-Loebl Microdensitometer and reduced to an intensity versus wavelength array using computer programs developed by H. Fast (1973), as follows. Digitizing scans were made along the stellar spectrum as well as across the calibration strips and the spectrum itself at several different wavelengths. Grain noise was then reduced by the application of a digital filter to remove spatial frequencies greater than $1/3$ of the Nyquist frequency. Next an equal-wavelength-interval array of $\log(\text{intensity})$ was generated; the wavelength scale was defined using "unblended" stellar (CN) lines of known wavelength while the intensity scale was determined from interpolation between the several calibration curves. Note that the photographic density of each spectrum point was first corrected to compensate for the non-uniform exposure (streaks) caused by the image slicer of the spectrograph. Finally the highest points were selected as representing the continuum and

| Star | Plate # | Date |
|--------|---------|-------------|
| UU Aur | 6485 | Nov. 21, 70 |
| X Cnc | 6486 | Nov. 21, 70 |
| Y CVn | 6487 | Nov. 21, 70 |
| 19 Psc | 6542 | Dec. 18, 70 |
| Z Psc | 6543 | Dec. 18, 70 |

TABLE 12. HIGH DISPERSION CARBON STAR SPECTRA

the array transformed to a normalized intensity array. Indicative of the extremely heavy line blanketing is the fact that typically there were no more than a half dozen such "continuum" peaks throughout the entire 400 Å region of interest. This relatively poorly determined continuum level has no effect on the subsequent analysis however; this will be dealt with more fully in a later section.

The one additional parameter to be derived from the spectra was the instrumental broadening; it was assumed that the instrumental profile was a Gaussian with a half-width to be determined. To this end the Argon comparison arc lines of a sample plate were digitized and converted to intensity. Not all the lines could be used, however, as the arc lines were more heavily exposed near the inside edge and were frequently saturated there. This resulted in an under-estimation of the true line strength and thus an overestimation of the width at the deduced half-intensity level. Using nineteen lines which were definitely not saturated resulted in an average half-width of 0.56 Å \pm 0.09 (st. devn).

SYNTHETIC SPECTRA - THEORY

Following Mihalas (1970) the flux radiating from a stellar atmosphere is given by

$$F_{\nu} = 2 \int_0^{\infty} S_{\nu}(\tau_{\nu}) E_2(\tau_{\nu}) d\tau_{\nu} \quad (4)$$

where F_{ν} is the flux per unit frequency interval, E_2 is the second exponential integral defined by

$$E_2(x) = \int_1^{\infty} \exp(-xt)/t^2 dt \quad (5)$$

and S_{ν} is the source function, here, for pure absorption lines, approximated by the Planck black body function

$$B_{\nu}(T) = [2h\nu^3/c^2] [1/(\exp(h\nu/kT) - 1)] \quad (6)$$

to conform to the LTE assumption of the model atmospheres.

The optical depth scale is given by

$$\tau_{\nu} = \int_0^{\tau_{\nu}} [k(\text{cont}) + l_{\nu}]/k(\text{std}) d\tau(\text{std}) \quad (7)$$

where $\tau(\text{std})$ is the standard optical depth as given by the model atmosphere, $k(\text{std})$ is the model opacity at a standard wavelength, $k(\text{cont})$ is the continuous opacity and l_{ν} is the opacity contribution of the lines

$$l_{\nu} = \sum_{sp} \alpha_{\nu}(sp) N(sp) \quad (8)$$

for all species (sp). N is the number density of the appropriate species and α_{ν} is the absorption cross-section of one atom (molecule) of that species at frequency ν under the

conditions at that point in the atmosphere.

The absorption cross-section per atom (molecule) at frequency ν is

$$\alpha_{\nu} = (\pi e^2 / mc) f \phi_{\nu} [n(i) / n(T)] \quad (9)$$

where f is the oscillator strength of the appropriate transition, ϕ_{ν} is the absorption line profile normalized to unit area, and $n(i) / n(T)$ is the fraction of the total number of atoms (molecules) that are in the lower state of the transition. For a Gaussian line profile

$$\phi_{\nu} = (1 / \sqrt{\pi} \Delta \nu_D) \exp\{-[(\nu - \nu_0) / \Delta \nu_D]^2\} \quad (10)$$

where $\Delta \nu_D$ is the line width and ν_0 is the central frequency. The line width $\Delta \nu_D$ is the Doppler width given by

$$\Delta \nu_D = \xi_0 \nu_{ij} / c, \quad \xi_0 = \{2kT / M + \xi_t^2\}^{1/2} \quad (11)$$

For a single rotational line of a diatomic molecule the oscillator strength is given by (Carbon 1973)

$$f_{ij} = f_{00} \frac{\tilde{\nu}_{ij}}{\tilde{\nu}_{00}} \frac{q_{v'v''}}{q_{00}} \frac{\sum |R_e(\bar{r}_{v'v''})|^2}{\sum |R_e(\bar{r}_{00})|^2} \frac{(2S+1)(2-\delta_{0,\Lambda''})}{(2J''+1)} S(HL) \quad (12)$$

where: f_{00} = (0,0)-band oscillator strength,

$\tilde{\nu}_{ij}, \tilde{\nu}_{00}$ = wavenumbers of transition (i, j) and the (0,0) band origin,

$q_{v'v''}$ = Franck-Condon factor for the (v', v'')-band,

$\sum |R_e(\bar{r}_{v'v''})|^2$ = sum of squares of the electronic transition moments,

$(2S+1)$ = multiplicity of the electronic transition,
 $(2-\delta_{0,\lambda''})$ = 1 for Σ states, = 2 for any other lower state,
 $(2J''+1)$ = rotational degeneracy of the lower state,
 $S(HL)$ = Honl-London factor, normalized to

$$\sum_{J'} S(HL) (J'' \rightarrow J') = 2J''+1. \quad (13)$$

The Honl-London factor is a measure of the line strength. Extensive formulae for transitions between various types of electronic states are given by Schadee (1964). It should be noted, however, that his formulae for ${}^2\Pi - {}^2\Sigma$ transitions (the CN red system) must be multiplied by 2 to satisfy the above normalization criterion. (N.B. In the notation used here a single prime refers to the upper level of a transition, a double prime refers to the lower level.)

The fractional number of molecules in the lower state of transition (ij) is given by (Tatum 1967)

$$\frac{n(i)}{n(T)} = \frac{2\phi (2J''+1) \exp\{-[hc/kT][T(el)+G(v'')+F(J'')] \}}{Q(el) Q(vib) Q(rot)} \quad (14)$$

This equation applies to Hund's coupling case (b) which is appropriate here since both the CN and C_2 transitions of interest come from a lower Σ -state. In this equation $\phi = 1/2$ for a heteronuclear molecule, whereas for a homonuclear molecule ϕ is a function of the nuclear spin; the energy of the lower level $[T(el)+G(v'')+F(J'')]$ is separated into three terms representing the electronic term value, the vibrational energy and the rotational energy; the denominator $[Q(T)]$ is the total

internal partition function, again separated into electronic, vibrational and rotational contributions. These are given by

$$Q(\text{el}) = \sum_{\text{all states}} g(\text{el}) \exp\{-(hc/kT)T(\text{el})\} \quad (15)$$

where $g(\text{el})$ is the degeneracy of the electronic state

$$g(\text{el}) = (2-\delta_{0,\Lambda}) (2S+1), \quad (16)$$

$$Q(\text{vib}) = \sum_{v=0}^{v_{\max}} \exp\{-(hc/kT)G(v)\}, \quad (17)$$

and

$$Q(\text{rot}) = kT/hcB(v''). \quad (18)$$

Collecting these terms and explicitly putting in a Gaussian line profile we arrive at the final expression

$$\alpha_{\nu} = \frac{\sqrt{\pi} e^2}{mc} \sum_{\text{all lines}} 2\phi f_{\infty} \frac{\tilde{\nu}_{ij}}{\tilde{\nu}_{00}} \frac{q_{v'v''}}{q_{00}} \frac{\sum |R_{v'v''}|^2}{\sum |R_{00}|^2} (2S+1) (2-\delta_{0,\Lambda}) S(\text{HL}) \cdot \quad (19)$$

$$\cdot \frac{\exp\{-(hc/kT)\chi_i\}}{Q(T) \Delta\nu_D} \cdot \exp[-(\nu-\nu_{ij})^2/\Delta\nu_D^2]$$

where the energy of the lower level has now been denoted by χ_i . The first group of terms is a constant for each individual line, the second group contains terms depending on the atmospheric level (temperature) whereas the last term depends primarily on the frequency.

SYNTHETIC SPECTRA - PRACTICEMolecular Parameters

The relevant molecular data for CN and C₂ have been summarized in Tables 13 and 14. The energy levels (χ_i) and frequencies (ν_{ij}) of the individual rotational lines have been computed for CN from the formulae of Fay, Marenin and van Citters (1971) and for C₂ from Marenin and Johnson (1970). For the bands used here the errors in these calculations are usually less than 0.1 cm⁻¹ for ¹²C¹⁴N and ¹²C¹²C and 0.2 cm⁻¹ for ¹³C¹⁴N up to N values of at least 60, the maximum used here; these equal 0.06 and 0.13 Å. Thus one would expect the errors for the other isotopic bands to be less than 0.25 Å, since the atomic masses are approximately equally accurate. To ensure that the wavelengths of the lines are as accurate as possible the computed wavelengths have been replaced by actual observed wavelengths wherever these are available. Observed wavelengths for the lines from the (2,0), (3,1), (7,4) and (8,5) bands of the Red system of ¹²C¹⁴N have been taken from the extensive tabulation of Davis and Phillips (1963); a few of the branches (P₁₂ and R₂₁ in particular) have been extrapolated somewhat past the tabular cutoffs, with the aid of the computed wavelengths, as the observed cutoffs were caused by the relatively cooler source temperatures they used. Observed wavelengths for the corresponding bands of ¹³C¹⁴N are from Wyller (1966), and for the Phillips system of ¹²C¹²C from Ballik and Ramsay (1963). In a very few instances missing rotational lines have been interpolated; in general missing lines have not been added, since it

is assumed that the fact that they are missing indicates that no line was in fact observed at the expected wavelength, probably caused by perturbations of the energy levels.

Note that the above lines are the only lines included in the synthetic spectra. This specifically excludes all atomic lines, lines of $^{12}\text{C}^{13}\text{C}$, and all telluric lines, even though the latter may be relatively numerous in some portions of the spectra.

The partition functions were calculated, as a function of temperature, for CN and C_2 using the energy levels in Tables 15A and 15B, and the above calculated vibrational $[G(v)]$ and rotational $[B(v'')]$ parameters of the lower level for each molecule.

Schematic layouts of the rotational structure of the appropriate states of CN and C_2 are presented in Figures 6 and 7, with the transitions giving rise to the first few rotational lines of each branch labelled. Note that the drawn fine structure separations of the levels are not to scale. The standard nomenclature is used to label the levels according to their parity (+, -), symmetry (s, a), rotational quantum number (N) and angular momentum (J) (for the C_2 singlet states $J=N$). The various branches are known as P, Q or R branches depending on whether $\Delta J = -1, 0$ or $+1$, respectively, and the individual rotational lines are labelled by the N value of their lower levels. The CN bands consist of 6 primary branches ($\Delta N = \Delta J$) and 6 satellite branches ($\Delta N \neq \Delta J$) with 4 of the satellite branches being internal (overlapping primary branches) and 2 (P_{12} and

R_{12}) external; the intensities of most of the satellite lines are much less than the primary lines. Because $^{12}\text{C}^{12}\text{C}$ is a homonuclear molecule with zero nuclear spin the anti-symmetric levels are forbidden, hence transitions can arise only from alternate levels.

| | |
|--|--------------------------|
| $f_{00} = 2.19 \times 10^{-3}$ | Arnold and Nicholls 1972 |
| $\tilde{\nu}_{00} = 9117.37 \text{ cm}^{-1}$ | |
| $q_{00} = 0.50015$ | Arnold and Nicholls 1972 |
| $q_{20} = 0.12685$ | " |
| $q_{31} = 0.19400$ | " |
| $q_{74} = 0.12095$ | " |
| $q_{85} = 0.08440$ | " |
| $\phi = 1/2$ for all levels | Tatum 1967 |
| $\sum R_e ^2 = \text{constant}$ | Carbon 1973 |
| $B(v=0) = 1.890658 \text{ cm}^{-1}$ | |
| $(2S+1) = 2$ | |
| $(2-\delta_{o,\Lambda''}) = 1$ | |

TABLE 13. SUMMARY OF RELEVANT MOLECULAR DATA FOR THE
RED SYSTEM OF CN ($A^2\Pi_{inv} - X^2\Sigma_g^+$)

| | |
|--|--------------------------|
| $f_{00} = 3.76 \times 10^{-3}$ | Cooper and Nicholls 1975 |
| $\tilde{\nu}_{00} = 8268.33 \text{ cm}^{-1}$ | |
| $q_{00} = 0.4157$ | Spindler 1965 |
| $q_{30} = 0.0589$ | " |
| $q_{41} = 0.1216$ | " |
| $q_{52} = 0.1429$ | " |
| $q_{51} = 0.0602$ | " |
| $q_{62} = 0.0962$ | " |
| $q_{73} = 0.1135$ | " |
| $q_{84} = 0.1085$ | " |
| $\phi = 1$ for s levels | Tatum 1967 |
| $\phi = 0$ for a levels | |
| $\sum R_e ^2 = 0.36$ for $\Delta v=0$ | Cooper and Nicholls 1975 |
| $= 0.42$ $\Delta v=3$ | (extrapolation) |
| $= 0.44$ $\Delta v=4$ | - " - |
| $B(v=2) = 1.774422$ | |
| $(2S+1) = 1$ | |
| $(2-\delta_{0,\Lambda''}) = 1$ | |

TABLE 14. SUMMARY OF RELEVANT MOLECULAR DATA FOR THE
PHILLIPS SYSTEM OF C_2 ($A^1\Pi_u - X^1\Sigma_g^+$)

| State | T(el) (cm ⁻¹) | g(el) |
|------------------|---------------------------|-------|
| B ² Σ | 25,751.8 | 2 |
| A ² Π | 9,117.37 | 4 |
| X ² Σ | 0.0 | 2 |

TABLE 15A. KNOWN ENERGY LEVELS OF THE CN MOLECULE

| State | T(el) (cm ⁻¹) | g(el) |
|--|---------------------------|-------|
| E ¹ Σ _g ⁺ | 55,034.6 | 1 |
| D ¹ Σ _u ⁺ | 43,240.23 | 1 |
| e ³ Π _g | 40,796.65 | 6 |
| C ¹ Π _g | 34,261.9 | 2 |
| d ³ Π _g | 20,022.50 | 6 |
| ¹ Σ _g ⁺ | 16,000 | 1 |
| c ³ Σ _u ⁺ | 13,312. | 3 |
| ¹ Δ _g | 10,000 | 2 |
| A ¹ Π _u | 8,391.00 | 2 |
| b ³ Σ _g ⁻ | 6,434.27 | 3 |
| a ³ Π _u | 716.24 | 6 |
| X ¹ Σ _g ⁺ | 0.0 | 1 |

TABLE 15B. KNOWN ENERGY LEVELS OF THE C₂ MOLECULE

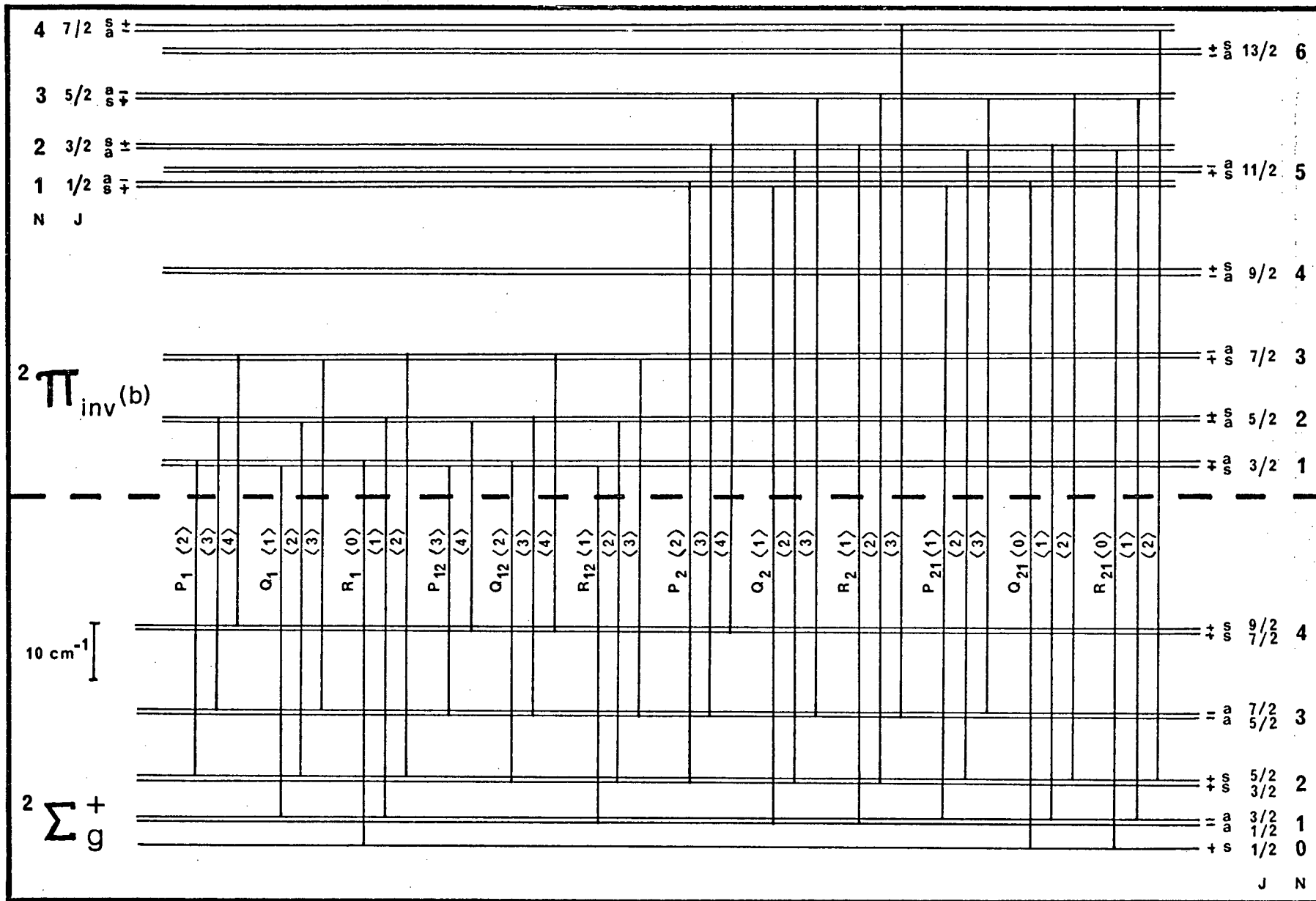


Figure 6a. Rotational Energy Level Structure for the Red System of CN (lower levels)

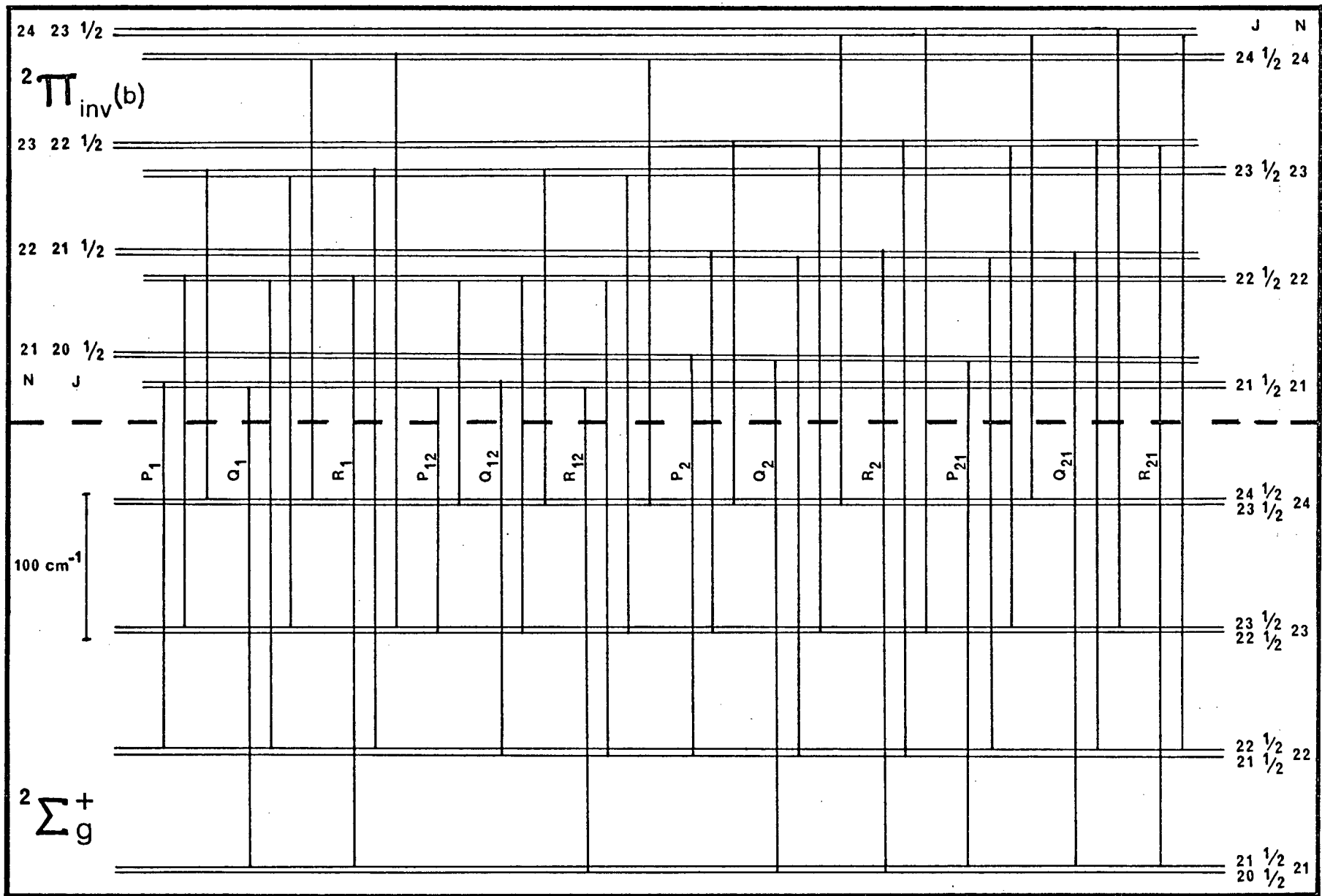


Figure 6b. Rotational Energy Level Structure for the Red System of CN (upper levels)

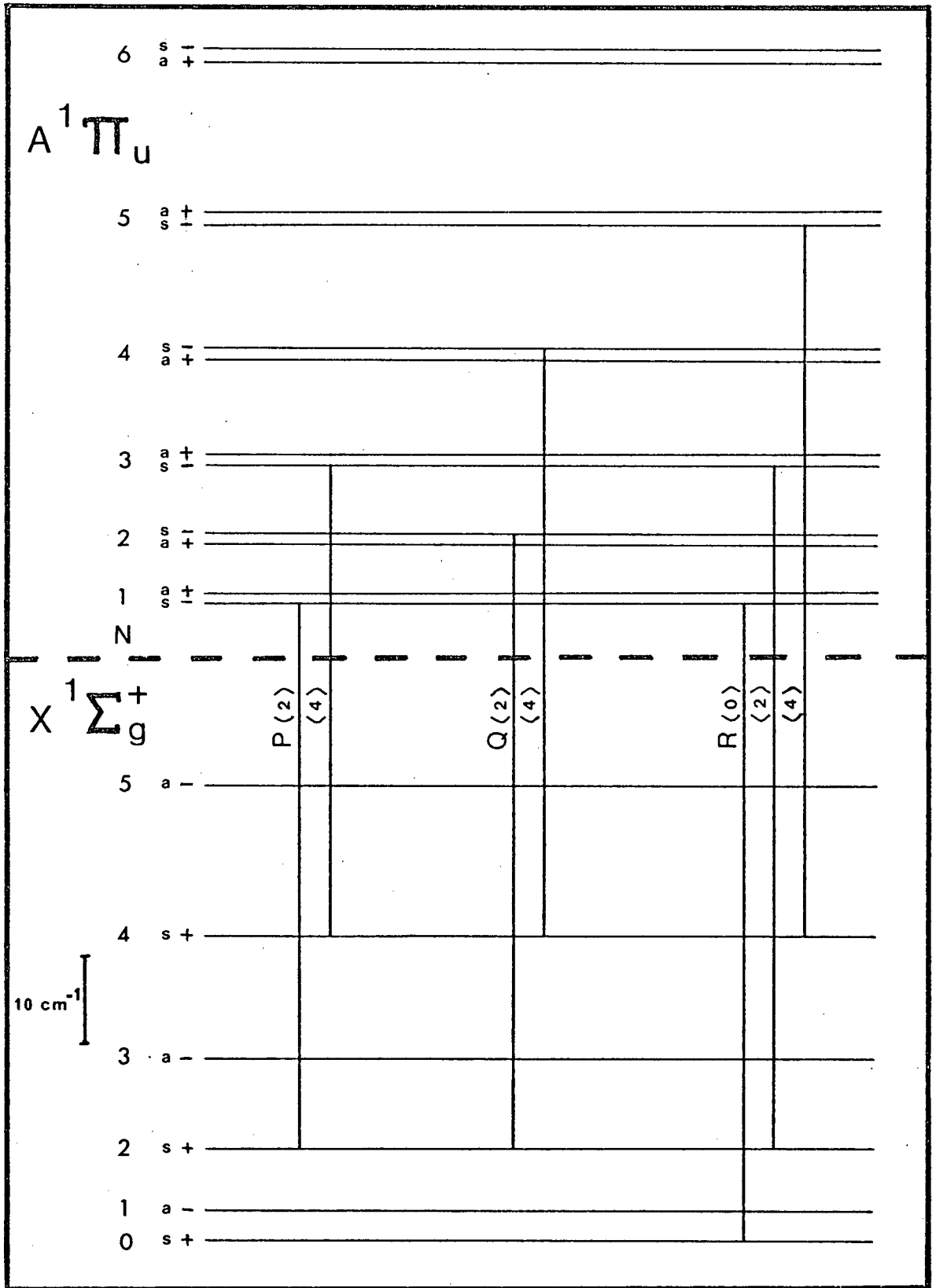


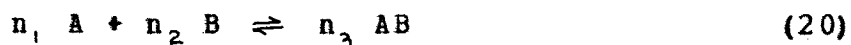
Figure 7. Rotational Energy Level Structure for the Phillips System of C_2

Molecular Equilibrium Calculation

In order to calculate the line and continuous opacities throughout the model atmosphere the densities of CN, C₂, H and H₂ are required in addition to the electron density, which is given directly in the model. To this end the equations of molecular equilibrium were solved for all the same species used in the models by Johnson. The computer program used for the solution basically follows the procedure used by Vardya (1965), although it has been modified to force the total pressure to equal the known pressure of the model. The basic program was kindly supplied by Dr. J. R. Auman.

The abundances used were the same as those used by Johnson; i.e. for H, He, C, N and O as specified for each model and the other elements from the solar composition as deduced by Lambert and his co-workers (Lambert 1968; Lambert and Warner 1968a, b, c; Warner 1968; Lambert and Mallia 1968). Dissociation constants were taken from polynomial fits to the data from the JANAF thermochemical tables (1960) or from the coefficients of Vardya (1965) or Morris and Wyller (1967), again as specified by Johnson.

Since the JANAF dissociation constants are of a different form from those required by Vardya's (1965) procedure it will be useful to consider the necessary conversion technique. The JANAF tables refer to equilibria of the kind



where A and B represent the reactants in their reference states, AB represents the product and n_1 , n_2 and n_3 are the number of molecules of each kind. The tabulated equilibrium constants (K') are then defined as

$$K'(AB) = \frac{[AB]^{n_3}}{[A]^{n_1} [B]^{n_2}} \quad (21)$$

where $[A] \equiv$ the partial pressure of reactant A in atmospheres. Note that the units of the K' 's are defined by the number of reactant molecules for each particular reaction and are of the form $(\text{atm}^{n_3 - n_2 - n_1})$.

As an example consider the specific case of the molecule NH:



since the reference states of N and H are N_2 and H_2 . Thus

$$K'(NH) = \frac{[NH]}{[H_2]^{1/2} [N_2]^{1/2}}, \quad (23)$$

also, e.g. $K'(H) = [H] / [H_2]^{1/2}$ for $1/2 H_2 \rightleftharpoons 1 H$.

The type of equilibrium constant (K) used by Vardya is defined as

$$K(AB) = p(AB) / p(A) p(B) \quad (24)$$

where $p(A) \equiv$ the partial pressure of reactant A in dynes cm^{-2} .

Hence we derive

$$K(\text{NH}) = \frac{[\text{NH}]}{[\text{N}][\text{H}]} = \frac{K'(\text{NH})}{K'(\text{N})K'(\text{H})}. \quad (25)$$

Finally, to convert to cgs units divide by (in this case) $1.013250 \times 10^6 \text{ dy cm}^{-2} / \text{atm.}$

To check that the calculated number density distribution of CN (in particular) corresponded to that of the actual model atmospheres two tests were performed. Using CN opacities from Johnson, Marenin and Price (1972), hydrogenic (H , H^- , H_2) continuous opacity as given in "Theory and Observation of Normal Stellar Atmospheres" (1969, ed. Gingerich), and Mutschlecner-Keller (1970, 1972) atomic line blanketing as modified by Johnson (1974) the output fluxes were computed as a function of frequency for several different models; these flux curves compared very well with Johnson's calculated fluxes. Secondly the CN density distribution was calculated from the tabulated values of the volume absorption coefficient at 1μ and the (interpolated) value of the CN mass absorption coefficient at 1μ (Johnson, Marenin and Price 1972). For this purpose it was assumed that the only opacity sources were CN and the hydrogenic species; although the models also incorporate CO and H_2O opacity this should be a good approximation for the 1μ wavelength used here. Atomic line blanketing was not included as it is not clear how Johnson calculated it at the 1μ standard wavelength, where he has a discontinuity in applying the blanketing. The resulting CN density was then compared with that from the

equilibrium calculations. The general agreement is quite good over the entire depth of the atmospheres, a range of several orders of magnitude, although in places the disagreement can rise to as much as a factor of 2.5. In view of the exceptionally large uncertainty in the dissociation energy of the CN molecule this is still thought to be quite acceptable agreement (Johnson 1975).

Spectrum Parameters

The main factor influencing the appearance of the synthetic spectrum is the amount of CN in the atmosphere. Since the available set of model atmospheres was calculated on a rather coarse grid of parameters [C/O, T(eff), C/H, log g] there is need for a finer gradation in the amount of CN to permit a better match to the observed spectrum. It was decided to do this by altering the metal [C, N, O] abundance by some factor [X(CNO)], thus providing for interpolation in model sequences with varying C/H ratio while keeping the C/O ratio the same. Since most of the C and O will form CO and only the leftover C can be used for CN and C₂ the CN abundance should scale as X(CNO)^{3/2} and C₂ as X(CNO)²; that this is in fact the case, to a good approximation, has been verified by recalculating the molecular equilibrium using the scaled abundances. Furthermore, spectra of neighbouring models along a C/H-varying sequence can be reproduced from each other quite well by this method. Needless to say, by tampering in this way we no longer have a proper model atmosphere, and that the more we have to change the X(CNO) factor the matchup becomes less satisfactory. Since we are not primarily interested in the structure of the atmosphere, however, but rather in the resulting spectrum, I feel that this is an acceptable procedure and will produce quite satisfactory interpolations as long as X(CNO) is "not too far" from unity.

Real spectral lines have Voigt profiles rather than Gaussian. This has been handled by using a Gaussian profile

$$\phi_{\nu} = \frac{1}{\sqrt{\pi} \Delta\nu_D} \exp\left\{-\left(\frac{\nu-\nu_0}{\Delta\nu_D}\right)^2\right\} \quad (26)$$

in the line core, and

$$\phi_{\nu} = \frac{1}{\sqrt{\pi} \Delta\nu_D} \frac{a}{\sqrt{\pi} (\nu-\nu_0)^2} \quad (27)$$

in the wings. This is a good approximation for small values of a .

Thus the synthetic spectrum depends on five parameters.

These are:

1. the model atmosphere used,
2. the CNO scaling factor [$X(\text{CNO})$],
3. the microturbulence [ξ_t],
4. the line profile wing strength [a],
5. the isotope abundance ratios.

Computational Procedure

The computer program used to calculate the emergent flux consists of a short main program and a few opacity subroutines written in Fortran, plus a longer section to handle the actual integration through the atmosphere and a few subroutines to do simple interpolations written in IBM Assembly Language. By using Assembly Language for the more intensive part of the program the execution time has been reduced by a factor of approximately 2.5.

Following is a schematized description of the program layout.

1. Partition functions $[Q(T)]$ and exponential integrals $[E_2(\tau_{std})]$ were calculated separately and explicitly put into the program.
2. Read in spectrum parameters: wavelength limits, micro-turbulence (ζ_t) , $X(\text{CNO})$ factor, line profile parameter (a) , isotopic abundance ratios.
3. Calculate the wavelength interval $[\Delta\lambda_i]$ about the current wavelength within which all spectral lines must be used;

$$\Delta\lambda_i = f(\zeta_t, a).$$
4. For each level of the atmosphere:
 - a. Read in model parameters: $\tau(\text{std})$, T , $n(e)$, κ , ρ , $N(\text{H})$, $N(\text{H}_2)$, $N(\text{CN})$, $N(\text{C}_2)$. (Note that the N's have been calculated by the molecular equilibrium program.)
 - b. Calculate: $B(T)$, $k(\text{cont})[N(\text{H}), N(\text{H}_2), n(e)]$,
 $k(\text{std}) [= \kappa\rho]$

- c. Calculate normalization factors for the various isotopes of CN and for C_2 , scaled by the X(CNO) factor
 $[= \text{const} \times N(\text{isotope}) / \Delta\lambda_D \cdot Q]$.
5. Integrate continuous opacity - gives continuum flux at ends of region to be synthesized.
 6. a. Increment wavelength counter
 b. Read in more spectral line parameters until we have all lines within $\Delta\lambda_i$ of the current wavelength
 7. For each atmospheric level:
 - a. Sum opacity contributions of all lines (within $\Delta\lambda_i$) using the appropriate profile and number density
 - b. Add on continuous opacity
 - c. Integrate - gives output flux
 - d. Normalize to continuum
 8. Go to 6.

When finished - broaden output spectrum by convolving with a Gaussian instrumental profile. (This is a separate program.)

The integration routine:

1. Normalize given k values: $k(\nu, \text{level}) / k(1\mu, \text{std, level})$.
2. Fit a (smooth) spline curve to the points.
3. Integrate along curve: $\rightarrow \tau(\nu, \text{level})$.
4. Calculate: $B_\nu [T(\text{level})] \cdot E_2[\tau(\nu, \text{level})]$,
 (E_2 values interpolated in the precalculated table.)
5. Integrate by summation under the $B \cdot E_2$ curve: \rightarrow Flux.

ANALYSIS TECHNIQUE

The method of analysis selected to compare the observed stellar spectra with the calculated synthetic spectra makes use of the coherence spectrum of the two traces to be compared. This method has been borrowed from the field of time series analysis and is there used to detect similarities between two time series. It is especially suitable when both time series contain noise; since neither the observed stellar spectrum (with its photographic noise) nor the synthetic spectrum (lacking atomic and telluric lines) is in fact an accurate representation of the actual stellar spectrum this situation certainly exists here. [Note that the word "spectrum" will be used with two different meanings: 1) the original astronomical meaning of an intensity vs wavelength representation, and 2) the time series meaning of (something) vs frequency representation. An astronomical spectrum is identical with a time series. The particular meaning intended must be found from the context.]

The technique involves calculating the auto- and cross-covariance functions of the two input time series, and their power spectra by Fourier-transforming these into the frequency domain and then normalizing the cross-spectrum by the auto-spectra, resulting in the coherence spectrum. The coherence plays the role of a correlation coefficient at each frequency. As a final step, to reduce the information in the entire coherence spectrum to a manageable quantity, the average coherence was calculated for all frequencies at which the

auto-power spectral density of the stellar spectrum was above some cutoff fraction of the peak power. This thus results in one number characterizing the goodness of fit between the two inputs. I shall call this number the coherency.

Computational Details

Let the two input time series be denoted by $x'(t)$ and $y'(t)$, $t=1,N$. The data are first reduced to give a zero mean value and detrended by subtracting a straight line fitted to the points. Next the time series are tapered by multiplying 10% from each end by a cosine-squared bell function. The series are then detrended again, extended with zeroes to give a length M , where M is a power of 2 (for reasons of computational economy), and finally extended again to a length of $2M$ (so as to eliminate aliasing in the power spectra), giving x and y (see Figure 8).

In the next step we calculate auto- and cross-covariance functions R_X , R_Y and R_{XY} . These are defined as

$$R_X(r) = \frac{1}{M} \sum_{n=1}^{M-r} x(n) x(n+r) \quad r=0, M-1 \quad (28)$$

and

$$R_{XY}(r) = \frac{1}{M} \sum_{n=1}^{M-r} x(n) y(n+r) \quad r=0, M-1 \quad (29)$$

and are most economically computed by the roundabout method of Fourier transforming the time series via the fast-Fourier-transform (FFT) technique to give $X(k)$ and $Y(k)$ for $k=0$ to $M-1$, then computing the raw auto- and cross-spectral estimates

$$\begin{aligned} G_X(k) &= X(k) \cdot X^*(k), \\ G_{XY}(k) &= |X^*(k) \cdot Y(k)|, \quad k=0, M-1 \end{aligned} \quad (30)$$

and computing the inverse FFT of these to yield R_X and R_{XY} .

The covariance functions are now multiplied by an appropriate "window function"; this has the effect of smoothing

the spectra in frequency space. The window used here is the Parzen weighting function

$$\begin{aligned} WP(r) &= 1-6(r/m)^2+6(r/m)^3, & r=0, m/2 \\ &= 2(1-(r/m)^2)^3, & r=m/2+1, m \\ &= 0, & r>m \end{aligned} \quad (31)$$

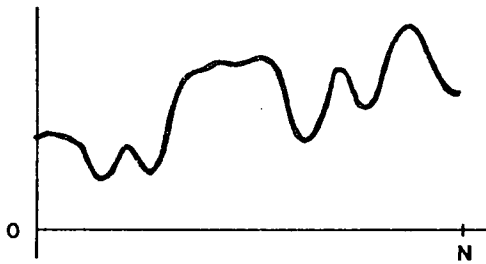
where m is the length of the non-zero part; the shorter this effective length, the greater the frequency smoothing. The use of the Parzen window ensures that the resulting coherence function stays between its theoretical limits of ± 1 .

Smoothed auto- and cross-spectral power densities are then computed from the windowed covariances by applying a forward FFT and calculating the power densities as in equations (30). The squared coherence function is then calculated as

$$C(k) = \frac{|\tilde{G}_{XY}(k)|^2}{\tilde{G}_X(k) \tilde{G}_Y(k)}, \quad k=0, M-1 \quad (32)$$

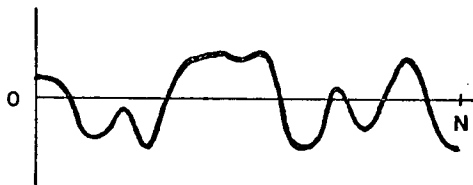
where the \sim 's represent the smoothed spectra.

Finally, to exclude spurious coherence values, the average coherence is calculated only for those frequencies at which the signal-to-noise ratio of the stellar auto-power spectrum is high, i.e. where the power is at least some specified fraction of the peak.



Initial time series:

$$x'(t), y'(t), t=1, N.$$



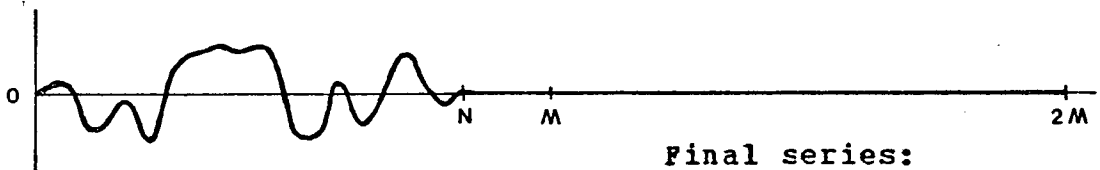
Detrended:

$$x''(t), y''(t), t=1, N.$$



Tapering function:

$$T(t)$$



Final series:

$$x(t) = x''(t) \cdot T(t), t=1, 2M.$$

$$M = 2^m \text{ such that } M/2 < N \leq M.$$

Figure 8. Pretreatment of Spectra

Comments

This analysis technique is basically an extension of the cross-correlation concept. A simple cross-correlation yields a sequence of values $[R_{XY}(r)]$ for the various lags (r) , with, if the correlation is good, a peak near the zero-lag point; the amplitude of this peak is then an indication of the "goodness of fit". Such an approach, however, makes no use whatsoever of the remainder of the correlation function, which has most of the information content of the original inputs. The coherence function is the transform of the correlation function and as such still contains all the information while changing it into a form we can use more easily.

The zero-mean condition on the original time series is a requirement for this technique to be applicable at all, the slope removal is not required but serves to minimize low frequency power that may spoil the power spectra (and coherence) quite spuriously. Because of this and the necessary normalization, the coherence is independent of both the mean level of the (stellar and synthetic) spectra and the amplitude of the features. This means that an error in the drawn continuum level is of no consequence, which is a big plus for carbon star spectra where the continuum is determined by only a few points. Note also that the smoothing of the power spectra (by the window function) is a required part of the procedure; otherwise the computed coherence will equal unity for all frequencies.

The above description has been drawn largely from the very

good explanation of Bendat and Piersol (1971); much relevant material may also be found in Jenkins and Watts (1968).

Tests

As an example and to test the accuracy of the method, a short (20 Å) sample spectrum was generated with all five parameters [model, X(CNO) factor, ξ_t , a , $^{13}\text{C}/^{12}\text{C}$] chosen randomly from a set known to produce plausible looking spectra. Parameter selection and program execution were done in such a manner that the particular parameters chosen was not known at the time. Random noise with peak amplitude 10% of the continuum was then added and the result smoothed, thus simulating a truly unknown spectrum. Various synthetic spectra were then produced and the parameter space was searched until the maximum coherency location was found. Since it was soon apparent that the a (line wing shape) value was quite small, all spectra were calculated with $a=0$ as this considerably reduced the computation time required.

When the coherency peak had been located, its parameters were compared to that of the "unknown" spectrum. Several different sets of random noise with 10% and 20% peak-to-peak amplitudes were then added to the unknown and the analysis repeated for each such new unknown. The derived parameter values are summarized in Table 16. The actual value of a was 0.01, only slightly different from zero; a significantly larger value (say 0.03) produced spectra which were readily distinguishable since the inter-line intensity in several critical places was systematically depressed by the profile wings.

Several things are worth noting: the deduced $^{13}\text{C}/^{12}\text{C}$ ratio

| Noise | | Coherency Peak | | | | Mean |
|-----------------|-----------|----------------|---------|---------|-----------|-------|
| Nr | Amplitude | Model | X (CNO) | ξ_t | $13C/12C$ | Level |
| 1 | 10% | K15 | 1.85 | 2.83 | 0.083 | 0.219 |
| -- | " -- | K16 | 1.20 | 2.86 | 0.091 | 0.215 |
| -- | " -- | K24 | 0.63 | 2.93 | 0.091 | 0.212 |
| 2 | 10% | " | 0.72 | 2.80 | 0.080 | 0.210 |
| 3 | 10% | " | 0.65 | 2.94 | 0.079 | 0.214 |
| 4 | 10% | " | 0.73 | 2.88 | 0.092 | 0.198 |
| 5 | 10% | " | 0.74 | 2.89 | 0.084 | 0.202 |
| 6 | 20% | " | 0.85 | 2.97 | 0.080 | 0.185 |
| 7 | 20% | " | 0.77 | 2.81 | 0.084 | 0.205 |
| actual unknown | | K24 | 0.80 | 2.90 | 0.080 | 0.207 |
| Mean K24 values | | | 0.73 | 2.89 | 0.084 | 0.204 |
| ± std. devn. | | | 0.07 | 0.06 | 0.005 | 0.010 |

TABLE 16. COHERENCY PEAKS FOR A TEST CASE

is in no case very far from the actual value; neither the deduced $^{13}\text{C}/^{12}\text{C}$ ratio nor the microturbulence depends strongly on the model atmosphere assumed, in spite of the differing $X(\text{CNO})$ values required; the mean levels of the spectra agree quite well with the unknown, again indicating that the scaling by the $X(\text{CNO})$ factor works. Visual inspection of the various unknowns frequently showed systematic differences sufficient to assign significantly different $^{13}\text{C}/^{12}\text{C}$ ratios; that the coherency method was not similarly affected shows the advantage of employing an analysis technique that uses the entire spectrum rather than just selected features.

It is also important that appropriate values be used in the coherency analysis; the two variables are the cutoff point of the window function (eqn 31) and the cutoff level for the power spectrum to determine which coherence points are to be included in the final average. The window function has here been terminated at the limit of the covariance function [i.e. m (eqn 31) = $M-1$ (eqn 28)] in order to get maximum frequency smoothing while also not completely discarding any part of the covariance. The power cutoff must be selected at a high enough level that most of the high frequency noise points are eliminated, yet not so high that all the weaker "real" spectral features are also discarded. To explore this, various cutoffs from 2% to 20% were used in the analysis of UU Aur. The parameter values of the coherency peaks for the several cutoffs are summarized below. For low cutoffs the peak coherency rises quite sharply up to about the 5% point; [The 1% point (whose peak was not located)

is also part of this trend.] after this the increase is much slower. This indicates that at the 5% level most of the

| Cutoff | X | ξ_t | $^{13}\text{C}/^{12}\text{C}$ | Coherency |
|--------|------|---------|-------------------------------|-----------|
| 20 % | .16 | 5 | .035 | .983 |
| 10 % | .140 | 4.7 | .037 | .9582 |
| 7.5 % | .138 | 4.9 | .039 | .9534 |
| 5 % | .137 | 4.8 | .040 | .9497 |
| 3 % | .125 | 5.4 | .057 | .9410 |
| 2 % | .105 | 5.6+ | .07 | .9378 |

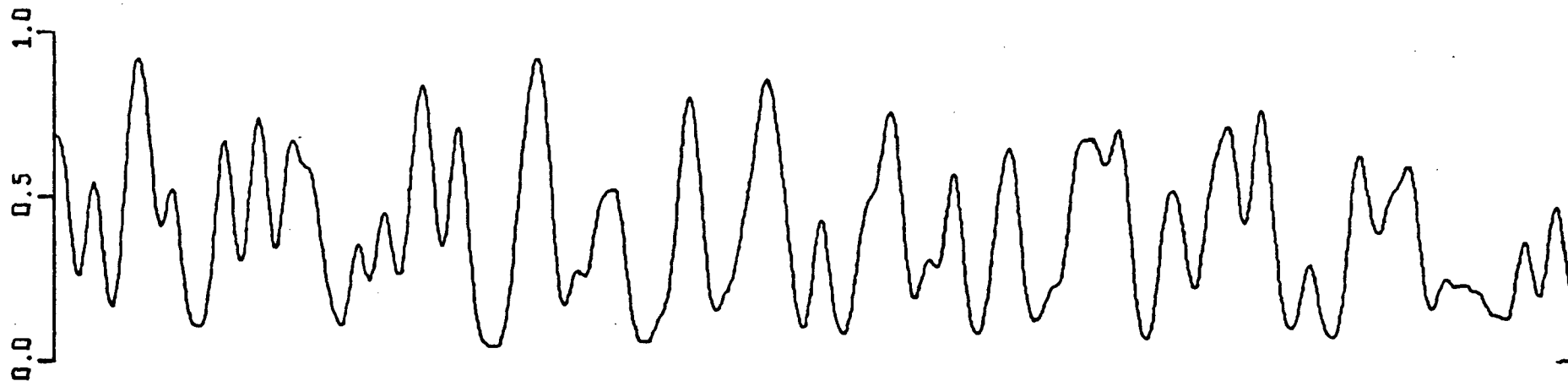
spurious coherence caused by "noise" has been eliminated. We also see that for cutoffs in the range 5% to 10% the deduced coherency peak locations are virtually identical, whereas outside this range the peak location deviates from these. For all subsequent analysis a coherency cutoff of 5% has been used.

Examination of the final results for the stellar spectra reveals that the deduced $^{13}\text{C}/^{12}\text{C}$ ratio is not a strong function of the microturbulence. It is somewhat more sensitive to the value of the X(CNO) factor. Thus, of the parameters characterizing the synthetic spectra, the coherency peak is most strongly dependent on the total amount of CN in the atmosphere [X(CNO)] and the isotope ratio; i.e. on the actual amounts of $^{12}\text{C}^{14}\text{N}$ and $^{13}\text{C}^{14}\text{N}$ present.

An examination of the final synthetic spectrum, which gives

the best coherency when compared to the star being analyzed (cf. Figures 9 and 13), often reveals that the fit is not equally good over the entire region synthesized, i.e., some sections fit better than others. This is not very surprising in view of the extent of the synthesized region. Since the idea is to get as good a fit as possible while using only a few parameters, the longer the section synthesized the more the fit can drift away from perfection. Part of this disagreement is unquestionably caused by the relatively poorly determined zero level of the observed spectrum. This is especially true here for Y CVn (in Figure 13) which is very heavily blanketed over a large part of the synthesized region.

BEST K26 MODEL



19 PSC

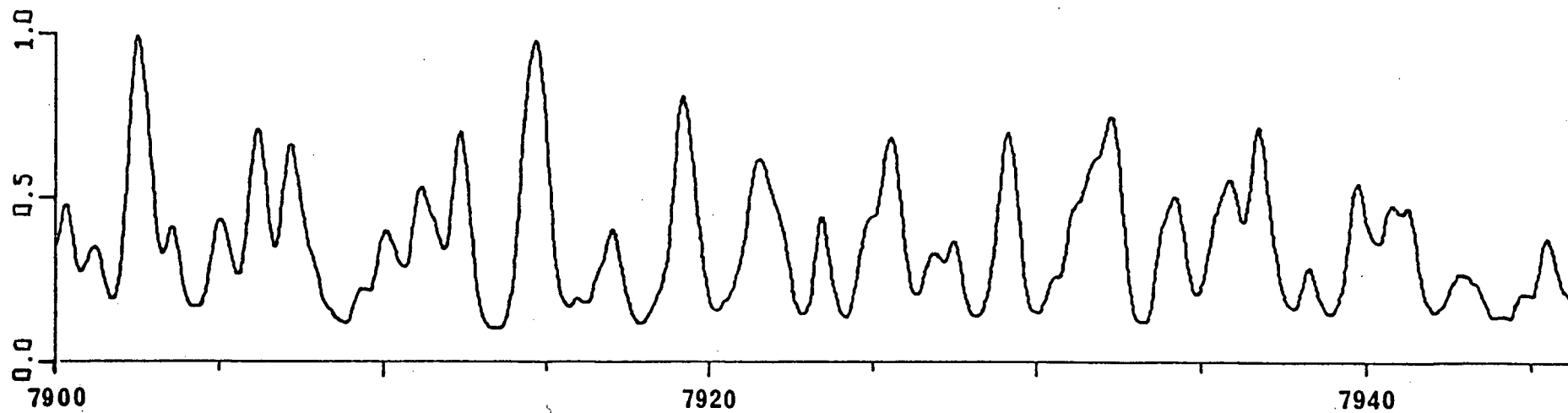
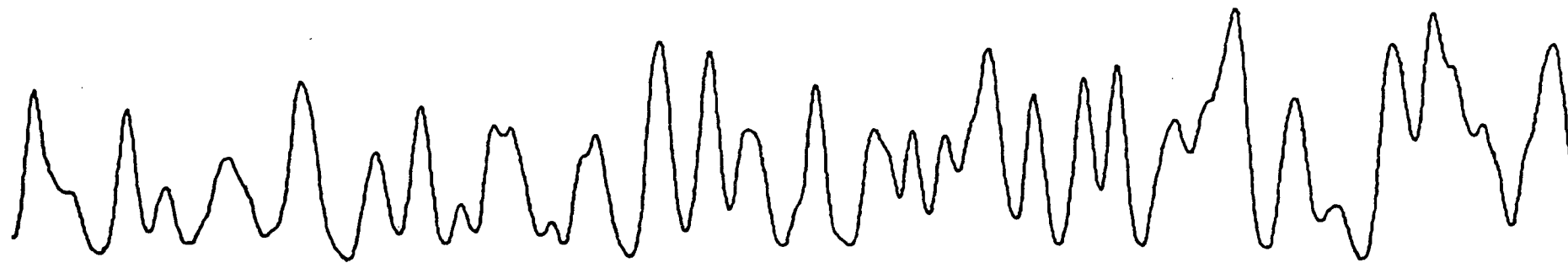
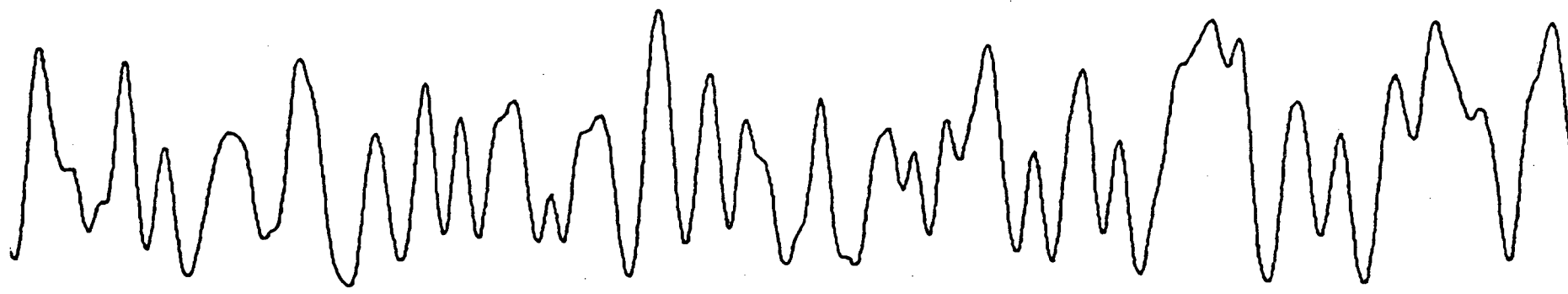


Figure 9. Calculated and Observed Spectra of 19 Psc



7950

7970

7990

Figure 9. (continued)

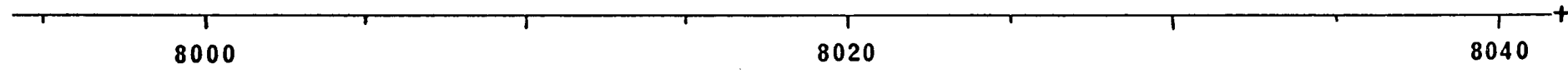
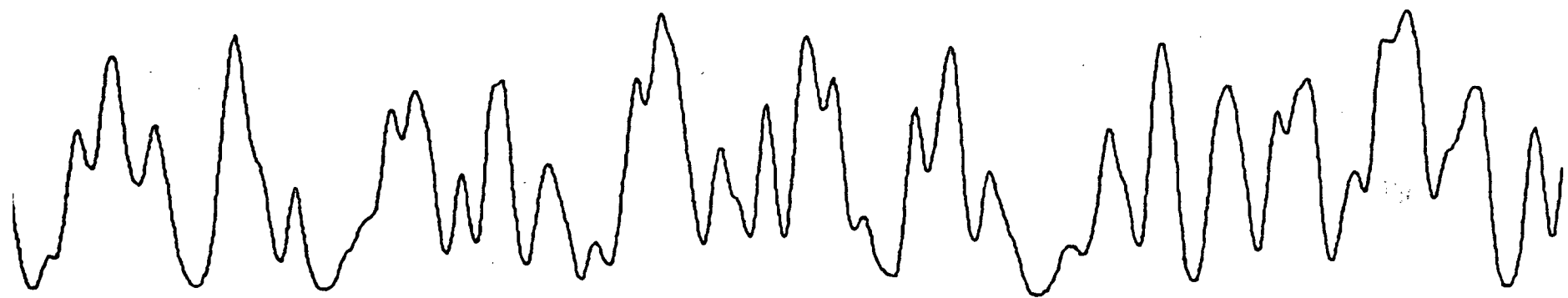
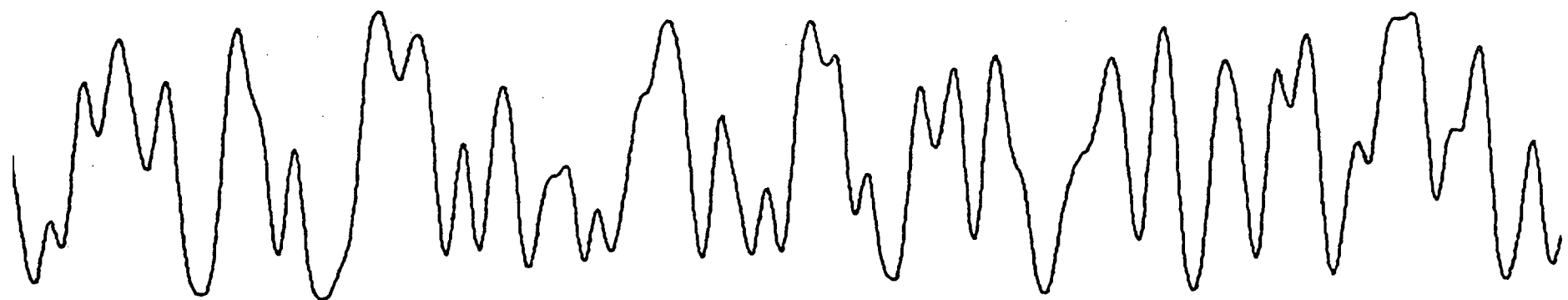


Figure 9. (concluded)

RESULTS

The $^{12}\text{C}/^{13}\text{C}$ Ratios

The detailed set of calculated coherency values is presented in Appendix IV; the deduced parameter values are also summarized in Table 17. Column 2 of the table gives the mean value of the observed spectrum and the average CN index (Baumert 1972); columns 4 to 8 all refer to the parameters of the deduced coherency peak for the model atmosphere in column 3. The uncertainty of the derived $^{13}\text{C}/^{12}\text{C}$ ratios is estimated to be <20% for each individual model. This is based on the deviations shown by the test cases, the curvature of the coherency curves near the peak, and the slight variations that could be caused by a different power cutoff level in the analysis. A further uncertainty is introduced by the model atmosphere itself, depending on how closely it approximates the real stellar atmosphere. This factor is unknown, but since there is no obvious dependence on the model chosen [models K12 and K26 are grossly different] we can assign an uncertainty to the average ratio of <25%. Note that the accuracy of the K24 model for 19 Psc is not as good as the others as only a small number of coherency points were calculated to check that the peak was in general agreement with the other two models.

Scalo (1977) has summarized previous $^{12}\text{C}/^{13}\text{C}$ ratio determinations for 22 carbon stars that were deduced from observations of the CN Red bands. Comparison with the present

| Star | Mean <CN> | Model | X (CNO) | ξ_t | $\frac{^{13}\text{C}}{^{12}\text{C}}$ | Mean | Peak Coh'y |
|--------|--------------|-------|---------|---------|---------------------------------------|-------|---------------|
| 19 Psc | 0.414 | K26 | 0.10 | 3.75 | 0.04 | 0.455 | .9410 |
| | 77 | K24 | 0.19 | 3.75 | 0.057 | 0.443 | .9380 |
| | | K12 | 0.80 | 3.5 | 0.050 | 0.491 | .9369 |
| Z Psc | 0.411 | K26 | 0.11 | 3.4 | 0.058 | 0.432 | .9415 |
| | 79 | K12 | 0.95 | 3.25 | 0.054 | 0.476 | .9378 |
| X Cnc | 0.313 | K26 | 0.17 | 3.8 | 0.032 | 0.345 | .9515 |
| | 89 | | | | | | |
| UU Aur | 0.318 | K26 | 0.14 | 4.8 | 0.040 | 0.351 | .9497 |
| | 100 | | | | | | |
| Y CVn | 0.226 | K26 | 0.20 | 5.0 | 0.40 | 0.200 | .9545 |
| | 119 | K12 | 1.3 | 5.3 | 0.45 | 0.265 | .9356 |

TABLE 17. SUMMARY OF DERIVED SPECTRAL PARAMETERS

results yield the following:

| | | |
|--------|-----------------------------|----------|
| 19 Psc | 5 values in the range 15-25 | here 21 |
| Z Psc | 1 value of 50 | here 18 |
| X Cnc | 1 value of 22 | here 31 |
| UU Aur | 2 values of 20 & 25 | here 25 |
| Y CVn | 5 values in the range 2-5 | here 2.4 |

Clearly the ratios for 19 Psc, UU Aur and Y CVn agree quite well. In view of the very great similarity of the spectra of 19 Psc and Z Psc, including the ^{13}C features, I can not accept such a great difference in the isotope ratios for these two stars. Both of the values for Z Psc and X Cnc were determined by the iso-intensity method, which is quite sensitive to the excitation temperature adopted. Although this method has recently been improved (Fujita and Tsuji 1976) by making use of the satellite lines in the stronger ^{12}CN bands for comparison with the ^{13}CN lines, thus using lines of more nearly equal strength, this technique was not used for either of these stars. For this reason I do not place great trust in those values and must prefer those deduced here.

With the recent availability of infrared spectra, isotope ratios have been determined from the $\Delta v=2$ CO bands at 2.2μ for a number of stars, including some carbon stars. These bands are strong for both carbon isotopes and the rotational lines are well separated. The $^{12}\text{C}/^{13}\text{C}$ ratios deduced from these bands are usually significantly lower than ratios determined from other

molecules, such as CN. For the stars studied here Johnson and Mendez (1970) give the following "estimates": 19 Psc 8-12, X Cnc 10-12, UU Aur 10-12, Y CVn 3-4; though without any details of their analysis. Thompson (1973) has, however, shown that these bands are not suitable for isotope ratio determinations because of their extreme degree of saturation, thus making the appearance of the spectrum rather insensitive to the amount of ^{13}C present. Perhaps more reliable ratios could be determined from the $\Delta v=3$ bands at 1.6μ , which should suffer less from saturation; this region is, however, more heavily overlaid by bands of CN and C_2 (cf. Querci and Querci 1975). No analysis of these bands has yet been done.

Turbulence

The microturbulence is one of the more important factors influencing the appearance of the spectrum. The value of the microturbulent velocity for a "typical" carbon star is, however, not known. For comparison Gustafsson, Kjaergaard and Andersen (1974) found a value of 1.7 km/s with little scatter for a sample of G and K giants. Tomkin, Luck and Lambert (1976) derived a mean value of 1.3 km/s for giants and 3.0 km/s for Ib supergiants, while Luck (1977) found 2.4 km/s for supergiants. That this question is still open is indicated by the fact that values have been cited for α Ori (M2 Ia) ranging from 2 to 10 km/s (Gautier et al. (1976); Hinkle et al. (1976)). For carbon stars Kilston (1975) derived values for 8 stars in the range 5 to 7 km/s, including 19 Psc (5.6) and Y CVn (6.3), while Fujita and Tsuji's (1964) study of Y CVn resulted in 6.6 km/s.

For the stars studied here the microturbulent velocity has been left as a free parameter to be determined. The derived values have already been summarized in Table 17. It should be remarked right away that, on the basis of some rather extensive tests, under no conditions is it possible to achieve a satisfactory visual match for 19 Psc with a microturbulent velocity as high as 6 km/s. This result was established prior to the main coherency calculations and is confirmed by them. Further, note that the derived values are not strongly dependent on the choice of model atmosphere. In view of the apparent trend that higher microturbulence corresponds to a greater depression of

the mean level of the observed spectrum, and to a larger CN index, it is tempting to speculate that the heavy line blanketing in some carbon stars is directly caused by a high value of the microturbulence. The observed change of mean level with turbulence is, however, about three times as large as one would expect from the variations of the synthetic spectra. Nonetheless, and in spite of using only five stars, at least part of the observed range in blanketing and CN strength is probably caused by the microturbulence.

Macroturbulence has not been included in this analysis. As has been mentioned, non-Gaussian (Voigt) line profiles were considered, but were not included in the final analysis for several reasons: the high degree of line crowding would terminate the extension of almost all profile wings, visual inspection of the resulting spectra did not indicate that the profile wings were generally important, and the necessary increase in computation time to calculate the extended wings was thus not deemed worthwhile. Because of the relatively poor ($1/2 \text{ \AA}$) instrumental resolution it is not possible to make a direct measurement of the stellar line widths. Macroturbulences for normal late-type giants are on the order of 5 km/s (e.g. Luck 1977).

A Note on the Carbon Abundance

A rough check on the nuclear processing that has occurred in these stars may be made by comparing the relative strengths of the CN and C₂ features in their spectra; in particular I want to examine the relative importance of CNO hydrogen burning and helium burning as revealed by the C, N and O content of the stars.

In order to form a carbon star by the mixing of nuclear processed material up to the surface, the C/O ratio of the processed material must be greater than unity. If only hydrogen burning CNO processing has occurred then the maximum producible C/O ratio is about 7 for a wide range of processing temperatures and the corresponding N/C ratio is about 25. As shown by Irgens-Jensen (1976) mixing this with an unprocessed envelope to give surface C/O > 1 also produces N/C > 10. One of the model atmospheres (K12) is a close approximation to this state (C/O=2, N/C=28). For comparison a model with greatly enhanced carbon was also selected (K26) (C/O=50, N/C=0.02); such abundances can not have resulted from CNO burning.

Computed spectra using these two atmospheres were compared with the observed spectrum of 19 Psc. Because of the relatively low carbon content the K12 spectrum is virtually free of C₂ lines; the C₂ content of the K26 atmosphere is higher by a factor of at least 10². In the 140 Å section of calculated spectrum, after adjusting the K26 model to produce a mean level equal to that of 19 Psc (no adjustment was necessary for K12),

11 places were found where K26 was significantly lower than K12. All of these places correspond to locations of C_2 lines and the differences were roughly proportional to the expected strengths of the C_2 features; thus it is safe to state that these additional features were caused by the C_2 and were not an artifact of the (grossly) different atmospheric structures. Comparison of these 11 features with the observed spectrum of 19 Psc showed that in every case the K26 spectrum was a better match than K12 and that in 9 out of the 11 cases the observed features were even stronger than in K26. As a control 10 places were found where the K12 spectrum was lower than K26 (opposite of the above); at these locations the comparison with 19 Psc showed that K12 and K26 each matched better 4 times with 2 places equally well matched. Thus it is seen that the stellar features are most likely really caused by C_2 and not by atomic or telluric lines, and that these features are stronger than those produced by the K12 model atmosphere (and possibly by K26 also). Samples of a few of the observed C_2 features are shown in Figure 10.

In order to increase the C_2 strength in the synthetic spectra we must either a) increase the CNO abundances as a whole, b) increase only the C abundance, or c) decrease the N abundance [decreasing O has the same effect as b)]. Only alternative a) is compatible with retaining the C:N:O ratios as produced by CNO processing but the required increase ($\sim \times 10^6$) is so large that the resulting CNO/H ratio is incompatible with any hydrogen left in the atmosphere. Hence the only reasonable

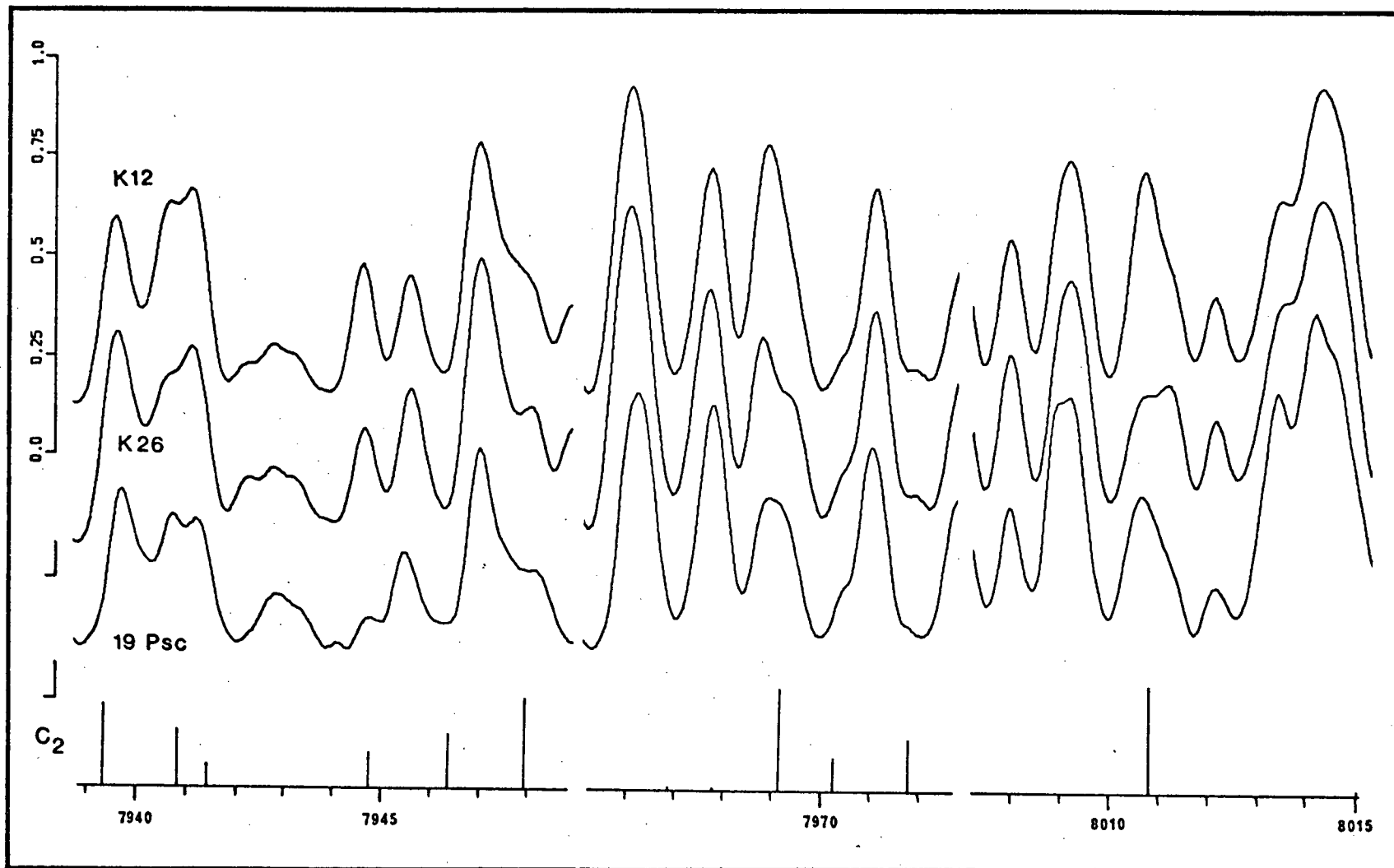


Figure 10. C₂ Features in the Spectrum of 19 Psc

alternative is to increase the C/N ratio; this can be done most readily by assuming that carbon from the helium burning regions has been admixed with the surface material.

Thus it is seen that the synthetic spectrum based on a model atmosphere closely resembling the expected result of CNO processing fails to reproduce the observed C_2 features. Only additional carbon enhancement (as from helium burning) can reasonably produce sufficient C_2 to match these features. Thompson (1977), using the $\Delta v=3$ sequence CO bands in three carbon stars, has recently also reported similar results. It may also be noted here that for those stars where more than one model atmosphere was used in the determination of the $^{12}C/^{13}C$ ratio, the resulting peak coherency was always greater for the model containing more carbon. Presumably this reflects the fact that the additional C_2 features produced a better matching synthetic spectrum.

The Search for ^{14}C and ^{15}N

One of the reasons carbon stars are interesting objects is that they are in an advanced stage of evolution and often show the evidence for this by the surface enhancement of some elements (e.g. ^{13}C and Tc). The case of Technetium is especially interesting since it is unstable, with a half-life of 2×10^5 years, and is apparently present only in stars which are long-period or irregular variables (Peery 1971). Since these elements must have been brought to the surface from the interior regions where they were made it is not inappropriate to also search for other elements which have been similarly transported to the surface. I have here made a search for ^{14}C and ^{15}N , the remaining CN nuclei that can be produced during CNO processing. Since ^{14}C is unstable, with a half-life of 5700 years, its presence would be proof of very recent mixing in a star.

The production of ^{14}C has been investigated by Cowan and Rose (1977) who concluded that enrichment is possible in the intershell region [between the helium- and hydrogen-burning shells] of a star undergoing helium shell flashes if hydrogen-rich material is injected into this region. Subsequent admixture of this material with the envelope could result in a measurable surface abundance of ^{14}C , depending on the relative masses of the intershell region and the envelope. The quantitative aspects of this study have, however, been questioned by Despain (1977), who concluded that the ^{14}C surface enhancement would be negligible [$^{14}\text{C}/^{12}\text{C} \leq 7 \times 10^{-4}$]. Cowan and Rose also

conclude that significant enhancement of ^{15}N will occur if "relatively large amounts" of matter are rapidly mixed into the intershell region. Despain, too, found ^{15}N enrichment on a short time scale. The production of ^{15}N is especially interesting since the hydrogen burning CNO reactions operating at equilibrium will very quickly (a few years) result in an $^{15}\text{N}/^{14}\text{N}$ ratio of about 4×10^{-5} for any burning temperature, yet the terrestrial ratio is 3.7×10^{-3} . Either the ^{15}N is exposed to CNO processing temperatures below and at the base of the envelope for only a very short time, or its observed abundance is the result of a different process altogether (e.g. spallation). Querci and Querci (1970) have tentatively identified ^{15}N in UU Aur with an $^{14}\text{N}/^{15}\text{N}$ abundance ratio of a few times 10^3 .

Wavelengths for the (2,0) band of the Red system of CN were calculated for the various isotopic forms [$^{14}\text{C}^{14}\text{N}$, $^{12}\text{C}^{15}\text{N}$, $^{13}\text{C}^{15}\text{N}$] and these lines were added to the input list for the synthetic spectrum calculations. Since none of these forms have been observed in the laboratory, it was not possible to ensure that the correct wavelengths were used (as was done for $^{12}\text{C}^{14}\text{N}$ and $^{13}\text{C}^{14}\text{N}$) and the computed wavelengths had to be used uncorrected. As was pointed out by Pay, Marenin and van Citters (1971) the value of the orbital electronic angular momentum (L) used in these calculations can't always be approximated by the L-values of the free-atom orbitals. Changing the L-value by one causes a change in the calculated wavelengths of 0.25 Å (for $^{13}\text{C}^{15}\text{N}$). Uncertainties caused by errors in the isotopic masses

are negligible.

A redetermination of the coherency peak, now a function of four variables [one of ^{14}C and ^{15}N added at a time], was deemed impractical. Instead the previously deduced values of $X(\text{CNO})$, ξ_t and $^{13}\text{C}/^{12}\text{C}$ were considered to be fixed and various small amounts of ^{14}C or ^{15}N were added, thus reducing the problem to but one variable. In view of the expected minor perturbations caused by these species this should be an adequate procedure.

In order to check the sensitivity to the amount of added material several tests were done. Synthetic spectra of the full 140 Å region were calculated with $^{14}\text{C}^{14}\text{N}$ added for several values of $^{14}\text{C}/^{12}\text{C}$ from 0 to 0.02; several different sets of random noise were then added to these spectra and the coherency calculated with respect to the noiseless spectra. Samples of the result of these tests are shown in Figure 11. Coherency curves are shown for eight different combinations of input $^{14}\text{C}/^{12}\text{C}$ ratio and noise. Each combination is represented by three curves, for power cutoff levels of 10, 5 and 3% (top, middle, bottom); the vertical placement of a curve is arbitrary, only the curve shape is important. The tests are divided into three groups with input isotope ratios of 0, 0.001 and 0.004, as indicated on the figure. The noise amplitude was 60% of the continuum for the tests shown; the third tests for ratios of 0 and 0.004 were done with more slowly varying noise (the noise was interpolated between the random values, which were calculated only every seventh point) in an attempt to better simulate

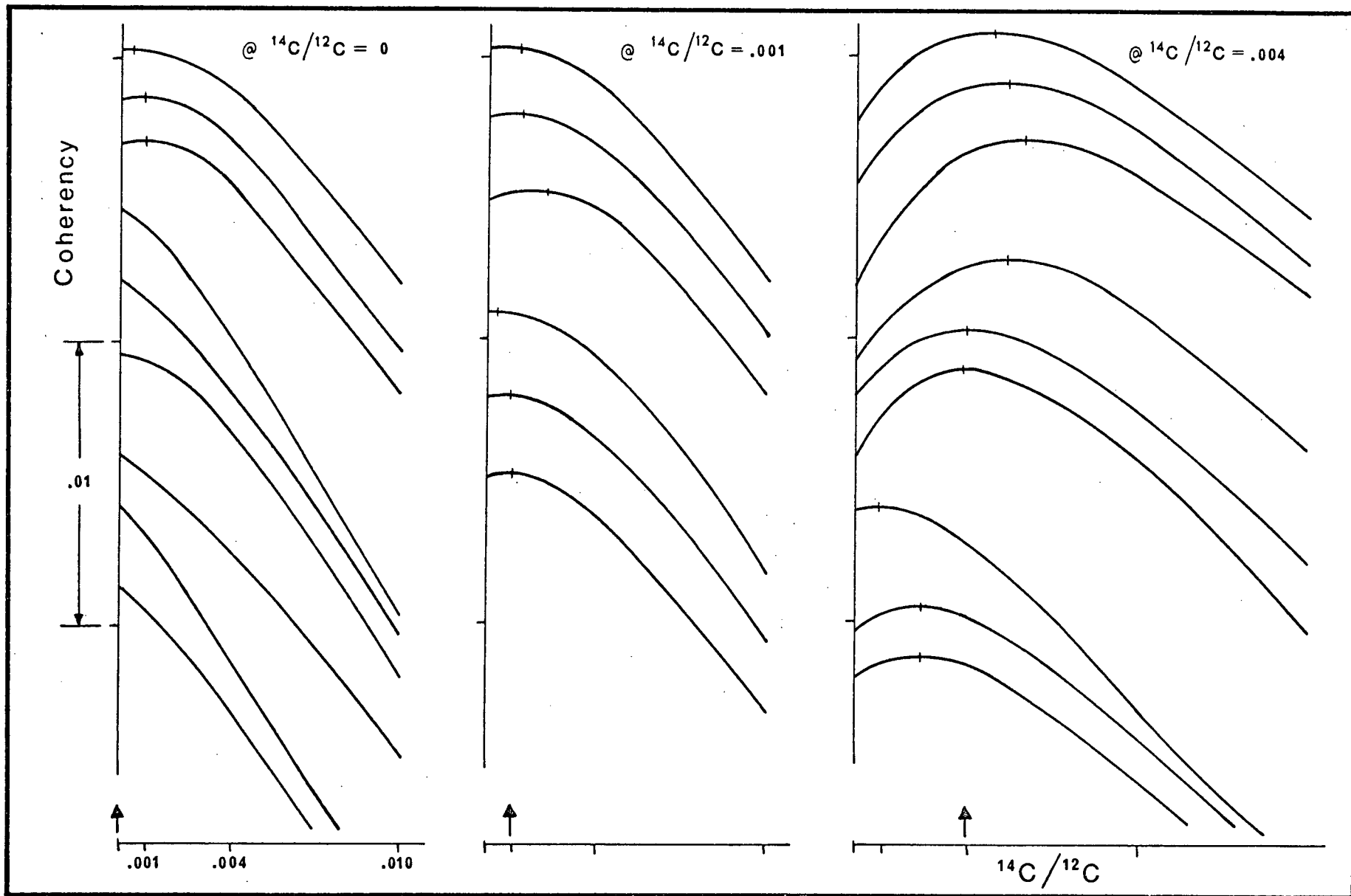


Figure 11. Coherency Curves for the ^{14}C Test Cases

the character of the noise "lines" being added. As can be seen, the peak locations in the coherency curves are usually independent of the power cutoff level although it is possible to get an occasional discordant curve. Clearly the curves for a ratio of 0.001 are not always distinguishable from 0; to get a reliable non-zero measure the coherency peak should be at a ratio ≥ 0.004 , and the peak value should be significantly higher than the zero intercept.

The results when the stellar spectra are analyzed for ^{14}C and ^{15}N are shown in Figures 12 and 13, respectively. The curves for X Cnc, UU Aur and Y Cvn are not distinguishable from the test cases without ^{14}C ; the curves for 19 Psc and Z Psc are peculiar in that the dropoff rate with increasing ^{14}C is much slower than for the test cases and the other three stars. Although the reason for this is not known, the peculiarity is not, however, of such a nature as to indicate the presence of ^{14}C . Thus, for all five stars, ^{14}C was not detected and $^{14}\text{C}/^{12}\text{C} < 0.004$, the detectability limit.

For ^{15}N similar remarks apply to 19 Psc, Z Psc, X Cnc and UU Aur. The coherency curves for Y Cvn, however, definitely indicate the presence of ^{15}N . To explore this further synthetic spectra were calculated wherein the amounts of $^{12}\text{C}^{15}\text{N}$ and $^{13}\text{C}^{15}\text{N}$ were varied independently. The resulting coherency values are presented in Table 18; the vertical and horizontal scales indicate the $^{15}\text{N}/^{14}\text{N}$ ratio used to calculate the abundances of $^{12}\text{C}^{15}\text{N}$ and $^{13}\text{C}^{15}\text{N}$, respectively; the curve in Fig. 13 is given

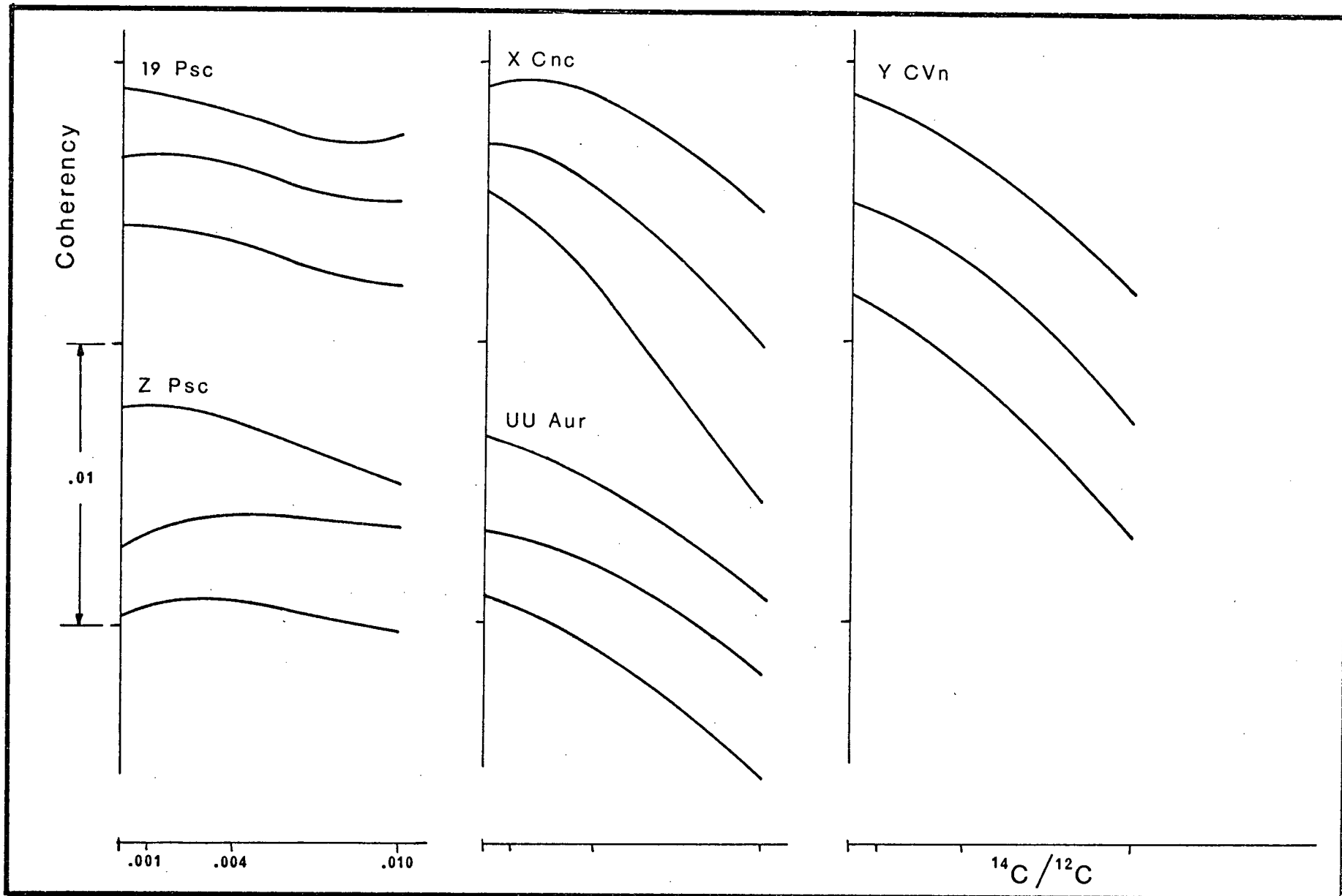


Figure 12. Coherency Curves for Stars vs ^{14}C Abundance

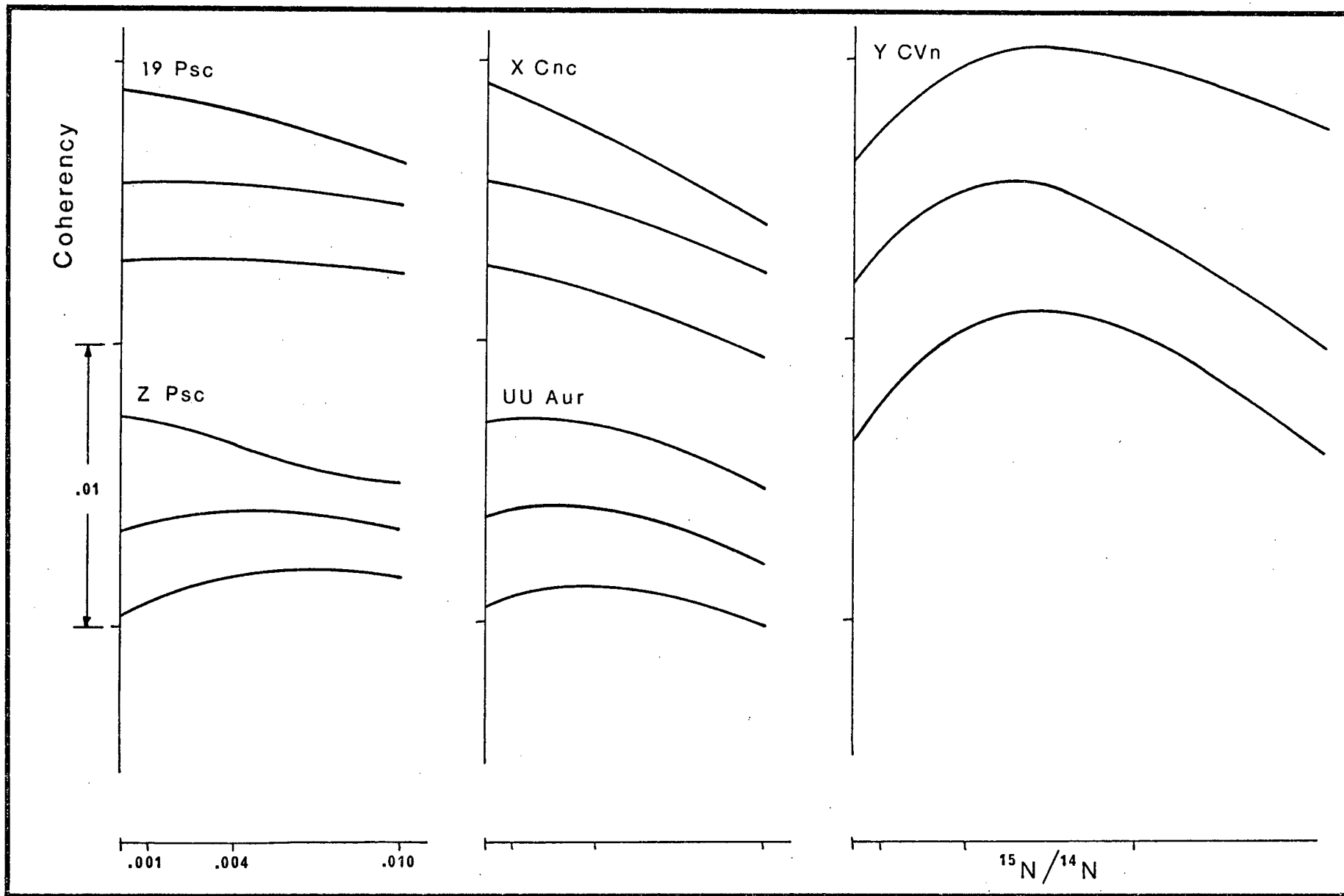


Figure 13. Coherency Curves for Stars vs ^{15}N Abundance

| | | | | | |
|------------------------------|-------------------------------|--------|--------|--------|------------------------------|
| | 0.020 | .95396 | .95331 | | .94999 |
| | 0.010 | .95887 | .95816 | .95657 | |
| $^{12}\text{C}^{15}\text{N}$ | 0.004 | .95889 | .95795 | .95605 | |
| | 0 | .95453 | | .95182 | |
| | $^{15}\text{N}/^{14}\text{N}$ | 0 | 0.004 | 0.010 | 0.020 |
| | | | | | $^{13}\text{C}^{15}\text{N}$ |

TABLE 18. COHERENCY FOR Y CVN VS $^{12}\text{C}^{15}\text{N}$ AND $^{13}\text{C}^{15}\text{N}$

by the diagonal entries. If ^{15}N is present the peak coherency should occur along the diagonal, this is not the case here. The observed peak corresponds to the presence of $^{12}\text{C}^{15}\text{N}$, with $^{15}\text{N}/^{14}\text{N} \sim 0.006$, but without $^{13}\text{C}^{15}\text{N}$. It should be noted, however, that it corresponds to a $^{13}\text{C}^{15}\text{N}/^{12}\text{C}^{14}\text{N}$ ratio of 0.0025, which is below the detectability threshold, so the absence of $^{13}\text{C}^{15}\text{N}$ is not too surprising. The observed behaviour may also be interpreted as some sort of contamination from the $^{13}\text{C}^{14}\text{N}$ features, which are displaced from the $^{12}\text{C}^{15}\text{N}$ features by only about 5 Å, although it is not clear how, by effectively including a second set of " $^{13}\text{C}^{14}\text{N}$ " features the coherency could be improved by the amount indicated.

An examination of the spectra (Figure 14) reveals 8 features that are significantly changed by the inclusion of ^{15}N . The observed spectrum of Y CVn is better represented by the "with ^{15}N " spectrum in 5 of these cases, 2 are equally well matched and 1 is definitely not compatible with ^{15}N . In view of the uncertainties in the wavelengths of the C^{15}N lines, a new wavelength set calculated with a different L-value was substituted and a new set of synthetic spectra calculated. The resultant coherency array had the same feature as before, although the peak was not as high; the spectrum showed a slightly different set of ^{15}N sensitive features, this time none of these was incompatible.

The fact remains that there are features in the spectrum of Y CVn that can not be explained by the constituents of these

synthetic spectra, nor by any telluric lines or atomic lines that appear in the Sun or Arcturus. Especially noteworthy is the feature at 8037.4 Å; this is a continuum point in 19 Psc, Z Psc, X Cnc and UU Aur. The most plausible origin of these features, without invoking ^{15}N , is $^{12}\text{C}^{13}\text{C}$ (or even $^{13}\text{C}^{13}\text{C}$), especially in view of the large amount of ^{13}C in Y CVn. This location is also depressed in WZ Cas, which, though not analyzed here, is reputed to have a high ^{13}C content. To check this possibility the wavelengths of the $^{12}\text{C}^{13}\text{C}$ and $^{13}\text{C}^{13}\text{C}$ lines were calculated, yielding wavelengths virtually identical to those used by Querci and Querci (1970). These calculations are probably accurate since their observed features at these wavelengths all fell on the linear part of the curve of growth and yielded a $^{12}\text{C}/^{13}\text{C}$ ratio about equal to that derived from the CN lines. Though comparison with Y CVn is difficult because of the heavy CN blanketing, it does show some indication that there is absorption caused by $^{12}\text{C}^{13}\text{C}$. The addition of these species can not, however, explain the observed " ^{15}N " features, as most of these avoid the calculated wavelengths. On the other hand there is also the occasional observed feature which stands up considerably higher than the synthetic spectrum.

The arguments in favour of the presence of ^{15}N are: 1) the existence of the coherency peak, with the characteristics we expect to be significant, since the indicated absence of $^{13}\text{C}^{15}\text{N}$ is not significant, and 2) most of the spectral features that would indicate the presence of C^{15}N are in fact observed. Contrary points are: 1) the single observed feature that does

not fit, though the uncertain wavelengths makes this of doubtful value, and 2) the observed matching features may be caused by something else. Since the positive arguments seem to be stronger, we are led to make a tentative identification of ^{15}N in Y CVn with an abundance ratio $^{14}\text{N}/^{15}\text{N} \sim 150$.

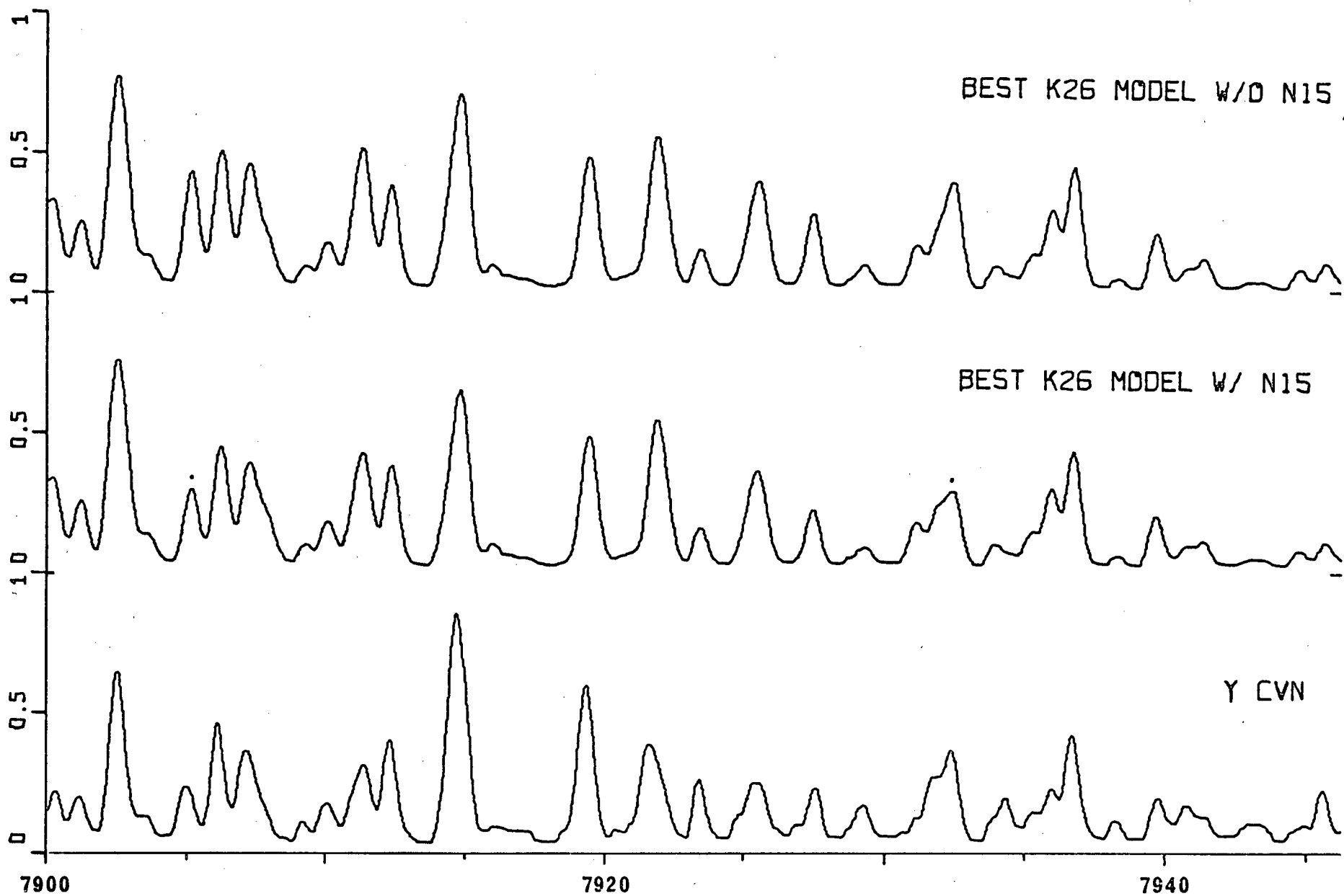


Figure 14. "¹⁵N Features" and the Spectrum of Y CVn

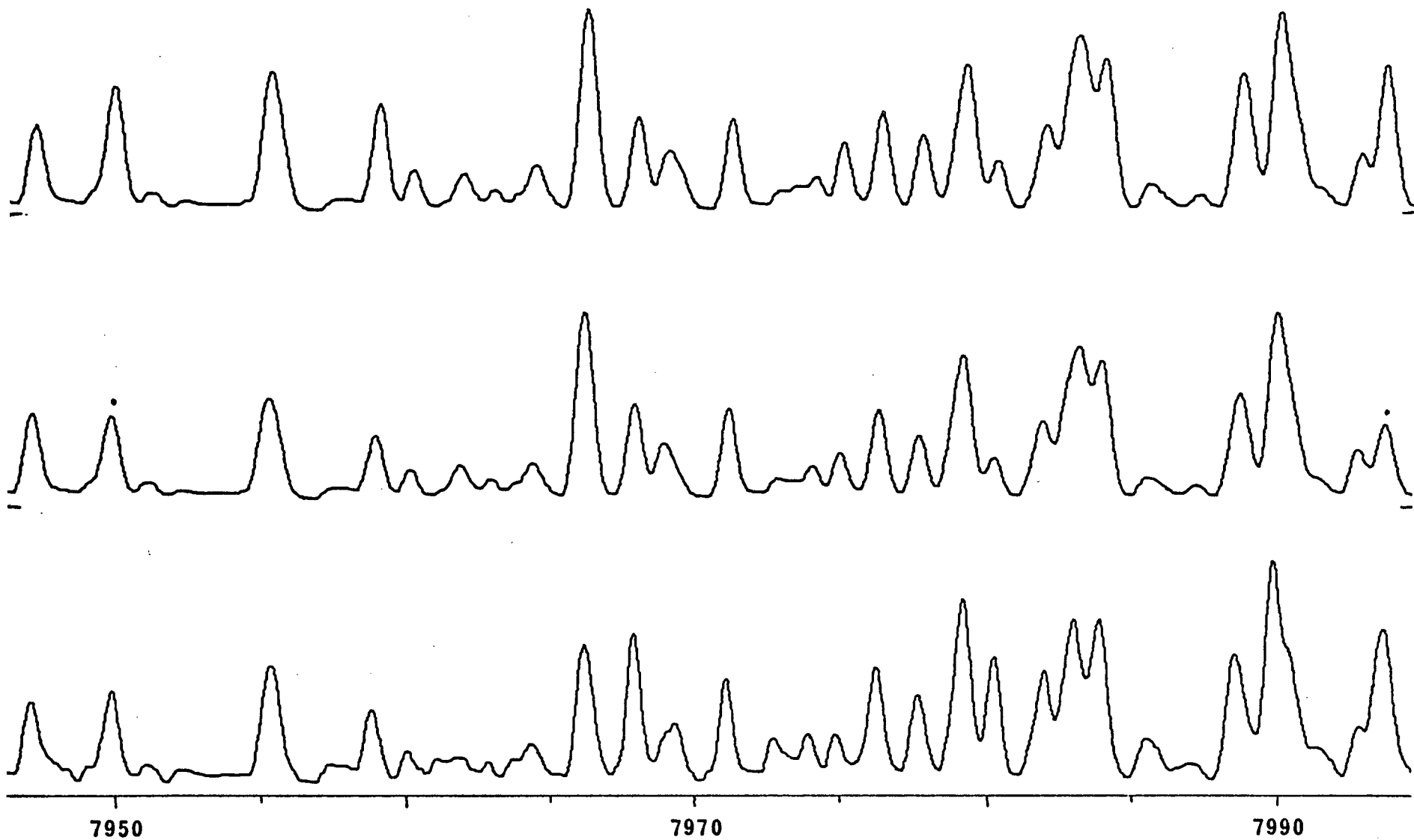


Figure 14. (continued)

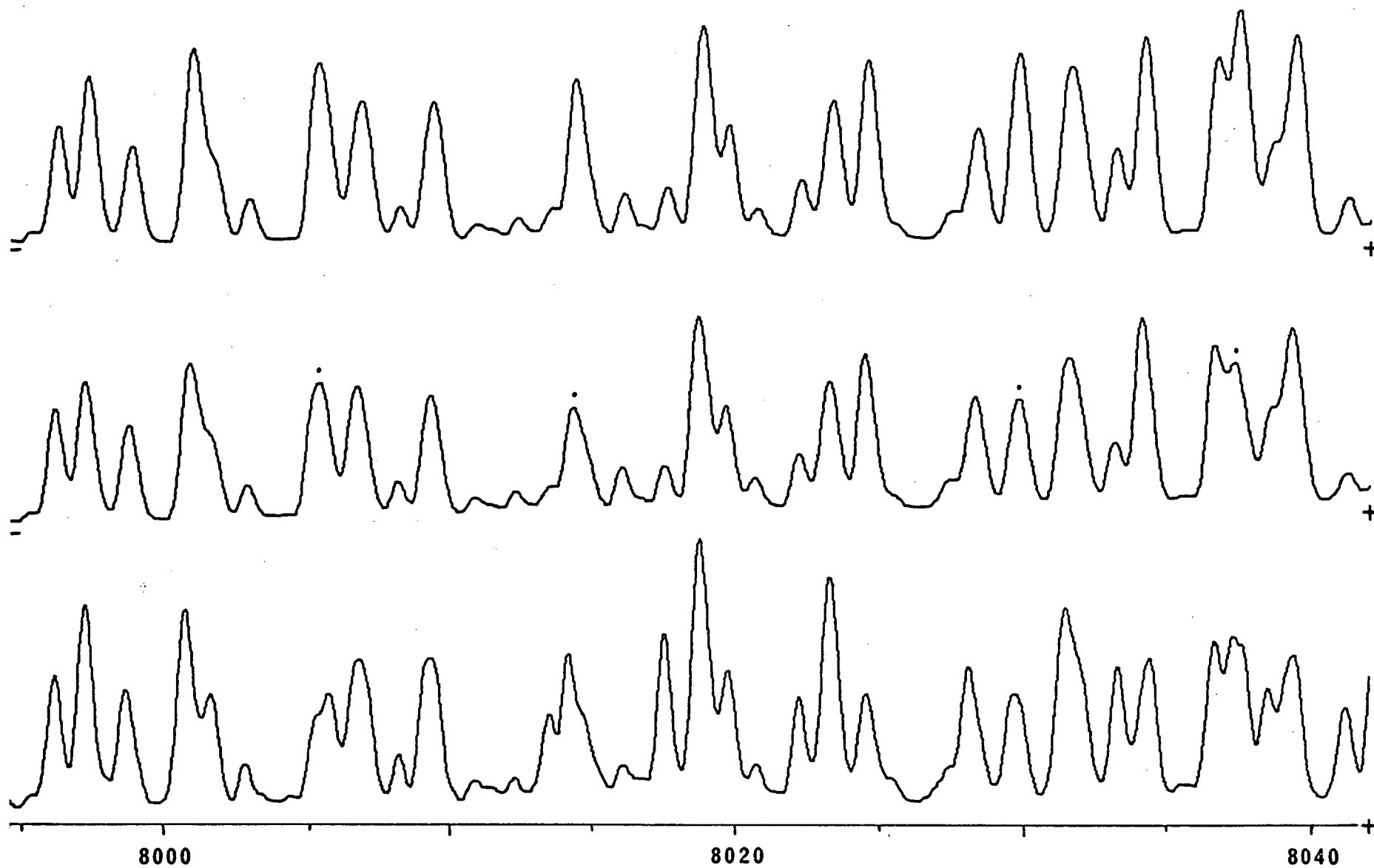


Figure 14. (concluded)

A RECAP OF THE COHERENCY TECHNIQUE

Since the coherency technique is a new tool for analyzing stellar spectra it seems appropriate to make a summary of its salient features in the light of what has been learned here.

First: its advantages.

1. It is an objective method, requiring minimal subjective input by the observer.
2. Errors in the level of the drawn continuum and in the scale of the observed spectrum have no effect whatsoever.
3. The information content of the entire spectrum is used. This makes it particularly applicable to molecular spectra where the features of interest are spread over a large range of the spectrum.
4. Particular lines do not need to be selected for analysis; the problem of blends does not enter. This means it should be applicable to the analysis of lower resolution spectra.
5. Weak lines, that are not correlated with the features of interest, (telluric, atomic, etc.) do not affect the result.
6. Isolated extraneous strong features have no effect.

Second: some possible drawbacks.

1. All the major components should be included in the synthetic spectrum to be compared against.
2. This means that the number of significant variables describing the synthetic spectra can become large. This has not been a problem here because of the nearly complete dominance of the carbon star spectra by the CN molecule.

3. Minor components are not accurately measurable. In this context "minor" means features which are of comparable strength to other spectral features ("noise") not included in the synthetic spectra. Even if some of these minor lines can be resolved, the coherency peak is likely to be significantly affected by the noise.

All things considered, it is a good way to get an objective measure of the major spectral variables. Though I have no concrete reason for saying so, having used spectra of only one dispersion, I feel that better resolution in the observational data should ease the analysis by making the effects of the variables more readily separable and give the coherency "surface" a stronger curvature near the peak, thus making it better defined. Some variables (e.g. the microturbulence) may even be directly measured using traditional techniques, thus reducing the number of remaining variables.

SUMMARY

The investigation of carbon stars in binary systems included most such suspected systems. Nine systems have been judged probably real; another half-dozen have been assigned lower weights, while for several more there is insufficient evidence to permit even a tentative judgement. Because of their faintness it has not been possible to acquire spectra of many of the companions; accurate radial velocities in particular would be valuable to allow one to confirm or reject the systems as real. The mean absolute visual magnitude of the carbon stars is -2.3 , while the bolometric magnitudes range between -4 and -8 . The average carbon star is thus somewhat more luminous than the normal giants, but the dispersion in luminosity is quite large. There is also some indication of a mass - luminosity relation for carbon stars.

A new, objective method of analyzing spectra, which requires minimal subjective input, has been introduced and demonstrated. It is particularly useful for carbon star spectra, which show extensive molecular bands with severe line blending and an uncertain continuum. The feasibility of calculating realistic synthetic spectra of carbon stars has also been demonstrated. The $^{12}\text{C}/^{13}\text{C}$ ratios deduced with this technique are in general agreement with ratios obtained via the curve-of-growth method from the same near infrared CN bands. The analysis also revealed an interesting possible correlation between the microturbulence and the CN index. The presence of

^{15}N has been tentatively identified in Y CVn, while ^{14}C was not found in any of the stars analyzed. The presence of ^{15}N is potentially a very important result; to confirm it we need to identify some specific lines of $^{12}\text{C}^{15}\text{N}$. To this end a thorough line identification study for Y CVn, using high-dispersion spectra, would be very valuable.

There is still a great shortage of realistic model atmospheres for carbon stars; in particular there is a need for models with abundances that reflect the helium-burning reactions. Since a CNO-type composition does not result in enough carbon to make adequate amounts of C_2 , and a carbon-enhanced model yields too much CN to give reasonable spectra without greatly scaling it down, it would appear that some nitrogen-poor (solar abundance or less) and carbon-enhanced models may be what are needed.

REFERENCES

- Abt, H. A., Meinel, A. B., Morgan, W. W. and Tapscott, J. W. 1968, An Atlas of Low-Dispersion Grating Stellar Spectra.
- Allen, C. W. 1973, Astrophysical Quantities, Athlone Press, London.
- Arnold, J. O. and Nicholls, R. W. 1972, J.Q.S.R.T. 12, 1435.
- Arp, H. C. 1965, Stars and Stellar Systems, Vol. 5, Galactic Structure, p. 401.
- Ballik, E. A. and Ramsay, D. A. 1963, Ap.J. 137, 84.
- Barnes, J. V. 1974, private communication.
- Baumert, J. H. 1972, Ph. D. thesis, Ohio State University.
- Baumert, J. H. 1974, Ap.J. 190, 85.
- Baumert, J. H. 1975, Ap.J.Lett. 200, L141.
- Bendat, J. S. and Piersol, A. G. 1971, Random Data: Analysis and Measurement Procedures, Wiley-Interscience, New York.
- Blaauw, A. 1963, Stars and Stellar Systems, Vol. 3, Basic Astronomical Data, p. 383.
- Blanco, V. M. 1956, Ap.J. 123, 64.
- Blanco, V. M. and Lennon, C. J. 1961, A.J. 66, 524.
- Bond, H. E. 1975, Ap.J. 202, L47.
- Cannon, R. D. and Stobie, R. S. 1973, M.N. 162, 207.
- Carbon, D. F. 1973, Ap.J. 183, 903.
- Catchpole, R. M. and Feast, M. W. 1973, M.N. 164, 11P.
- Climenhaga, J. L. 1960, Publ. D.A.O. 11, 307.
- Cooper, D. M. and Nicholls, R. W. 1975, J.Q.S.R.T. 15, 139.
- Cowan, J. J. and Rose, W. K. 1977, Ap.J. 212, 149.
- Crabtree, D. R., Richer, H. B. and Westerlund, B. E. 1976, Ap.J.Lett. 203, L81.
- Crull, H. E. 1972, private communication.

- Davis, S. P. and Phillips, J. G. 1963, The Red System of the CN Molecule, University of California Press, Berkeley.
- Dearborn, D. S. P. and Eggleton, P. P. 1976, Q.Jl.R.A.S. 17, 448.
- Despain, K. H. 1977, Ap.J. 212, 774.
- Dickens, R. J. 1972, M.N. 159, 7P.
- Eggen, O. J. 1972, Ap.J. 174, 45.
- Fast, H. 1973, private communication.
- Fay, T., Marenin, I. and van Citters, W. 1971, J.Q.S.R.T. 11, 1203.
- Feast, M. W. and Lloyd Evans, T. 1973, M.N. 164, 15P.
- Franz, O. G. and White, N. M. 1973, Bull. A. A. S. 5, 43.
- Fujita, Y. 1970, Interpretation of Spectra and Atmospheric Structure in Cool Stars, Univ. of Tokyo Press, Tokyo.
- Fujita, Y. and Tsuji, T. 1964, Proc. Japan Acad. 40, 404.
- Fujita, Y. and Tsuji, T. 1976, Proc. Japan Acad. 52, 296.
- Garrison, R. F. 1977, private communication.
- Gaustad, J. E. and Conti, P. S. 1971, P.A.S.P. 83, 351.
- Gautier, T. N., Thompson, R. I., Pink, U. and Larson, H. P. 1976, Ap.J. 205, 841.
- Gingerich, O. J. (ed.) 1969, Theory and Observation of Normal Stellar Atmospheres, M.I.T. Press, Cambridge.
- Gordon, C. P. 1968, P.A.S.P. 80, 597.
- Gustafsson, B., Kjaergaard, P. and Andersen, S. 1974, Astr.Ap. 34, 99.
- Hagen, G. L. 1970, Atlas of Open Cluster Colour-Magnitude Diagrams, Publ. D.D.O., Vol. 4.
- Harding, G. A. 1962, Observatory 82, 205.
- Hartwick, F. D. A. and Hesser, J. E. 1973, Ap.J. 183, 883.
- Hartwick, F. D. A., Hesser, J. E. and McClure, R. D. 1972, Ap.J. 174, 557.
- Hayes, D. S. 1970, Ap.J. 159, 165.

- Herbst, W., Racine, R. and Richer, H. B. 1977, P.A.S.P. (in press).
- Hinkle, K. H., Lambert, D. L. and Snell, R. L. 1976, Ap.J. 210, 684.
- Honeycutt, R. K. 1972, P.A.S.P. 84, 823.
- Iben, I., Jr. 1967, A.R.A.A. 5, 571.
- Iben, I., Jr. 1975, Ap.J. 196, 525.
- Irgens-Jensen, S. 1976, Astr.Ap. 51, 107.
- JANAF Thermochemical Tables 1960-69, (Midland, Mich.: Dow Chemical Co.)
- Jenkins, G. M. and Watts, D. G. 1968, Spectral Analysis, Holden-Day, San Francisco.
- Johnson, H. L. 1966, A.R.A.A. 4, 193.
- Johnson, H. L. 1968, Stars and Stellar Systems, Vol. 7, Interstellar Matter, p. 167.
- Johnson, H. L. and Borgman, J. 1963, B.A.N. 17, 115.
- Johnson, H. L. and Mendez, M. E. 1970, IAJ 75, 785.
- Johnson, H. R. 1974, NCAR Technical Note / STR-95.
- Johnson, H. R. 1975, private communication.
- Johnson, H. R., Marenin, I. R. and Price, S. D. 1972, J.Q.S.R.T. 12, 189.
- Kilston, S. 1975, P.A.S.P. 87, 189.
- Lambert, D. 1968, M.N. 138, 143.
- Lambert, D. and Mallia, E. 1968, M.N. 140, 13.
- Lambert, D. and Warner, B. 1968a, M.N. 138, 181.
- Lambert, D. and Warner, B. 1968b, M.N. 138, 213.
- Lambert, D. and Warner, B. 1968c, M.N. 140, 197.
- Lee, T. A. 1970, Ap.J. 162, 217.
- Luck, R. E. 1977, Ap.J. 212, 743.
- Marenin, I. R. and Johnson, H. R. 1970, J.Q.S.R.T. 10, 305.

- Matthews, T. A. and Sandage, A. R. 1963, Ap.J. 138, 30.
- Mendoza V, E. E. and Johnson, H. L. 1965, Ap.J. 141, 161.
- Mihalas, D. 1970, Stellar Atmospheres, W. H. Freeman and Company, San Francisco.
- Morris, S. and Wyller, A. A. 1967, Ap.J. 150, 877.
- Mutschlecner, P. and Keller, C. 1970, Solar Phys. 14, 294.
- Mutschlecner, P. and Keller, C. 1972, Solar Phys. 22, 70.
- Oke, J. B. and Schild, R. E. 1970, Ap.J. 161, 1015.
- Olson, B. I. 1971, M. Sc. thesis, University of British Columbia.
- Olson, B. I. and Richer, H. B. 1975, Ap.J. 200, 88.
- Pearse, R. W. B. and Gaydon, A. G. 1941, The Identification of Molecular Spectra, Wiley & Sons, London.
- Peery, B. F., Jr. 1971, Ap.J.Lett. 163, L1.
- Peery, B. F., Jr. 1975, Ap.J. 199, 135.
- Querci, M. and Querci, F. 1970, Astr.Ap. 9, 1.
- Querci, M. and Querci, F. 1975, Astr.Ap. 42, 329.
- Richer, H. B. 1971, Ap.J. 167, 521.
- Richer, H. B. 1972, Ap.J. Lett. 172, L63.
- Rybski, P. M. 1973, P.A.S.P. 85, 653.
- Sackmann, I.-J. 1977, Ap.J. 212, 159.
- Sackmann, I.-J., Smith, R. L. and Despain, K. H. 1974, Ap.J. 187, 555.
- Sanford, R. F. 1940, P.A.S.P. 52, 408.
- Sanford, R. F. 1944, Ap.J. 99, 145.
- Scalo, J. M. 1977, Ap.J. 215, 194.
- Scalo, J. M. and Ulrich, R. K. 1973, Ap.J. 183, 151.
- Schadee, A. 1964, B.A.N. 17, 311.
- Schmidt, K. H. 1956, Mitt. Univ. Sternwarte Jena, No. 27.

- Schmidt-Kaler, Th. 1965, Landolt-Bornstein, Neue Series VI/1, p. 297.
- Smith, M. G. and Wing, R. F. 1973, P.A.S.P. 85, 659.
- Smithsonian Astrophysical Observatory Star Catalog 1966, Smithsonian Publication 4652.
- Spindler, R. J. 1965, J.Q.S.R.T. 5, 165.
- Stromgren, B. 1966, A.R.A.A. 4, 433.
- Tatum, J. B. 1967, Ap.J. Supp. 16, No. 124, 21.
- Thompson, R. I. 1973, Ap.J. 184, 187.
- Thompson, R. I. 1977, Ap.J. 212, 754.
- Tomkin, J., Luck, R. E. and Lambert, D. L. 1976, Ap.J. 210, 694.
- Underhill, A. B. and Walker, G. A. H. 1966, M.N. 131, 475.
- Vandervort, G. L. 1958, A.J. 63, 477.
- Vardya, M. S. 1966, M.N. 134, 347.
- Walker, M. F. 1972, M.N. 159, 379.
- Wallerstein, G. 1973, A.R.A.A. 11, 115.
- Warner, B. 1968, M.N. 138, 229.
- Westerlund, B. E. 1959, Uppsala Astr. Obs. Ann. 4, nr 7.
- Westerlund, B. E. 1964, I.A.U. Symp. 20, The Galaxy and the Magellanic Clouds, p. 239.
- Willstrop, R. V. 1965, Memoirs R. A. S. 69, 83.
- Wilson, R. E. 1953, General Catalogue of Stellar Radial Velocities (Carnegie Institution of Washington, Washington, D.C.).
- Wyller, A. A. 1966, Ap.J. 143, 828.
- Yamashita, Y. 1972, Ann. Tokyo Astr. Obs. 13, 169.

APPENDIX I

RADIAL VELOCITIES OF CARBON STARS

Radial velocities for most types of stars are usually measured in the blue spectral region (3700 - 4600 A) for two reasons: viz. this is where the photographic plates are most efficient, and there is a good selection of atomic lines available for all spectral types. Carbon stars are, however, usually extremely weak in the blue, and hence long exposures are required to get good blue spectra. The near infrared (7000 - 9000 A) is a much more efficient region for taking spectra of carbon stars (using N plates), while still further into the infrared photographic plates become inefficient and/or observational methods become more elaborate. This region is, however, heavily blanketed by bands of CN and C₂, making it well nigh impossible to find any unblended atomic lines. This problem is even more severe at low dispersions when almost every spectral feature is a blend of several lines.

Since several of the carbon stars in the list of suspected binary systems had poorly determined velocities (Sanford 1944) it was deemed desirable to acquire better data in this regard. Furthermore fully 1/6 of the stars on Sanford's list have velocities determined from a single classification dispersion spectrum only. If one could come up with a set of standard wavelengths for use on low dispersion near infrared spectra this situation could be greatly improved.

The spectra used for this study were obtained by Dr. H. B. Richer at Cerro Tololo in 1969. They are at 124 A/mm dispersion and cover the spectral range 7400 - 8900 A; also used were some high dispersion (13 A/mm) spectra of the same region obtained at the Dominion Astrophysical Observatory, Victoria.

Tracings of the high dispersion spectra were used to choose a set of lines which were reasonably strong and had no (or few) comparably strong nearby neighbours. These lines were then measured on the low dispersion spectra of the 11 stars with "a"-quality velocities (Sanford 1944) listed in Table 19. All these stars are late-type carbon stars except V Ari, which is a CH star. Since the near infrared spectra of most carbon stars show very little variation (Richer 1971), this is not important and the standard wavelengths are applicable to all carbon stars showing the CN bands in sufficient strength to make most of the lines measurable.

The stellar spectra were digitized using the department's automated Joyce-Loebl Microdensitometer, with a sampling interval of 5 microns (about 0.6 A), and the line position measurements were made by a computer program (see next Appendix) which fits spline functions to the observed points and then calculates both the line center-of-gravity and minimum from the reconstructed spectrum. The wavelengths of both of these were then plotted versus the expected velocity of the star (corrected for the earth's orbital motion) and only those features with the tightest correlation retained.

Seventeen lines were thus chosen to define the radial velocity system; these are listed in Table 20. The same features are also indicated on the tracing of T Ind in Fig. 15. Because of the great complexity of carbon star spectra the listed features may not be used unquestioningly, however, but only if the line shape is such as to conform to that in the stars used in defining the system. These necessary qualifications are noted in Table 21. A rough idea of how frequently a feature may be found acceptable can be estimated from the number of lines used to define that rest wavelength (column "N" in Table 20). Note that features 1 and 4 in the tracing in Fig. 15 would not be considered acceptable by these criteria.

This technique was applied to nine of the program stars. An average of 12 lines were measured for each star resulting in an average probable error of the mean of 4 km/s. This internal accuracy is comparable to Sanford's "c"-quality velocities, as defined by his error bars.

| Star | Expected Velocity | Sp. Type | |
|-----------|----------------------|----------------|---------------|
| | | Sanford (1944) | Richer (1971) |
| V Aql | +65 | N | C5 |
| AQ Sgr | +42 | N | C5 |
| T Ind | +24 | N | C5 |
| DS Peg | +19 | N | C5 |
| HD 173291 | +10 | N | C5 |
| TT Tau | -12 | N | C5 |
| HD 180953 | -16 | N | C5 |
| AQ And | -19 | N | C6 |
| TT Cyg | -33 | N | C6 |
| RS Cyg | -37 | Ne | C5 |
| V Ari | -191 | R0, CH | C5 |

TABLE 19. STARS WITH "A"-QUALITY VELOCITIES USED TO ESTABLISH STANDARD WAVELENGTHS IN THE INFRARED

| Feature No. | Rest Wavelength | Main Contributor | St. Devn (km/s) | N |
|-------------|-----------------|---------------------|-----------------|----|
| 1 | 7479.287 | CN | 6.1 | 9 |
| 2 | 7692.477 | CN | 8.5 | 11 |
| 3 | 7714.804 | Ni, C ₂ | 10.3 | 11 |
| 4 | 7765.840 | C ₂ , CN | 4.0 | 8 |
| 5 | 7851.035 | CN (bh) | 15.5 | 10 |
| 6 | 7995.146 | CN | 10.0 | 10 |
| 7 | 7999.598 | CN | 13.4 | 11 |
| 8 | 8021.041 | CN | 12.4 | 10 |
| 9 | 8187.644 | CN | 13.7 | 8 |
| 10 | 8297.700 | CN | 11.8 | 8 |
| 11 | 8338.297 | CN | 7.9 | 8 |
| 12 | 8343.629 | CN | 10.3 | 7 |
| 13 | 8405.211 | CN | 14.3 | 9 |
| 14 | 8426.466 | CN, Ti | 10.0 | 9 |
| 15 | 8487.968 | CN | 6.7 | 5 |
| 16 | 8498.941 | Ca II, CN | 11.9 | 10 |
| 17 | 8662.238 | Ca II | 12.6 | 7 |

TABLE 20. STANDARD WAVELENGTHS AND ACCURACIES OF FEATURES DEFINING THE RADIAL VELOCITY SYSTEM

| Feature No. | Set on | Additional qualifications |
|-------------|--------|--|
| 1 | Min | Reasonably symmetrical minimum. |
| 2 | CG | |
| 3 | CG | |
| 4 | CG | Ought to have the typical width. |
| 5 | Min | Min should be close to steep edge. |
| 6 | CG | Must resolve 7992 line. |
| 7 | CG | |
| 8 | CG | |
| 9 | Min | Must have sharp min close to steep edge. |
| 10 | Min | Must have sharp min close to steep edge. |
| 11 | Min | Must have sharp min & very steep edge. |
| 12 | Min | Must have sharp min. |
| 13 | Min | Should be fairly deep line. |
| 14 | CG | |
| 15 | Min | Extremely sharp minimum. |
| 16 | CG+Min | |
| 17 | CG | |

All lines to be set on the minimum (Min) should have their minimum following smoothly from the adjacent maximum without any abrupt changes in the slope of the profile.

Lines to be set on the center-of-gravity (CG) should be reasonably symmetrical. These lines generally have a typical width of 3 to 4 pts (about 2 A).

TABLE 21. ACCEPTANCE CRITERIA FOR WAVELENGTH STANDARDS

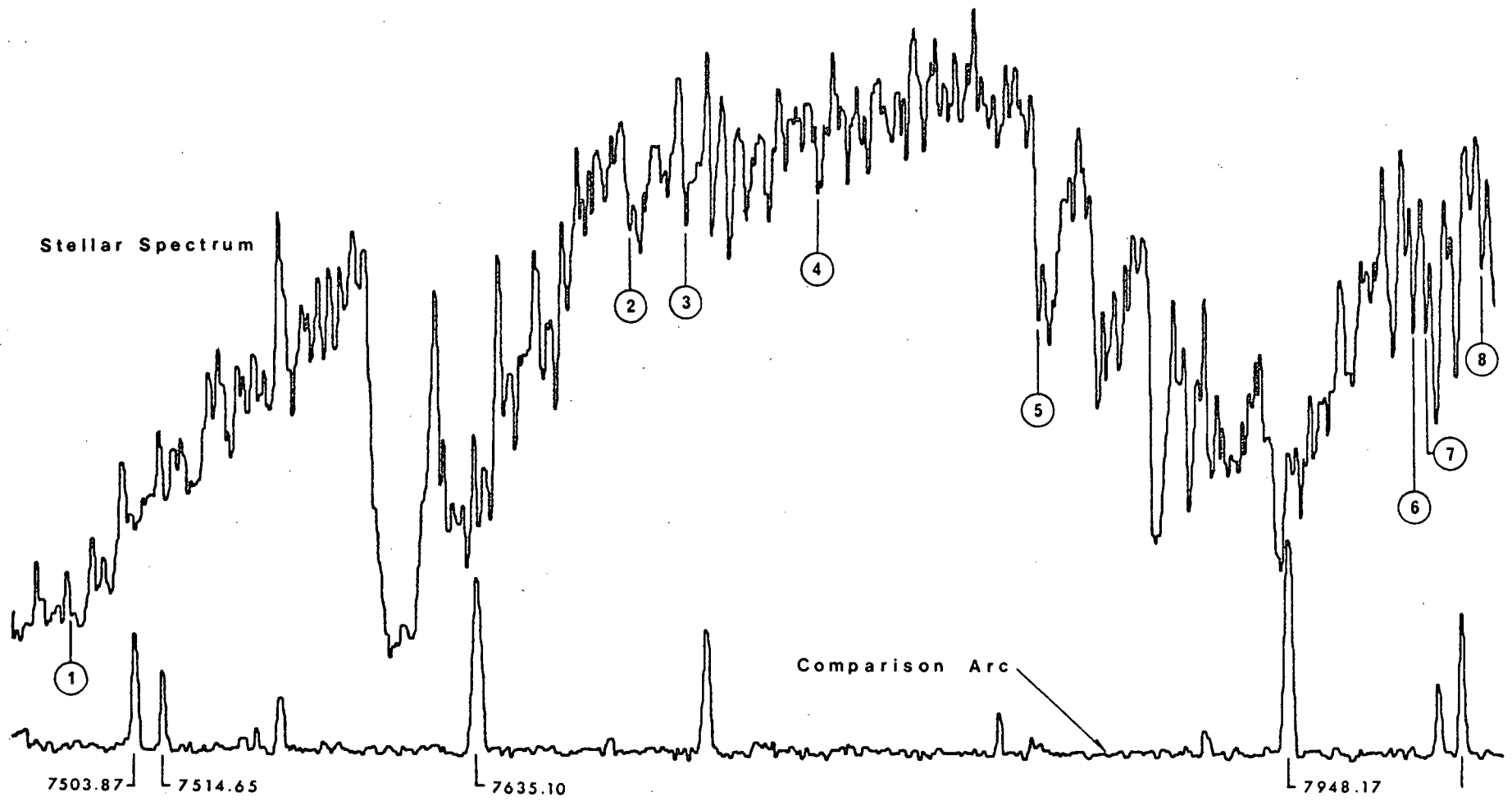


Figure 15. Identification of Wavelength Features for Near Infrared Radial Velocity System

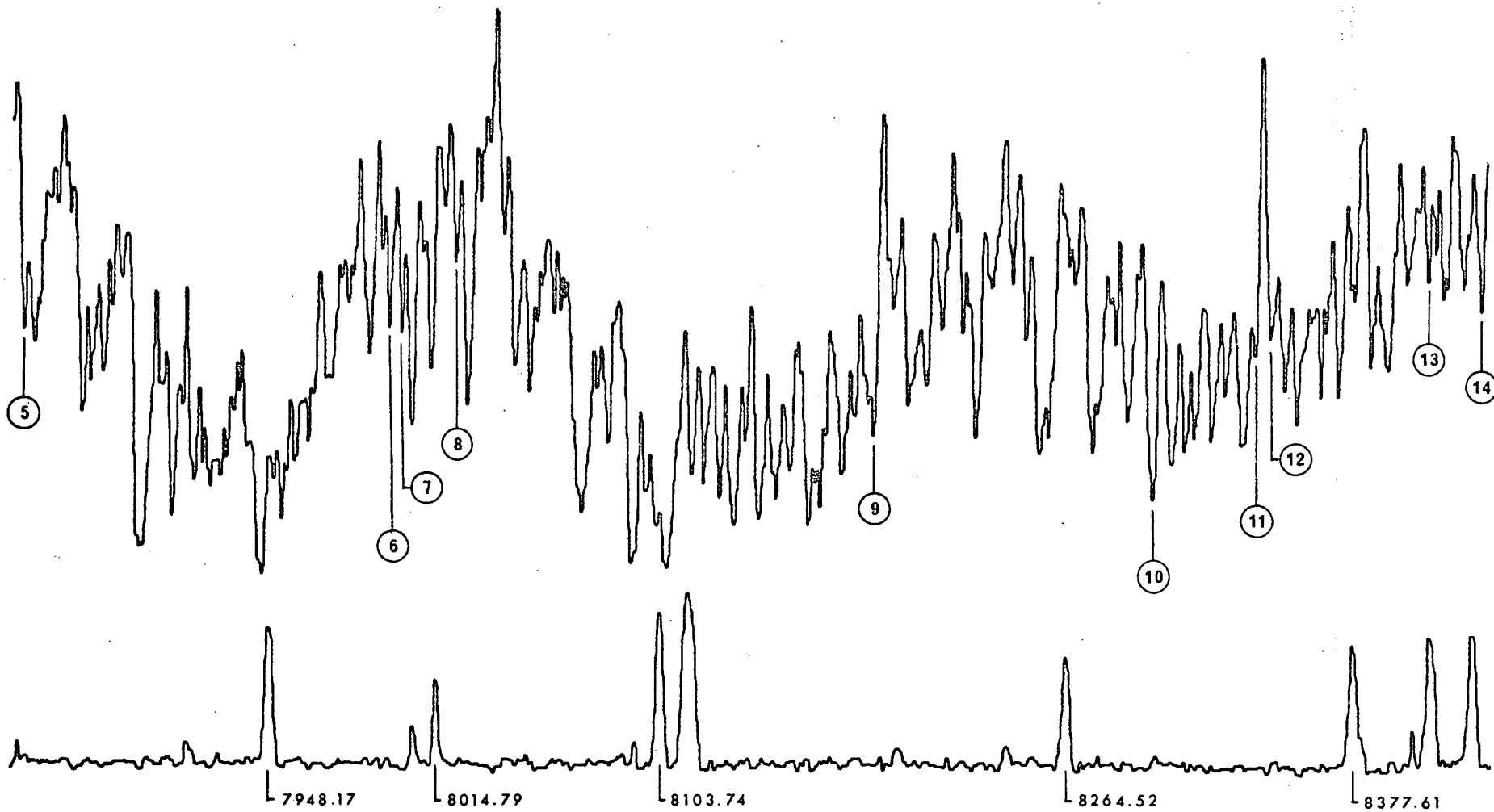


Figure 15. (continued)

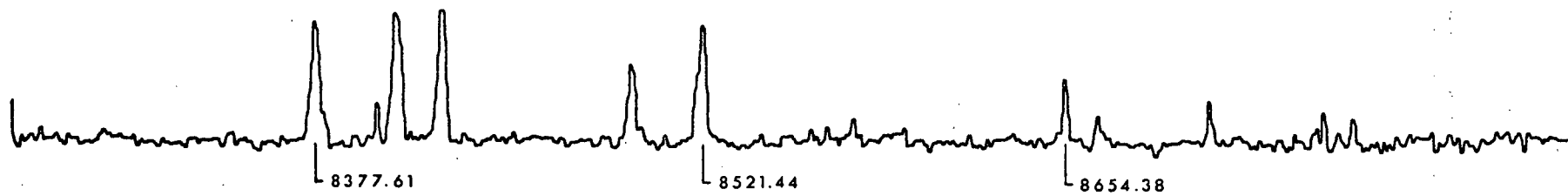
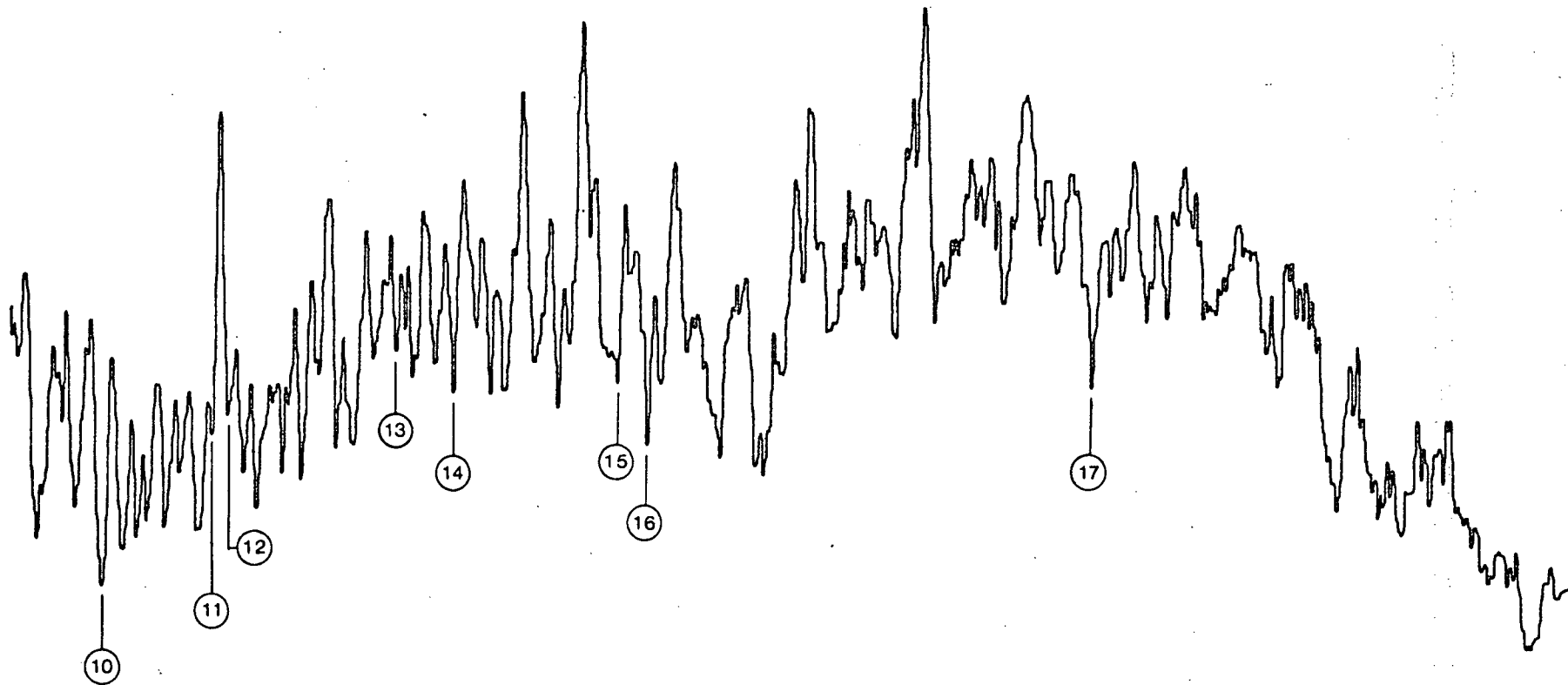


Figure 15. (concluded)

APPENDIX II

USE OF MICRODENSITOMETER AND COMPUTER PROGRAMS
TO MEASURE RADIAL VELOCITIES

The method of measuring radial velocities outlined in the previous Appendix and described in more detail here is, unfortunately, rather laborious and time-consuming. Although this University does have a Grant oscilloscope measuring machine, this instrument does not have sufficient sensitivity to permit setting on many of the weak features indicated in Fig. 15. The wavelength standards derived here do not, of course, depend on the measurement technique but only require that the instrument used be sufficiently sensitive with a 5 micron slit width to show contrast comparable to that of Fig. 15. For the following it is assumed that the reader is familiar with the operation of the Joyce-Loebl Autodensidater (see e.g. Olson 1971).

The Autodensidater is used to generate a digitized spectrum punched on paper tape. This spectrum must be decoded and stored before further processing is done. The positions of the comparison arc lines are found using the "ARC" program and a dispersion curve is fitted to those positions. Finally the "STELLAR2" program is used to find the positions of the stellar features and calculate their wavelengths.

Since the comparison arc lines must be recorded at the same time as the stellar spectrum, a mask has been constructed to fit immediately in front of the Autodensidater analyzing slit. This

permits rapid switching back and forth between the stellar and arc spectra.

A scan should normally start near 7450 Å and end past 8700 Å. The mask should be used to switch over to record the comparison arc for those lines marked in Fig. 15, except 8654 Å which is too close to the stellar 8662 Å line. To get this line, return past 8521 Å and record only the arc; this will allow calculation of the offset to 8654 Å. The paper tape should be started by keying in the characters "000*999*" and ended by a "D".

The card deck setups for the six applicable programs are given below. Input is in either free format of integer, real or logical type (I, R, L) or literal data in 'A' format.

The tape is decoded using the "DENSITY" program:

```

$RUN DENSITY 1=DensityFile
1. NrPts (I)
$END

```

NrPts should be a multiple of 2000; max. = 30000.

The plate density values should next be printed out using the "PRINTT" program:

```

$RUN PRINTT 1=DensityFile

```

The arc line positions are calculated and punched on cards using the "ARC" program. This program requires the point index of the peak of each line as input; this can be gotten from the printed density values.

```
$RUN ARC 1=DensityFile 8=*PUNCH*
```

```
1. Line positions      Max = 50                      (I...)
```

```
Repeat card 1 as required.
```

```
$END
```

The dispersion curve coefficients are calculated by the "OLQF" program. The input is the same as that required by the UBC library program *OLQF.

```
$RUN OLQF
```

```
1. Nr. of Pts, Order to fit, "0", "T".              (3I,L)
```

```
2. Pos'n, Wavelength                                (2R)
```

```
Card 2 repeated "Nr of Pts" times.
```

```
$END
```

This program should be run with judicious deletion of lines until the fit is adequate.

The wavelengths of the stellar features are calculated using the "STELLAR2" program:

```

$RUN STELLAR2 1=DensityFile
1. Dispersion curve coefficients      Max = 5          (5R)
2. Line positions                    Max = 100       (I...)
    Repeat card 2 as required.
$END

```

The density values near the stellar lines may be plotted to assist in judging whether a line profile is acceptable:

```

$RUN PLOTT 1=DensityFile
1. Literal title                      (20A4)
2. Low & High pt indices of region to be plotted;
    Low & High density values to be plotted.      (4I)
    Repeat card 2 as desired.
$END

```

The radial velocity may now be calculated by the usual method from the measured line wavelengths and the rest wavelengths of Table 20.

Appendix II
Listing of Computer Programs

```

C      "DENSITY"
C
      INTEGER*2 IDATA, IDPLT(30000)
      NCOUNT = 0
      MISSTP = 0
      NCALLS = 0
      CALL FREAD (-2, 'ENDFILE', 1)
      CALL FREAD (5, 'I:', NDATA, &10)
10  IF (NDATA.LT.1) NDATA=30000
      NDATA = (NDATA+1999)/2000*2000
      DO 9 J = 1, NDATA
      NCALLS = NCALLS + 1
      CALL JCLBL (IDATA, NCOUNT, NBOGUS, MISSTP, &8)
      IF (IDATA.EQ.1000) GO TO 8
      IDPLT(J) = IDATA
9  CONTINUE
8  WRITE (6,4) NCALLS, NCOUNT, MISSTP
4  FORMAT('NR OF JCLBL CALLS', 10X, '=' , I6, '/', 'NR OF DATA COUNTS'
+ ' BY JCLBL =', I6, '/', 'NR OF TAPE ERRORS', 10X, '=' , I6)
      ND= ((NCALLS+1999)/2000)*2000
      DO 1 J = 1, ND, 2000
      K = J + 1999
      WRITE (1) (IDPLT(I) , I=J,K)
1  CONTINUE
      STOP
      END

C
      SUBROUTINE JCLBL (IDATA, NCOUNT, NBOGUS, MISSTP)
      INTEGER*2 IDATA, IA(4)
      NZERO = 0
201 DO 200 N = 1, 4
      CALL PTAPE (I, &210, &210)
      I = IABS(I)
      IF (I.GT.128) I = I - 128
      IF (I.EQ.42) GO TO 202
      IF (N.EQ.4) GO TO 205
      IA(N) = I - 48
      IF (IABS(I-53).LE.5) GO TO 200
      IF (I.EQ.68) IDATA = 1000
      IF (IDATA.EQ.1000) RETURN
      IF (I.EQ.0) NZERO = NZERO + 1
      IF (NZERO.LT.9000) GO TO 201
      IF (NZERO.GE.9000) IDATA = 1000
      RETURN
200 CONTINUE
202 IF (N.EQ.4) GO TO 204
      IF (NCOUNT.EQ.0) GO TO 201
205 MISSTP = MISSTP + 1
      DO 206 J = 1, 4
      CALL PTAPE (I, &210, &210)
      IF (IABS(I).GT.128) I = IABS(I)-128
      IF (J.EQ.4.AND.I.EQ.42) WRITE (6, 101) NCOUNT
      IF (J.EQ.4.AND.I.EQ.42) NCOUNT = NCOUNT + 1

```

Appendix II
Listing of Computer Programs

```

      IF (I.EQ.42) GO TO 207
206 CONTINUE
207 IDATA = 0
      NCOUNT = NCOUNT + 1
      WRITE (6,101) NCOUNT
101 FORMAT (' DUE TO TAPE ERROR, DATA=0 AT POINT =',I6)
      RETURN
204 IDATA = 100*IA(1) + 10*IA(2) + IA(3)
      NCOUNT = NCOUNT + 1
      RETURN
210 WRITE (6,152) NCOUNT,NZERO
152 FORMAT (' END OF TAPE AT PT',I5,10X,'NZERO =',I5)
      RETURN 1
      END

```

```

C      "OLQF"
C
      DIMENSION X(50),Y(50),YF(50),YD(50),WT(50),S(10),SG(10),
* A(10), B(10),P(10),YL(50)
      REAL*8 DISP,XO,YO,LAM
      LOGICAL LK
      CALL FREAD (-2,'ENDFILE',1)
210 LK=.FALSE.
      CALL FREAD (5,'3I,L:',M,K,NWT,LK,&220)
      DO 200 I = 1, M
      CALL FREAD (5,'3R:',X(I),Y(I),WT(I))
200 CONTINUE
      CALL OLQF (K,M,X,Y,YF,YD,WT,NWT,S,SG,A,B,SS,LK,P)
      KP = K + 1
      KPP = K + 2
      WRITE (6,150) K
150 FORMAT ('4',T50,'DEGREE OF CHOSEN POLYNOMIAL WAS',I4,/,/,
+ T10,'X',T26,'Y',T38,'Y--FITTED RESIDUALS',5X,
+ 'RESID 1ST ORD',7X,'SIGMA',13X,'P',/)
      XO = DBLE(X(1))
      YO = DBLE(Y(1))
      DISP = (DBLE(Y(M))-YO)/(DBLE(X(M))-XO)
      DO 230 J = 1, M
      LAM = DISP * (X(J)-XO) + YO
      YL(J)=LAM-Y(J)
230 CONTINUE
      WRITE(6,151) (X(I),Y(I),YF(I),YD(I),YL(I),SG(I),P(I),I=1,KP)
151 FORMAT (1X,E16.7,E16.6,E16.6,F12.3,4X,F12.3,4X,2E16.8)
      WRITE (6,152) (X(I),Y(I),YF(I),YD(I),YL(I),I=KPP,M)
152 FORMAT (1X,E16.7,E16.6,E16.6,F12.3,4X,F12.3)
      GO TO 210
220 WRITE (6,150) NWT
      STOP
      END

```

Appendix II
Listing of Computer Programs

```

C      "ARC"
C
      INTEGER*2 IN(4000)
      INTEGER IPOS(50)/50*0/
      REAL PP(6),WL(9)/7503.87,7514.65,7635.10,7948.17,8014.79,
* 8103.74,8264.52,8377.61,8521.44/
      REAL*8 S,SS
      LOGICAL PCHWL/.FALSE./
      READ (1) (IN(I),I=1,2000)
      READ (1,END=200) (IN(I),I=2001,4000)
200 CALL FREAD (-2,'ENDLINE','STREAM')
      CALL FREAD (5,'I V:',IPOS)
      CALL FREAD (-2,'NUMBER',NP)
      WRITE (6,152)
152 FORMAT ('1STAR NAME =',T40,'PLATE NO =',T80,'ARC POSNS',//)
      IF (NP.EQ.15) PCHWL = .TRUE.
      DO 204 JJ = 1, NP
      P = 0.0
      MID = IPOS(JJ)
      Y0 = IN(MID-1)
      Y1 = IN(MID)
      Y2 = IN(MID+1)
      B = 2.0*Y1 - 1.5*Y0 - 0.5*Y2
      C = 0.5*Y0 - Y1 + 0.5*Y2
      IF (C.EQ.0.0) GO TO 317
      P = -0.5*B/C + FLOAT(MID-1)
317 DO 300 J = 1, 10
      JA = MID-J
      IF (IN(JA-1).GT.IN(JA)) GO TO 301
300 CONTINUE
301 DO 302 J = 1, 10
      JB = MID+J
      IF (IN(JB+1).GT.IN(JB)) GO TO 303
302 CONTINUE
303 IMN = IN(JA)
      IF (IN(JB).GT.IMN) IMN = IN(JB)
      IMX = IN(MID)
      HT = IMX-IMN
      DO 305 IL = 3,8
      HLV = IMN + 0.1*IL*HT
      DO 306 J = JA, MID
      IF (IN(J).LE.HLV .AND. IN(J+1).GT.HLV) GO TO 307
306 CONTINUE
307 PP(IL-2) = J + (HLV-IN(J))/(IN(J+1)-IN(J))
      DO 308 J = MID,JB
      IF (IN(J).GE.HLV .AND. IN(J+1).LT.HLV) GO TO 309
308 CONTINUE
309 PP(IL-2) = (J+(HLV-IN(J))/(IN(J+1)-IN(J))+PP(IL-2))/2.0
305 CONTINUE
      N = 6
314 S = 0D0
      SS = 0D0
      DO 310 J = 1, N

```

Appendix II
Listing of Computer Programs

```

      S = S + DBLE(PP(J))
      SS = SS + DBLE(PP(J))**2
310  CONTINUE
      AVG = S/N
      SD = DSQRT ((SS-S**2/DFLOAT(N))/DFLOAT(N-1))
      IF (SD.LE.0.1 .OR. N.LE.3) GO TO 311
      XD = 0.0
      DO 312 J = 1, N
      IF (ABS(AVG-PP(J)).GT.XD) XD = ABS(AVG-PP(J))
312  CONTINUE
      M = 0
      DO 313 J = 1, N
      IF (ABS(AVG-PP(J)).GE.XD) GO TO 313
      M = M+1
      PP(M) = PP(J)
313  CONTINUE
      N = M
      GO TO 314
311  WRITE (6,150) MID,P,AVG,N,SD
150  FORMAT ('0MIDPT =',I5,10X,'PEAK =',F10.3,10X,'CENTER =',
+ F10.3,10X,I2,' PT ST.DEV =',F6.3)
      IF (PCHWL) GO TO 320
      IF (JJ.LE.9) WRITE (8,151) AVG
      GO TO 204
320  IF (JJ.LE.9) WRITE (8,151) AVG,WL(JJ)
151  FORMAT (F10.3,F10.2)
204  CONTINUE
      STOP
      END

```

```

C      "PRINTT"
C
      INTEGER*2 ID(2000)
200  READ (1,END=201) ID
      WRITE (6,150) ID
150  FORMAT (25I5)
      GO TO 200
201  STOP
      END

```

Appendix II
Listing of Computer Programs

```

C      "STELLAR2"
C
      DIMENSION X(25),Y(25),IPS(100),XO(100)
      DIMENSION T(220),SS(220),SS1(220),SS2(220)
      REAL*4 COF(5)
      INTEGER*2 IN(4000)
      EPSLN = 1.0E-4
      READ (1) (IN(I),I=1,2000)
      READ (1,END=207) (IN(I),I=2001,4000)
207 CALL FREAD (5,'R V:',COF)
      CALL FREAD (-2,'NUMBER',NCF)
      CALL FREAD (-2,'ENDLINE','STREAM')
      CALL FREAD (5,'I V:',IPS)
      CALL FREAD (-2,'NUMBER',NPOS)
      WRITE (6,150)
150 FORMAT ('1STAR =',T40,'PLATE NO =',T80,'STELLAR LINES',//)
      WRITE (6,159) (COF(J),J=1,NCF)
159 FORMAT (' WAVELENGTH COEFFS: ',5G16.7)
      WRITE (6,161)
161 FORMAT ('0',T29,'MINIMUM',T60,'CENTER OF GRAVITY',T97,
+ 'DEPTH      WIDTH      AREA',/,T25,'POSN      WAVELENGTH',T62,
+ 'POSN      WAVELENGTH',T98,'(DU)      (DP)      (DU.DP) ')
      DO 250 NT = 1, NPOS
      MID = IPS(NT)
      IB = MID - 10
      IE = MID + 10
      DO 251 J = 1, 10
      IX = MID - J
      IF (IN(IX+1)-IN(IX).GE.100) GO TO 252
      IF (IX.LE.3) GO TO 252
251 CONTINUE
      GO TO 253
252 IB = IX + 1
253 DO 254 J = 1, 10
      IX = MID + J
      IF (IN(IX-1)-IN(IX).GE.100) GO TO 255
254 CONTINUE
      GO TO 256
255 IE = IX - 1
256 NPTS = IE - IB + 1
      IF (NPTS.LE.10) WRITE (6,155) MID
155 FORMAT ('0NOT ENOUGH PTS FOR SPLINE AROUND MINIMUM AT',I5)
      IF (NPTS.LE.10) GO TO 250
      IX = 0
      DO 257 J = IB, IE
      IX = IX + 1
      X(IX) = FLOAT(J)
      Y(IX) = IN(J)
257 CONTINUE
      M = 10*NPTS - 9
      DO 300 J = 1, M
      T(J) = IB + 0.1 * (J-1)
300 CONTINUE

```

Appendix II
Listing of Computer Programs

```

CALL SPLINE (NPTS,M,EPSLN,X,Y,T,PROXIN,SS,SS1,SS2)
XM = FLOAT(MID)
CALL SPLINV (XM,V,SL,SD)
IF (SL.EQ.0.0) GO TO 249
ISP = IFIX (SIGN(1.1,SL))
260 SLP = SL
XMP = XM
XM = XMP - 0.5*ISP
CALL SPLINV (XM,V,SL,SD)
IF (SL.EQ.0.0) GO TO 249
IS = IFIX (SIGN(1.1,SL))
IF (IS.EQ.ISP) GO TO 260
263 AA = (SL-SLP)/(XM-XMP)
BB = SL - AA*XM
XMN = -BB/AA
CALL SPLINV (XMN,V,SLN,SD)
ISN = IFIX(SIGN(1.1,SLN))
IF (ISN.NE.ISP) GO TO 261
IF (ABS(XMN-XMP).LE.0.0015) GO TO 265
XMP = XM
SLP = SL
ISP = IS
GO TO 262
261 IF (ABS(XMN-XM).LE.0.0015) GO TO 265
262 XM = XMN
SL = SLN
IS = ISN
GO TO 263
265 XM = XMN
249 DO 301 J = 3, M
IF (T(J).GT.XM) GO TO 302
IBOTM = J
301 CONTINUE
302 IBB = J+1
DO 303 I = IBB,M
IF (SS(I).LE.SS(I-1)) GO TO 305
JR = I - 10
JL = I - 20
IF (JL.LE.IBB) JL = IBB - 1
IH = (JL+I)/2
IF (JR.LT.IH) JR = IH
D = SS(JR) - SS(JL)
IF (D.LE.0.0) GO TO 303
XT = (SS(I)-SS(JL))*(JR-JL)/D+JL
XT = IB + 0.1*(XT-1.0)
IF (T(I)-XT.LT.0.4) GO TO 303
LRT = (I+JR)/2
GO TO 306
303 CONTINUE
305 LRT = I-1
306 IBB = IBB - 3
IE = IBB-2
DO 307 IX = 1, IE

```

Appendix II
Listing of Computer Programs

```

I = IBB - IX
IF (SS(I).LE.SS(I+1)) GO TO 308
JR = I + 20
JL = I + 10
IF (JR.GE.IBB) JR = IBB + 1
IH = (I+JR)/2
IF (JL.GT.IH) JL = IH
D = SS(JR) - SS(JL)
IF (D.GE.0.0) GO TO 307
XT = (SS(I)-SS(JL))*(JR-JL)/D + JL
XT = IB + 0.1*(XT-1.0)
IF (XT-T(I).LT.0.4) GO TO 307
LLT = (I+JL)/2
GO TO 309
307 CONTINUE
308 LLT = I+1
309 IF (SS(LLT).GT.SS(LRT)) GO TO 310
VEL = SS(LLT)
DO 311 J = IBB, LRT
IF (SS(J).GT.VEL) GO TO 312
311 CONTINUE
312 LRT = J-1
GO TO 314
310 VEL = SS(LRT)
DO 313 J = LLT, IBB
IF (SS(J).LE.VEL) GO TO 315
313 CONTINUE
315 LLT = J
314 XLEN = (LRT-LLT)/10.0
HHT = VEL - SS(IBOTM)
IO = 1
IF (XLEN.GT.1.0) GO TO 319
AREA = 0.0
IO = 0
XWT = 1.0
GO TO 325
319 AR = 0.0
DO 320 J = LLT, LRT
AR = AR + (VEL-SS(J))
320 CONTINUE
AREA = AR/10.0
AR2 = AR/2.0
AR = 0.0
DO 321 J = LLT, LRT
AR = AR + (VEL-SS(J))
IF (AR.GE.AR2) GO TO 322
321 CONTINUE
322 FR = (AR2-(AR-(VEL-SS(J)))) / (VEL-SS(J))
XWT = J-1+0.5*FR
XWT = IB+0.1*(XWT-1.0)
325 W1 = 0.0
W2 = 0.0
DO 331 J = 1, NCF

```

Appendix II
Listing of Computer Programs

```

W1 = W1 + COF(J)*XM**(J-1)
W2 = W2 + COF(J)*XWT**(J-1)
331 CONTINUE
  IF (IO.EQ.0) W2 = 0.0
323 WRITE (6,160) NPTS,MID,XM,W1,XWT,W2,HHT,XLEN,AREA
160 FORMAT ('0',I2,' PTS AT',I5,4X,2F11.3,15X,2F11.3,15X,
+ 2F8.1,F12.3)
250 CONTINUE
  STOP
  END

```

```

C
  SUBROUTINE SPLINE (N,M,EPSLN,X,Y,T,PROXIN,SS,SS1,SS2)
C COMPUTES NATURAL CUBIC SPLINE. ALSO GETS INTEGRAL OVER KNOTS.
C FINALLY, EVALUATES SPLINE (S',S'') AT VARIOUS ABSCISSAE.
C SOURCE: GREVILLE IN <MATH METHODS FOR DIGITAL COMPUTERS>
C VOL II RALSTON/WILF INTERPOLATION ON N PAIRS,
C (X,Y)-VALUES AT M T-VALUES. INTEGRAL = PROXIN.
C SPLINE AND DERIVATIVES IN M SS-,SS1-,SS2-VALUES.
C SS2(X) ARE FOUND BY SOR WITH CONVERGENCE PARAMETER EPSLN.
  REAL X(25),Y(25),B(25)
  REAL T(220),SS(220),SS1(220),SS2(220)
  REAL H(25),DELY(25),H2(25),DELSQY(25),S2(25),C(25),S3(25)
  N1 = N-1
  H(1) = X(2)-X(1)
  DELY(1) = (Y(2)-Y(1))/H(1)
  DO 52 I = 2, N1
  H(I) = X(I+1)-X(I)
  H2(I) = H(I-1)+H(I)
  B(I) = 0.5*H(I-1)/H2(I)
  DELY(I) = (Y(I+1)-Y(I))/H(I)
  DELSQY(I) = (DELY(I)-DELY(I-1))/H2(I)
  S2(I) = 2.0*DELSQY(I)
52 C(I) = 3.0*DELSQY(I)
  S2(1) = 0.0
  S2(N) = 0.0
  OMEGA = 1.071797
  5 ETA = 0.0
  DO 10 I = 2, N1
  W = (C(I)-B(I)*S2(I-1)-(0.5-B(I))*S2(I+1)-S2(I))*OMEGA
  IF (ABS(W).LE.ETA) GO TO 10
  ETA = ABS(W)
  10 S2(I) = S2(I)+W
  IF (ETA.GE.EPSLN) GO TO 5
  DO 53 I = 1, N1
53 S3(I) = (S2(I+1)-S2(I))/H(I)
  AR = DELY(N1)+H(N1)*S2(N1)/6.0
  AL = DELY(1)-H(1)*S2(2)/6.0
  PROXIN = 0.0
  DO 62 I = 1, N1
62 PROXIN = PROXIN+0.5*H(I)*(Y(I)+Y(I+1))
  # -H(I)**3*(S2(I)+S2(I+1))/24.
  IF (M.LE.0) RETURN
  GO TO 15

```

Appendix II
Listing of Computer Programs

```

ENTRY SPLINV(ARG,SP,SP1,SP2)
C COMPUTES SPLINE AND ITS 1ST 2 DERIVS AT 'ARG'; RETNS SP,SP1..
  M = 1
  T(1) = ARG
15 DO 61 J = 1, M
  I = 1
  IF (T(J)-X(1)) 58,17,55
55 IF (T(J)-X(N)) 57,59,580
56 IF (T(J)-X(I)) 60,17,57
57 I = I+1
  GO TO 56
58 SS(J) = AL*(T(J)-X(1))+Y(1)
  SS1(J) = AL
  SS2(J) = 0.0
  GO TO 61
580 SS(J) = AR*(T(J)-X(N))+Y(N)
  SS1(J) = AR
  SS2(J) = 0.0
  GO TO 61
59 I = N
60 I = I-1
17 HT1 = T(J)-X(I)
  HT2 = T(J)-X(I+1)
  PROD = HT1*HT2
  SS2(J) = S2(I)+HT1*S3(I)
  DELSQS = (S2(I)+S2(I+1)+SS2(J))/6.0
  SS(J) = Y(I)+HT1*DELY(I)+PROD*DELSQS
  SS1(J) = DELY(I)+(HT1+HT2)*DELSQS+PROD*S3(I)/6.0
61 CONTINUE
  SP = SS(1)
  SP1 = SS1(1)
  SP2 = SS2(1)
  RETURN
  END

```

Appendix II
Listing of Computer Programs

```

C      "PLOTT"
C
      REAL*4 MULT,TITLE(20)
      INTEGER*2 IN(4000),HEX00/ZFOFO/,NX,NH,
* F(9) / ('1','H9','I','5',' ',' ','X','1H','*') /
      READ (5,1001) TITLE
1001 FORMAT (20A4)
      CALL FREAD (-2,'ENDFILE',1)
      READ (1) (IN(I), I=1,2000)
      READ (1,END=2030) (IN(I),I=2001,4000)
2030 CALL FREAD (5,'4I:',NMIN,NMAX,IBOT,ITOP,&9999)
      IF (NMAX.LE.NMIN .OR. NMAX.LE.0) GO TO 2030
      IF (NMIN.LE.0) NMIN = 1
      IF (NMAX.GT.4000) NMAX = 4000
      IF (IBOT.LT.0 .OR. IBOT.GE.999) IBOT = 0
      IF (ITOP.LE.0 .OR. ITOP.GT.999) ITOP = 999
      IF (ITOP-IBOT.GE.124) GO TO 2010
      IF (999-IBOT.GE.124) GO TO 2011
      ITOP = 999
      IBOT = 875
      GO TO 2010
2011 IF (ITOP.GE.124) GO TO 2012
      ITOP = 124
      IBOT = 0
      GO TO 2010
2012 IMID = (ITOP+IBOT) / 2
      ITOP = IMID + 62
      IBOT = IMID - 62
2010 MULT = 124.0 / FLOAT(ITOP-IBOT)
      ZER = 1.001 - MULT*IBOT
      SC = 1.0 / MULT
      WRITE (6,1051) TITLE,IBOT,ITOP,SC
1051 FORMAT ('1',20A4,/,,' BOTTOM VALUE =',I5,10X,' TOP VALUE =',
+ I5,15X,'SCALE =',F7.3,' / PRINT POSN',/)
      DO 2001 NPT = NMIN, NMAX
      NX = IN(NPT)*MULT + ZER
      IF (NX.GE.1 .AND. NX.LE.125) GO TO 2040
      IF (NX.LE.0) WRITE (6,226) NPT
      IF (NX.GT.125) WRITE (6,227) NPT
      GO TO 2001
2040 NH = NX/100
      F(5) = NH + HEX00
      NX = NX-100*NH
      F(6) = NX/10*256 + NX-NX/10*10 + HEX00
      WRITE (6,F) NPT
2001 CONTINUE
      GO TO 2030
9999 WRITE (6,1052)
1052 FORMAT ('1')
      STOP
      226 FORMAT ('9',I5,'<')
      227 FORMAT ('9',I5,125X,'>')
      END

```

APPENDIX III

THE RATIO OF TOTAL TO SELECTIVE ABSORPTION

It has long been known that the ratio of total to selective absorption [R] for the (UBV) photometric system is not a constant depending only on the shape of the interstellar reddening curve, but is also a function of the colour of the star being observed (e.g. Blanco 1956). This additional effect is caused by the wide bandpass of the (UBV) filters, allowing the effective wavelengths of the filters to shift with different stellar intensity gradients. This must be taken into account if we want to derive the intrinsic colours of the carbon stars or their distances, since their colour excesses will not be the same as for the bluer companions.

Previous studies of this effect show that the value of R increases toward later spectral types, but the actual numerical results for very cool stars are not agreed upon. Blanco and Lennon (1961) found an increase from 3.1 for early-type stars to 3.7 for α Ori (M2 Ia, $B-V=1.86$), the ratio being insensitive to colour excess for the early-type stars but steadily decreasing with colour excess from about type K0 onwards. Schmidt (1956) found R to increase with colour excess for all spectral types except N, and found a value of 4.25 for three carbon stars, which was relatively insensitive to the excess. Similarly, Honeycutt (1972) found R to be relatively constant at a value of 3.8 for two carbon stars with $B-V = 2.5$.

In an attempt to eliminate these discrepancies and to define the variation of the R-values with intrinsic colour and colour excess this problem was re-examined.

The ratio of total to selective absorption is given by

$$R = A(V) / E(B-V) = A(V) / [A(B) - A(V)] \quad (33)$$

$$\text{where } A(i) = -2.5 \log \left\{ \frac{\int_0^\infty \tau^X(\lambda) \phi_i(\lambda) I(\lambda) d\lambda}{\int_0^\infty \phi_i(\lambda) I(\lambda) d\lambda} \right\}. \quad (34)$$

The transmission function of the i 'th filter-cell combination is given by $\phi_i(\lambda)$, and the star's spectral intensity distribution by $I(\lambda)$, and the transmission function of X units of interstellar matter by $\tau^X(\lambda)$

$$\text{where } \tau(\lambda) = 10^{** -[\delta_m(\lambda) - \delta_m(\infty)]/2.5} \quad (35)$$

$\delta_m(\lambda)$ is the usual ordinate of the interstellar reddening curve and $\delta_m(\infty)$ is the value of the interstellar absorption extrapolated to infinite wavelength.

The reddening curve has been taken from Underhill and Walker (1966) and normalized to give $A(V) = 0$ and $E(B-V) = 1$:

$$\begin{aligned} \delta_m(\lambda) &= 2.23 (\lambda^{-1} - 1.83) \text{ for } \lambda^{-1} < 2.25 \\ \delta_m(\lambda) &= 1.42 (\lambda^{-1} - 1.59) \text{ for } \lambda^{-1} > 2.25. \end{aligned} \quad (36)$$

The parameter $\delta_m(\infty)$ is essentially a free parameter and has been

set to 3.12 to give a value of $R = 3.20$ for early-type stars. This is a widely accepted value which seems to hold for most regions in the galaxy. Johnson (1968) concludes that 3.0 is the minimum possible value and cites several cases of much higher values. Other authors prefer R values in the range 3.1 to 3.2 (e.g. Johnson and Borgman 1963, Schmidt-Kaler 1965).

The filter transmission functions have been taken from Matthews and Sandage (1963), while the stellar intensity distributions are mainly from Willstrop (1965), supplemented by the early-type calibrations of Hayes (1970) and of Oke and Schild (1970). Willstrop's data cover the wavelength range 4000 Å to 6500 Å at 25 Å intervals for many types of stars, including one S-star, one R-star and two N-stars. The short wavelength range necessitated extrapolation to the filter limits of 3600 Å and 7200 Å. This did not affect the results, however, since the agreement with Hayes and with Oke and Schild (corrected for Balmer line absorption) for those stars in common was quite good. Nor were the late-type stars affected (where the extrapolation was less certain), as a result of the low spectral intensity shortward of 4000 Å and the low filter transmission longward of 6500 Å. The numerical integrations used points at 100 Å intervals after it had been ascertained that closer spacing affected the results negligibly.

The results are presented in Figures 16 and 17. Note that the result for the N-stars ($B-V=2.4$) is in good agreement with that found by Schmidt, while the value for the M-stars ($B-V=1.6$,

$R=3.7$) compares favourably with the observational result of Lee (1970), who found $R = 3.6 \pm 0.3$ from infrared photometry of M-stars. The results for blackbodies of various temperatures are also shown in Fig. 17. These have been used as a guide in extrapolating the observed variation to redder stars.

To quantize these results, polynomials were fitted to the reddening curves of Fig. 16; polynomials were again used to define the variation of the coefficients with intrinsic colour. The coefficients of this second set of polynomials are given in Table 22.

During the course of these calculations it was noticed that the visual absorption $A(V)$ is a function of the star's intrinsic colour as well as the actual amount of intervening interstellar matter (X). Using the definition of X as in eqn. 35 this relation is given by

$$A(V) = [1.042 - 0.020*(B-V)_0] X - 0.00385 X^2 \quad (37)$$

to good accuracy for all types of stars. This effect is caused by the shift of the effective wavelength of the V filter and simply means that the redder stars are absorbed less. This term will produce a differential change in $A(V)$ of about 0.1 magnitude for a colour excess of $E(B-V) = 1.0$ only if two stars differ in intrinsic colour by $(B-V) > 3.0$. Hence this term would usually be quite negligible.

The accuracy of the calculated R values can be no better than that of the zero point value $R = 3.2$, which is generally

assigned an uncertainty of ± 0.2 or 0.3 (p.e.). The relative accuracy for comparison of early and late-type stars, however, should be somewhat better than this.

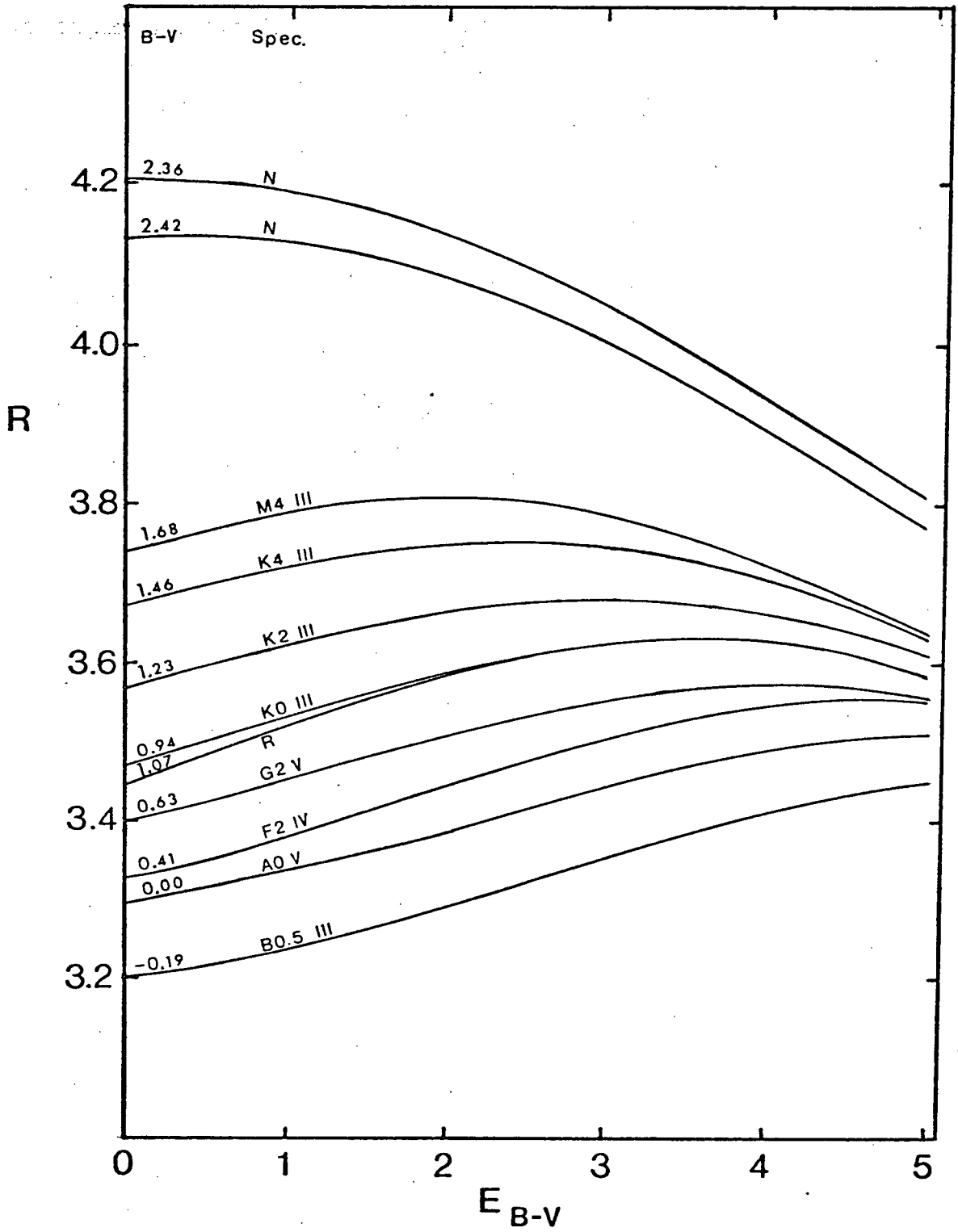


Figure 16. R vs $E(B-V)$ for various types of stars

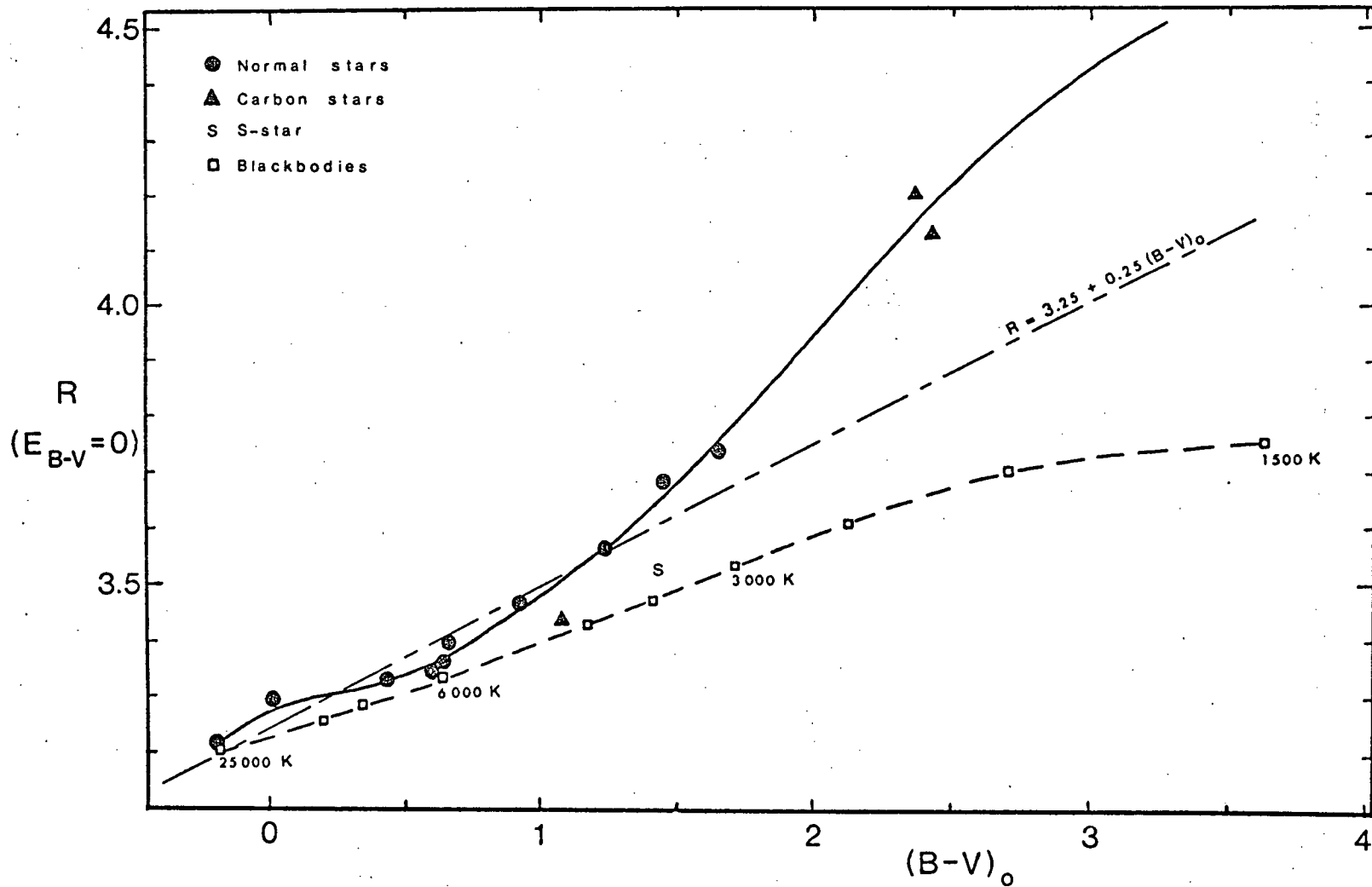


Figure 17. R [$@ E(B-V)=0$] vs $(B-V)_0$

| i | q(0,i) | q(1,i) | q(2,i) | q(3,i) |
|---|-----------------------------|-----------------------------|-----------------------------|-----------------------------|
| 0 | 3.28067 | 2.02458 x 10 ⁻² | 1.69810 x 10 ⁻² | -2.39331 x 10 ⁻³ |
| 1 | 2.47655 x 10 ⁻¹ | 3.24753 x 10 ⁻² | -5.09329 x 10 ⁻³ | -8.21006 x 10 ⁻⁴ |
| 2 | -3.92830 x 10 ⁻¹ | 6.86755 x 10 ⁻² | -2.18495 x 10 ⁻² | 2.29100 x 10 ⁻³ |
| 3 | 4.51732 x 10 ⁻¹ | -6.65211 x 10 ⁻² | 7.44152 x 10 ⁻³ | -3.98584 x 10 ⁻⁴ |
| 4 | -1.46818 x 10 ⁻¹ | 1.69069 x 10 ⁻² | 3.39048 x 10 ⁻⁶ | -8.54519 x 10 ⁻⁵ |
| 5 | 1.49948 x 10 ⁻² | -1.40081 x 10 ⁻³ | -1.34500 x 10 ⁻⁴ | 1.72167 x 10 ⁻⁵ |

$$q(m) = \sum_{i=0}^5 q(m,i) * (B-V)_0 ** i$$

$$R[E(B-V), (B-V)_0] = \sum_{m=0}^3 q(m) * E(B-V) ** m$$

TABLE 22. COEFFICIENTS OF POLYNOMIALS TO DETERMINE R FROM E(B-V) AND (B-V)₀.

APPENDIX IV

COHERENCY TABLES

This appendix contains, in tabular form, the computed coherency values for each synthetic spectrum when compared with the various observed stellar spectra. The tabular entries are the average coherency values calculated with a 5% power cutoff level. The model parameters for each entry are indicated on the left for the microturbulence and $^{13}\text{C}/^{12}\text{C}$ ratio [R] and along the bottom for the X(CNO) value. Note that these parameter values are not always in a uniform sequence; irregularities are sometimes indicated by double lines separating the columns. Each table is also marked with the parameter values of the deduced coherency peak and the mean synthetic spectrum level [\bar{S}] at the peak.

The location of the coherency peak was determined by mental interpolation in the table, with the aid of pencil and graph paper. An attempt was made to derive the peak location by least-squares fitting a three-dimensional ellipsoid to the coherency data, but this was not successful as, in fact, an ellipsoid is a poor approximation of the actual functional dependence of the coherency on the three parameters.

19 Psc with model K12

Coherency peak at $(X, \xi, R, \bar{S}) = (0.80, 3.5, 0.050, 0.491)$

| | | | | | | |
|-----|--------|--------|--------|--------|--------|--------|
| 4.0 | | | | | | |
| .07 | | | .93462 | | | |
| .05 | | .93530 | .93623 | .93504 | | |
| .03 | | | .93258 | | | |
| 3.5 | | | | | | |
| .10 | | | .92939 | | | |
| .07 | | | .93499 | .93202 | | |
| .06 | | | .93633 | | | |
| .05 | .93147 | .93579 | .93692 | .93573 | .93346 | .93053 |
| .03 | | | .93348 | .93527 | | |
| 3.0 | | | | | | |
| .07 | | | .93393 | .93132 | | |
| .05 | | .93491 | .93601 | .93516 | | .93036 |
| .03 | | | .93280 | .93490 | | |
| | 0.50 | 0.65 | 0.80 | 0.95 | 1.10 | 1.25 |

19 Psc with model K24

Coherency peak at $(X, \xi, R, \bar{S}) = (0.19, 3.75, 0.057, 0.443)$

| | | | | | | |
|-----|--------|--------|--------|--------|--------|--------|
| 4.5 | | | | | | |
| .05 | | | .93674 | | | |
| 4.0 | | | | | | |
| .10 | | | .93246 | | | |
| .07 | | | .93680 | | | |
| .05 | | .93617 | .93779 | | .93299 | |
| .03 | | | .93498 | | | |
| 3.5 | | | | | | |
| .07 | | | .93670 | | | |
| .05 | | | .93772 | | | |
| .03 | | | .93541 | | | |
| 3.0 | | | | | | |
| .05 | .93041 | | .93628 | .93410 | .93040 | .92263 |
| | 0.10 | 0.15 | 0.20 | 0.25 | 0.30 | 0.40 |

19 Psc with model K26

Coherency peak at $(X, \xi, R, \bar{S}) = (0.10, 3.75, 0.04, 0.455)$

| | | | | | | |
|------|--------|--------|--------|--------|--------|--------|
| 4.0 | | | | | | |
| .07 | | | | .93835 | | |
| .05 | | | | .94022 | | |
| .03 | | | | .93950 | | |
| 3.75 | | | | | | |
| .04 | | | .94034 | .94098 | | |
| 3.5 | | | | | | |
| .10 | | | | .93294 | | |
| .07 | | | | .93780 | | |
| .05 | | .93977 | | .94054 | .93249 | |
| .03 | | | | .94008 | | |
| 3.0 | | | | | | |
| .05 | .93322 | | | .93976 | .93176 | .91370 |
| | 0.05 | 0.08 | 0.09 | 0.10 | 0.15 | 0.25 |

Z Psc with model K12

Coherency peak at $(X, \xi, R, \bar{S}) = (0.95, 3.25, 0.054, 0.476)$

| | | | | | | |
|-----|--------|--------|--------|--------|--------|--------|
| 4.0 | | | | | | |
| .07 | | .93629 | | | | |
| .05 | .93276 | .93570 | .93611 | | | |
| 3.5 | | | | | | |
| .10 | | .93427 | | | | |
| .07 | | .93745 | .93597 | | | |
| .06 | | .93776 | | | | |
| .05 | .93395 | .93717 | .93767 | .93667 | .93473 | .93227 |
| .03 | | .93093 | .93453 | | | |
| 3.0 | | | | | | |
| .07 | | .93691 | .93583 | .93363 | | |
| .05 | .93360 | .93682 | .93775 | .93705 | | |
| .03 | | | .93482 | .93665 | | |
| 2.5 | | | | | | |
| .05 | | | .93536 | | | |
| | 0.65 | 0.80 | 0.95 | 1.10 | 1.25 | 1.40 |

Z Psc with model K26

Coherency peak at $(X, \xi, R, \bar{S}) = (0.11, 3.4, 0.058, 0.432)$

| | | | | | | |
|-----|--------|--------|--------|--------|--------|--------|
| 4.0 | | | | | | |
| .10 | | | .93911 | | | |
| .07 | | | .94058 | | | |
| .06 | | | | .94025 | | |
| .05 | | | .93911 | | | |
| .03 | | | .93300 | | | |
| 3.5 | | | | | | |
| .10 | | | .93936 | | | |
| .07 | | .94081 | .94133 | .94099 | .93992 | |
| .06 | | | | .94144 | | |
| .05 | .93594 | | .94036 | .94129 | .94122 | .93784 |
| .03 | | | .93427 | | .93773 | .93903 |
| 3.0 | | | | | | |
| .10 | | | .93784 | | | |
| .07 | .93819 | | .94071 | | .93926 | .93395 |
| .05 | | | .94035 | | .94116 | .93800 |
| .03 | | | | | | .93887 |
| | 0.08 | 0.09 | 0.10 | 0.11 | 0.12 | 0.15 |

X Cnc with model K26

Coherency peak at $(X, \xi, R, \bar{S}) = (0.17, 3.8, 0.032, 0.345)$

| | | | | | | |
|-----|--------|--------|--------|--------|--------|--------|
| 4.5 | | | | | | |
| .05 | .94883 | .94906 | | | | .94449 |
| .03 | | .94906 | | | | |
| 4.0 | | | | | | |
| .07 | | .94531 | | | | |
| .05 | | .94954 | | | | |
| .04 | | | .95092 | .95042 | | |
| .03 | | .95067 | .95134 | .95144 | .95072 | |
| .02 | | .94565 | | .94881 | .95001 | |
| 3.5 | | | | | | |
| .05 | | .94887 | | | | .94348 |
| .03 | .94759 | .95077 | .95132 | .95144 | .95058 | |
| .02 | | .94613 | | | | |
| 3.0 | | | | | | |
| .05 | | .94643 | | | | |
| | 0.13 | 0.15 | 0.16 | 0.17 | 0.19 | 0.20 |

UU Aur with model K26

Coherency peak at $(X, \xi, R, \bar{S}) = (0.14, 4.8, 0.040, 0.351)$

| | | | | | | |
|------|--------|--------|--------|--------|--------|--------|
| 6.0 | | | | | | |
| .05 | | | | .94810 | | |
| 5.5 | | | | | | |
| .07 | | .94763 | .94753 | .94710 | .94721 | |
| .05 | | | .94873 | .94891 | | |
| .04 | | | | .94893 | | |
| 5.0 | | | | | | |
| .07 | .94736 | | | | | |
| .05 | .94724 | | .94929 | .94944 | | |
| .04 | | | | .94947 | | |
| .03 | | | | .94809 | | |
| 4.75 | | | | | | |
| .07 | | | | .94739 | | |
| .05 | | | .94938 | .94936 | .94889 | |
| .04 | | | | .94955 | .94966 | .94915 |
| .03 | | | | .94825 | .94889 | |
| 4.5 | | | | | | |
| .05 | | | | .94906 | | .94772 |
| | 0.10 | 0.11 | 0.12 | 0.13 | 0.14 | 0.15 |

Y CVn with model K12

Coherency peak at $(X, \xi, R, \bar{S}) = (1.3, 5.3, 0.45, 0.265)$

| | | | | | | |
|-----|--------|--------|--------|--------|--------|--------|
| 6.0 | | | | | | |
| .40 | .93475 | .93482 | .93436 | .93361 | | |
| 5.5 | | | | | | |
| .50 | | | .93556 | | | |
| .40 | | .93553 | .93561 | .93528 | .93498 | |
| .30 | | | .93459 | | | |
| 5.0 | | | | | | |
| .50 | | | | | .93487 | |
| .40 | | | .93517 | .93521 | .93495 | .93436 |
| .30 | | | | | .93446 | |
| 4.5 | | | | | | |
| .40 | | | | | .93293 | |
| | 1.00 | 1.20 | 1.40 | 1.60 | 1.80 | 2.20 |

Y CVn with model K26

Coherency peak at $(X, \xi, R, \bar{S}) = (0.20, 5.0, 0.40, 0.200)$

| | | | | |
|-----|-----|--------|--------|--------|
| 5.5 | | | | |
| | .40 | .95368 | .95364 | |
| 5.0 | | | | |
| | .50 | .95260 | .95401 | .95355 |
| | .40 | | .95453 | .95337 |
| | .30 | | .95366 | |
| 4.5 | | | | |
| | .70 | | .95108 | .95226 |
| | .50 | | .95350 | .95379 |
| | .40 | | | .95340 |
| | .30 | | .95276 | .95171 |
| 4.0 | | | | |
| | .50 | | | .95116 |
| 3.5 | | | | |
| | .60 | | .94618 | |
| | .50 | .94395 | .94701 | .94740 |
| | .40 | | .94690 | |
| | .30 | | .94503 | |
| | | 0.15 | 0.20 | 0.25 |
| | | | | 0.30 |

$$C(0.21, 4.9, 0.41) = .95452$$

$$C(0.22, 4.8, 0.42) = .95443$$

APPENDIX V

PARAMETERS OF SPECIFIC MODEL ATMOSPHERES

| Model | K12 | K24 | K26 |
|--------|-----------------------|-----------------------|-----------------------|
| T(eff) | 3500 | 3500 | 3500 |
| log g | 0 | 0 | 0 |
| He/H | .1 | .1 | .1 |
| C/H | 3.55×10^{-5} | 3.55×10^{-3} | 3.55×10^{-2} |
| N/H | 9.75×10^{-4} | 8.15×10^{-4} | 8.15×10^{-4} |
| O/H | 1.78×10^{-5} | 7.10×10^{-4} | 7.10×10^{-4} |
| C/O | 2 | 5 | 50 |